UNIVERSITY OF CALIFORNIA

Los Angeles

The Effect of Dynamic Surface Tension on Oxygen Transfer Coefficient in Fine Bubble Aeration System

A dissertation submitted in partial satisfaction of the

requirements for the degree of Doctor of Philosophy

In Civil Engineering

By

Tai L. Huo

1998

The dissertation of Tai. L. Huo is approved.

Thomas C. Harmon

Keith D. Stolzenbach

Irwin H (Mel) Suffet

Michael, K. Stenstrom, Committee Chair

University of California, Los Angeles

1998

DEDICATION

To Mom and Kid

TABLE OF CONTENTS

TABLE OF CONTENTS (Cont'd)

TABLE OF CONTENTS (Cont'd)

LIST OF FIGURES

LIST OF FIGURES (Cont'd)

LIST OF FIGURES (Cont'd)

LIST OF FIGURES (Cont'd)

LIST OF TABLES

ACKNOWLEDGMENTS

I would like to express my appreciation to my advisor, Professor Michael K. Stenstrom, for his guidance, understanding, and unconditionally support. It has been an honor to work with him. I would like to thank the other members of my committee: Professor Harmon, Professor Stolzenbach, and Professor Suffet.

Special thanks to Mr. Edward Ruth for his valuable suggestions and technical support in troubleshooting my experimental setup.

Finally, I would like to thank Mom and Kid for their unconditional support and love.

VITA

ABSTRACT OF THE DISSERTATION

The Effect of Dynamic Surface Tension on

Oxygen Transfer Coefficient in Fine Bubble Aeration System

by

Tai L. Huo

Doctor of Philosophy in Civil Engineering

University of California, Los Angeles, 1998

Professor Michael K. Stenstrom, Chair

A bench-scale bubble aeration device was built and applied to the dynamic surface tension (DST) effect on oxygen transfer rate (OTR) study. A 2 cm x 2 cm square pyrex glass tube (1 ft long) served as the aeration tank. An upward capillary (with 0.15 mm internal diameter) and upward micro-oxygen electrode were submerged in surfactant solution inside of the tube. Data acquisition system was interfaced with both pressure transducer and dissolved oxygen (DO) meter. The pressure transducer measured system pressure change while the DO meter measured surfactant solution DO concentration

during aeration. Both signals were analyzed by a computer for recording and processing. The sodium dodecyl sulfate (SDS) and iso-amyl alcohol were used for this research. The lowest concentration this device could detect DST changes was 45 mg/l for SDS and 0.020% for iso-amyl alcohol. Precision as high as ±6.0% for aeration test results also achieved using this device.

The unique feature of this device was that it measured DST and OTR simultaneously. As a result of this feature, a linear relationship between DST and $K_L a$ for both surfactants was obtained in this study. The results demonstrated that the dynamic surface tension of surfactant can be used for a predictive tool in accessing the surfactant impact on oxygen transfer rate.

Alpha factors (the ratio of the transfer rate in process water to clean water) have been using as a tool in translating clean water results to process conditions. The original intention to use alpha factor was to account for the differences of wastewater characteristics; however, this has been problematic because the complexity nature of wastewater. This device and technique hold promise for relating transfer rate and alpha factor to contaminant concentration.

INTRODUCTION

Aeration is an essential part of wastewater treatment and is usually the largest single energy consuming part of a treatment plant. Therefore, the oxygen transfer efficiency is a major concern for aeration device design. It has been a standard practice for manufacturers to evaluate oxygen transfer rate of an aerator according to the Clean Water Standard published by the American Society of Civil Engineers (ASCE, 1993). Due to many factors influencing oxygen transfer mechanisms in aeration, the oxygen transfer rate of full-scale wastewater treatment aerators often differs from that predicted by manufacturer by as much as 70%. The difference between the expected and the actual performance of the aerator can cause substantial additional modification costs and time delays in order to meet treatment requirements.

The main difference between expected and actual oxygen transfer rate can be explained using the oxygen transfer model :

$$\frac{dC}{dt} = K_L a \left(C_\infty^* - C_t \right) \tag{1}$$

where

$\frac{dC}{dt}$ = The rate of oxygen concentration changes in the liquid phase

K_L = Liquid film coefficient

a = Interfacial area normal to mass transfer

$K_L a$ = Overall volumetric oxygen transfer coefficient

C_∞^* = Oxygen saturation concentration

C_t = Oxygen concentration at any time t.

This oxygen transfer model was derived by Lewis and Whitman (1924) based on two-film theory. In the two-film theory, the concentration gradient near interface is assumed to be at steady state and linear. However, during aeration, the time of exposure of a fluid to mass transfer is so short that steady state does not develop. Although penetration and surface renewal theories, which were developed later, more closely account the actual transfer mechanisms, the two-film oxygen transfer model is still used because of its simplicity.

The second reason for the deviation is due to the nature of clean water test. As mentioned earlier, many factors influence oxygen transfer mechanisms in aeration. The primary result of this test is expressed as the Standard Oxygen Transfer Rate (SOTR). The SOTR is a hypothetical mass of oxygen transferred per unit time at zero dissolved oxygen concentration, water temperature of 20 °C and barometric pressure of 1.00 atmosphere, under specified gas flow and power conditions. The SOTR can be converted to field Oxygen Transfer Rate (OTR) in process water by applying the following correction factors:

$$K_L a_{pw} = \alpha \cdot K_L a_{tw} \tag{2}$$

$$C^*_{\infty\,pw} = \beta \cdot C^*_{\infty\,tw} \tag{3}$$

$$K_L a(\mathrm{T}) = K_L a_{20} \cdot \theta^{\mathrm{T}-20} \qquad (4)$$

where

T = temperature (°C)

pw = subscript indicating process water

tw = subscript indicating tap water

20 = subscript indicating 20°C

$\alpha, \beta, 6$ = correction factors

The conversion equation for the major difference between clean water and process conditions is:

$$\mathrm{OTR} = \alpha \left(\frac{\beta \cdot C^*_{\infty,\mathrm{tw}} - C_L}{C^*_{\infty,20}} \right) \theta^{\mathrm{T}-20} \cdot \mathrm{SOTR} \qquad (5)$$

where

C_L = Desired value of dissolved oxygen concentration under normal operation

There are several smaller effects on the correction, but they are not need for the purposes of this dissertation (ASCE, 1993). Theoretically, the OTR predicted from a clean water test is reliable so long as the aeration device, turbulence, and basin geometry of the test aeration system and process application are similar and the water contaminants have predictable effects on $K_L a$.

However, wastewater contains surfactants, unique contaminants, which tend to adsorb at the air-water interface during aeration, and reduce oxygen transfer. The rate of adsorption is time dependent so that the reduction of oxygen transfer coefficient (K_L) is also time dependent. Because of the steady state liquid film and clean water assumptions in oxygen transfer testing, the effect of surfactants on oxygen transfer coefficient in clean water testing is neglected (refer to Section IX-B-2). After realizing that surface tension is a time varying property, it is desirable to incorporate the impact of the time-dependence in a clean water test and eventually into aeration design. The goal is to relate the oxygen transfer coefficient with a parameter that reflects the liquid property. It is believed that this parameter can be identified by learning how liquid surface tension changes during aeration. The reason for choosing surface tension is that it is the major property associated with surface-active agents. As long as surfactants are present, the surface tension of the liquid will be impacted.

Surface tension can be static or dynamic depending on which measuring technique is used. A number of researches have tried to relate the static surface tension to oxygen transfer rate. The static surface tension measurements have also been investigated with regard to alpha values but were inconclusive (Stenstrom and Gilbert, 1981). It is thought that since oxygen transfer coefficient is a time-dependent parameter, the dynamic surface tension (DST) measurements are a better choice than static surface tension (SST) measurements to correlate the mass transfer coefficient with the liquid properties.

In 1988, dynamic surface tension effects on oxygen transfer in activated sludge system were studied (Masutani and Stenstrom, 1988). A mathematical equation was derived to predict $K_L a$ by DST, SST and flow-rate. This research builds upon this previous work.

In Masutani's study, the clean water test was performed in a 55-gallon tank with baffles using two fine bubble diffuser stones, however, the DST was measured by MBPM with the surfactant solution was retrieved from the aeration tank. The DST obtained by this "off-line" method does not represent the real DST during aeration. From literature studies, dynamic surface tension of a solution depends on many factors, such as, temperature of solution, impurities of surfactant, capillary immersion depth, capillary internal diameter, and capillary length. Among them, the capillary I.D. introduces the largest error to final DST. In order to obtain the true DST of surfactant solution during aeration process, not only the capillary I.D. must equal to the size of bubble diffuser's orifice but also the bubbling rate should be the same so that temperature for two measurements are the same.

The objective of this research was to design a bench scale measuring device, which simultaneously measures DST, $K_L a$, and bubble diameter of surfactant solutions. Two model surfactants were carefully chosen to demonstrate the effectiveness of this device in obtaining the parameters, which were used in studying of the relationship between oxygen transfer and dynamic surface tension.

LITERATURE REVIEW

I. Surfactants

Surfactants, or surface-active agents, are organic substances, which tend to adsorb to the surfaces of a system and change the surface free energies of those systems. Each surfactant molecule is composed of two groups with properties of an opposite nature -- an oil-soluble lipophilic group and a water-soluble hydrophilic group. These two groups serve to combine with oil and water to lower the surface free energy. The surface free energy is the minimum work required to create a new surface. The work per unit area is a measurable quantity. It is called surface tension (Fujimoto, 1985).

Surfactants can be classified as ionic or nonionic surfactant based on whether they ionize when dissolved in water. Ionic surfactants can be further sub-classified to anionic, cationic and amphoteric surfactants depending on the type of ion resulting from ionization.

Surfactant molecules in dilute solution tend to adsorb to the water-air interface to form a monomolecular film. As its concentration increases, the surfactant molecules start to gather together to form aggregates (i.e. micelles) within the water. The minimum concentration at which surfactant molecules begin to form micelles is called Critical Micelle Concentration (C.M.C.) which is an important technical term in surfactant chemistry.

The surface concentration is an important feature of surfactants in evaluating their performance. The surface concentration at the solid-liquid interface can be determined by an adsorption isotherm. The most commonly used isotherm in this adsorption process is Langmuir adsorption isotherm:

$$\frac{x}{m} = \frac{a \cdot b \cdot C_e}{1 + b \cdot C_e} \tag{6}$$

where

x = Mass of adsorbate on solid phase; [g]

m = Mass of adsorbent; [g]

C_e = Remaining adsorbate concentration in solution at equilibrium; [g/m^3]

a = Empirical constant

b = Saturation coefficient; [m^3/g]

a and b can be determined by plotting $\frac{C_e}{(x/m)}$ versus C_e on arithmetic paper (Tchobanoglaus, 1987). Unlike solid-liquid interfaces, the surface concentration at liquid-gas and liquid-liquid interfaces are calculated indirectly from the surface tension data by use of the Gibbs equation :

$$\Gamma = -\frac{1}{4.606 \cdot R \cdot T}\left(\frac{\partial \sigma}{\partial \log C}\right) \tag{7}$$

where

Γ = The surface excess concentration (mol/cm^2)

σ = Surface tension (dyne/cm)

C = Surfactant concentration in bulk solution (mol/L)

T = Temperature (K)

R = Ideal gas constant, 8.31×10^7 ergs/ mol· K

The surface concentration can be obtained from the slope of a plot of σ versus log C at constant temperature (Rosen, 1978). (Note: Equation (7) is for solutions of ionic surfactant in the absence of any other solutes.)

II. Adsorption Kinetics of Surface-Active Agents

There are two principles adsorption mechanisms and both have been measured in various experiments for a long time. They are a diffusion-controlled mechanism and a kinetic-controlled mechanism. Addison and coworkers (1943-1946) did the most comprehensive experimental studies to determine the real adsorption mechanism of surfactants. They presented a convenient mathematical description of their results instead of a physical description of the kinetics of adsorption. Unfortunately, all their work can not be used to determine if diffusion or adsorption barriers (due to activation energy barriers, orientations, etc.) control the surfactant adsorption process. Ward and Tordai (1946) presented a physically founded model of diffusion-controlled adsorption. Now, it seems to be clear that surfactant adsorption is diffusion-controlled process.

For a dilute surfactant solution (i.e. concentration below C.M.C.), the generally accepted physical model of adsorption kinetics is two-step. The first step is the diffusion of molecules in the bulk phase to the subsurface close to the interface. It is caused by the concentration gradient produced by the adsorption of surfactant molecules at the very beginning of the process. The second step is to transport the molecules from the dissolved phase to the adsorbed state on the surface.

The Ward and Tordai equation is the first model that correlated the surface concentration Γ to the time dependence of surfactant concentration, $\Phi(\tau)$, in the subsurface

$$\Gamma(t) = 2C_0\sqrt{\frac{D\cdot t}{\pi}} - \sqrt{\frac{D}{\pi}}\int_0^t \frac{\Phi(\tau)}{\sqrt{t-\tau}}\,d\tau \qquad (8)$$

where

Γ = Surface concentration (or adsorption) at time t

C_0 = Equilibrium bulk concentration

D = Surfactant diffusivity

Φ = Surfactant concentration in the subsurface layer

The application of Equation (8) to experimented data is not easy due to integrated form. Therefore, approximations are frequently used. Because surface tension is a measurable quantity, the approximations of Equation (8) are presented in surface tension form by assuming a linear relationship between Γ and Φ using the Gibbs Equation (Equation 7).

There are two limiting cases for approximation: long time approximation which is valid if $t >> 5$ msec and short time approximation which is valid if $t << 5$ msec.

Long time approximation

$$\sigma = \sigma_\infty + \frac{2RT\Gamma_\infty^2}{C_0}\frac{1}{\sqrt{\pi Dt}} \tag{9}$$

where

σ = Surface tension at time t

σ_∞ = Equilibrium surface tension

Γ_∞ = Equilibrium adsorption (surface concentration)

R = Universal gas constant

T = Absolute temperature

Small time approximation

$$\sigma = \sigma_0 - 2RTC_0\sqrt{\frac{Dt}{\pi}} \tag{10}$$

where

σ_0 = Surface tension of pure water

Equations (9) and (10) are particular cases of the more general Equation (8). All three equations were derived originally for a quiescent interface of constant area. However, none of the methods to measure surface tension at different times have a quiescent

interface of constant area. For example, when using the Maximum Bubble Pressure Method, which measures the surface tension of an expanding bubble, there are two effects that can additionally influence the adsorption kinetics. One is the convection that is caused by the advancing bubble in the solution. The other is the expansion of the surface during bubble growth. Miller (1980) presented an expression that accounted for these two effects:

$$\Gamma(t) = 2C_0\sqrt{\frac{3Dt}{7\pi}} - \sqrt{\frac{D}{\pi t^{1/3}}}\int_0^{\frac{3}{7}t^{1/3}} \frac{\Phi\left(\frac{3}{7}t^{1/3}\right)}{\sqrt{\frac{3}{7}t^{1/3}-\tau}}\,d\tau \qquad (11)$$

The approximations of Equation (11) (Joos *et al.*; 1981 and 1991) are:

Long time approximation:

$$\sigma = \sigma_\infty + \frac{2RT\Gamma^2}{C_0}\sqrt{\frac{7\pi}{12Dt}} \qquad (12)$$

Small time approximation:

$$\Gamma = \Gamma^\infty\left[1-\exp\left(\frac{-(\sigma_0-\sigma)}{RT\Gamma^\infty}\right)\right] \qquad (13)$$

and

$$\Gamma = 2C_0\sqrt{\frac{3Dt}{7\pi}} \qquad (14)$$

where

Γ^∞ = Equilibrium adsorption

Bendure (1971) used the MBPM for studying the adsorption kinetics. He evaluated his data using Equations (9) and (10) instead of Equations (12), (13) and (14). He justified their use because he claimed that the surfactant adsorption occurs inside of the capillary for most of the period of bubble life. Therefore, adsorption takes place with constant area which satisfy the assumptions of Equations (9) and (10).

Experimental studies on adsorption kinetics of surfactant mixtures were published by Bogaert *et al.* (1979) and Fainerman (1992). The first person who considered the influence of micelles on adsorption kinetics processes (when solution concentration is above C.M.C.) was Lucasson (1976). The conceptual model is similar to adsorption below C.M.C., except we have to include the bulk transport of micelles by diffusion, as well as the formation and dissolution of micelles in the first step of adsorption kinetics model (refer to the beginning of this section).

III. Surface Tension Measuring Techniques

The distinguishing feature of surface-active agents is that they lower the surface tension of a pure liquid by adsorbing strongly at relatively low bulk concentration. Since surface tension is a measurable quantity, there are many existing methods for measuring the surface or interfacial tension of a liquid. The more accurate methods measure the pressure difference on the two sides of a curved surface, which possess surface tension. They include the capillary rise, maximum bubble pressure, and drop-weight methods. Less accurate methods are sometime used because they are convenient and fast. Methods

in this category include the ring and the Wilhelmy method. They measure the force needed to extend and detach a liquid film by means of a support (either a ring or a plate).

It is customary to divide surface tension measuring techniques into static and dynamic methods. Static methods measure the tension of a stationary surface that has been formed over an appreciable time. They include the capillary rise method, Du Noüy Ring method, Pendant drop method, etc. Dynamic methods measure the surface tension of a freshly formed surface. The drop weight, maximum bubble pressure, and oscillating jet methods are examples of dynamic methods (Matijevic, 1969).

The surface tension evolution can be described using Figure 1. When the surface area of a solution is suddenly increased by stretching, a part of the bulk liquid is forced to enter the surface layer by convection. The fresh surface is called zero age and its surface concentration is the same as the bulk concentration. The surface tension of a surface of zero age is called pure dynamic surface tension. As time increases, the surface concentration of the adsorbed molecules increases and the surface tension decreases with time during the aging of the surface. This surface tension is called dynamic surface tension. As time approaches infinity, the surface tension of the solution approaches an asymptote. This surface tension is equilibrium surface tension or static surface tension of the solution. Static (equilibrium) surface tension has significance alone, but the dynamic surface tension has no significance unless related directly to surface age. When the liquid

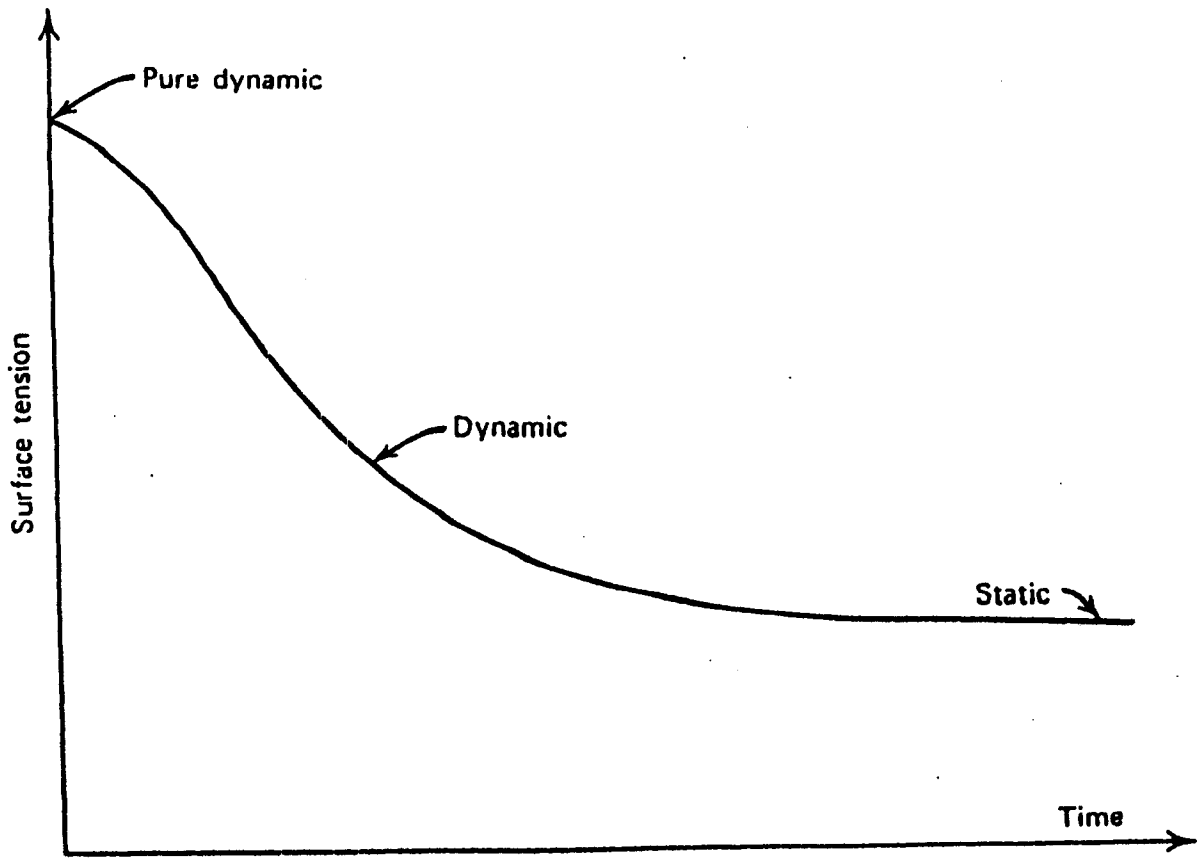

Figure 1. Surface tension is a function of time during surface aging (after Defay and Pe′tre′, 1993).

is pure, the only change at the surface with age will be the orientation of the surface molecules. Such orientation almost happens instantaneously. When one or more components of a system are preferentially adsorbed at the surface, the solute molecules diffuse to the subsurface until an equilibrium adsorbed layer is established. Therefore, the surface tension of this system usually changes from a value almost equal to that of the solvent to the equilibrium value of the solution.

A. Capillary Rise Method

The Capillary Rise Method is the easiest static method for measuring surface tension. When a capillary tube is wetted by a liquid, the liquid rises in the capillary because this change is in the direction of reducing surface area. When the liquid reaches equilibrium, as shown in Figure 2, the force of gravity pulling downward must be equal and opposite to the force of capillary rise (Roberson, 1993). At the equilibrium position, the weight of liquid between line A and line A' is equal to the surface tension of the liquid. Therefore, surface tension can be calculated from the following equation:

$$\sigma = \frac{1}{2} \cdot h \cdot r \cdot \rho \cdot g \qquad (15)$$

where

σ = Surface tension [dyne/cm]

h = Height difference between menisci [cm]

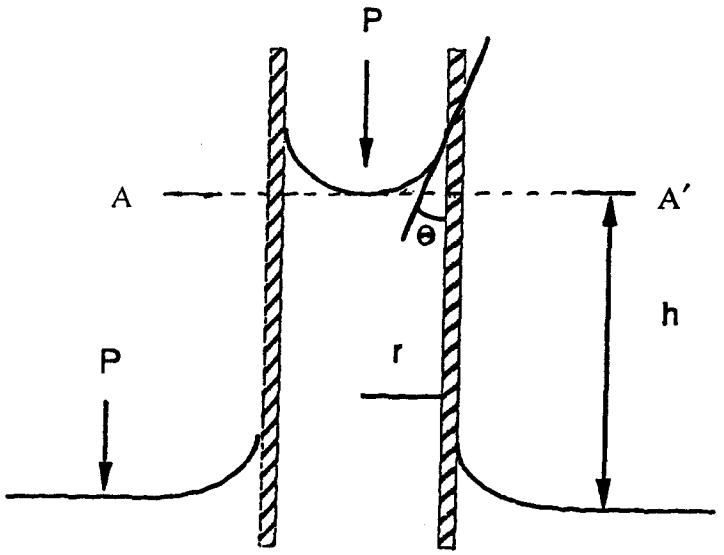

Figure 2. Capillary Rise Method.

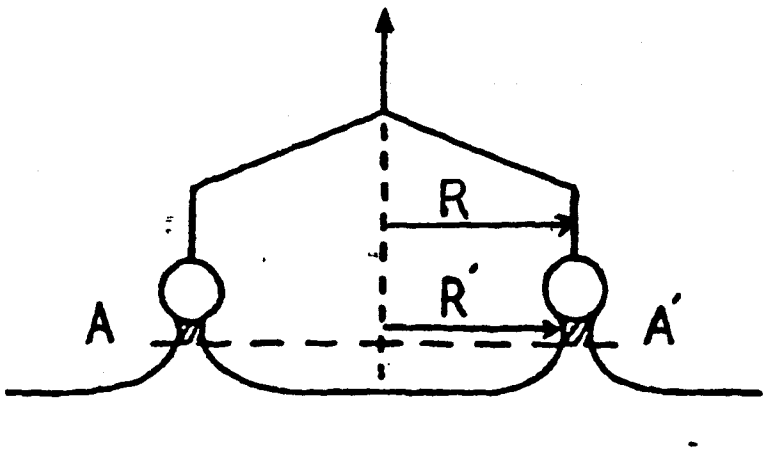

Figure 3. The position of Du Noüy ring right before film rupture.

r = Radius of capillary [cm]

ρ = Density of liquid [g/cm^3]

g = Acceleration due to gravity [cm/sec^2]

The advantage of this method is that it is inexpensive and easy to perform. However, in order to obtain sufficient accuracy using this method, the diameter of capillary tube must be small (< 0.1 cm), the inside wall of capillary must be clean (e.g. cleaned thoroughly with chromic acid) so that contact angle ($\angle 6$) is zero. This method is not suitable for measuring the surface tension of a surfactant solution because the surfactant molecule adsorbs on the glass and make it repellant, thereby increasing the contact angle to a value above zero.

B. Du Noüy Ring Method

The ring method depends upon the determination of the maximum pulling force necessary to detach a circular ring of round wire from the surface of a liquid with a zero contact angle. Du Noüy was not the first to measure the surface tension by ring method, but by describing a convenient form of apparatus, his name has become inseparable from the method. The apparatus he designed is a torsion balance. Instead of measuring the tension by means of weights, the torsion of the wire is used to counteract the tension of the liquid film and to break it (Du Noüy , 1919).

The elementary theory of ring method is that the maximum force required to detach the ring from the surface is equal to the total perimeter of the wire times the liquid surface tension.

$$m g = \sigma \cdot 4\pi r \qquad (16)$$

where

m = Mass of the ring, [g]

σ = Liquid surface tension, [dyne/cm]

g = Gravity of acceleration, [cm/sec^2]

r = Radius of the ring, [cm]

However, Harkins and Jorden (1930), Frend and Frend (1930), showed that Equation (16) was incorrect. They derived a correction factor (f); as follows:

$$\sigma = \frac{m g}{4\pi r} \cdot f \qquad (17)$$

The physical significance of the correction factor can be understood by refering to Figure 3. In the position of maximum pull, it can be seen from Figure 3 that the rupture of the surface occurs at plane A A$'$ and leaves a small but significant volume of liquid attached to the ring. Therefore, the force that is applied to raise the ring to the breaking point is actually equal to the weight of the ring plus the weight of the liquid lifted.

The correction factor, f, takes account of both the extra volume effect and the discrepancy between the measured radius, R, and the radius, R', of the meniscus in the plane of rupture. Huh and Mason (1975), conducted a rigorous study of ring tensiometry, concluding that the ring produced excellent results for static surface tension measurement using the Harkins-Jordan correction factors.

The ring method is one of the static surface tension measurements. It is less accurate than capillary rise method. Ring method's advantage is that it is extremely rapid, very simple and does not need to be calibrated using solutions of known surface tension (Freud and Freud, 1930). Nevertheless, when properly applied to pure liquid, the accuracy can be as high as $\pm 0.25\%$. The following outlines are important if higher accuracy is demanded:

- The theory of ring method is based on force balance (gravitational force and surface tension). Therefore, the buoyancy effect of an immersed ring should be avoided by making the ring with very thin wire (0.007 inch) and immersion depth as shallow as possible (1/8 inch).
- The plane of the ring must be horizontal to the liquid surface.
- The ratio between the measuring vessel and the ring radius can not be too small. (The diameter of the vessel should be greater than 8 cm)
- The ring must be completely wet with the liquid.
- Vibration must be avoided.

The disadvantage of this method is that it is inappropriate for the determination of surface tensions of surfactant solutions (Padday and Russel, 1960; Boncher, Grinchuk, and Zettlemoyer, 1967). Reproducibility of results is always difficult to achieve. Nevertheless, surface tension of surfactant solutions is frequently measured using the ring method because of its simplicity.

Hommelen (1959) found that evaporation will produce erroneous results when measuring the surface tension of surfactant solutions. He also noted that the main difficulty in applying this method to surfactant solutions is the uncertainty of when adsorption equilibrium is reached.

The surface tension of sodium dodecyl sulfate (SDS) solution was measured by ring method (Libra, 1993). She found that the surface tension increased with time, but stabilized after about 30 minutes. She also discovered that the values of surface tension were more reproducible if the solution was shaken before being poured into the container, followed immediately by measurement.

Lunkenheimer and Wante (1981) in their research using ring tensiomatry found that the distance between the upper edge of the vessel and the solution level significantly affects result reproducibility. They discovered that the adsorption layer of surfactant solution is extended to hydrophilic vessel wall. With the additional surface, it takes longer for surface-active agents to reach equilibrium. Readings taken before equilibrium result in a

surface concentration dilution effect due to expansion of adsorption surface area (Addison and Hutchinson, 1948; Hermann, 1965).

C. Drop Weight Method

The Drop Weight Method is a dynamic surface tension measurement method. As mentioned earlier, dynamic surface tension is function of time, as well as composition. Therefore, unlike static (equilibrium) methods, the dynamic methods are good for studying aging effects and adsorption kinetics of solutions.

The first person to notice that a drop is not a definite quantity was Tate, a pharmacist (Matijevoc, 1969). Later, Lahnstein found that the weight of a liquid drop hanging on an orifice was supported by liquid surface tension. When this force was exceeded, the drop falls away from the orifice. The relationship is called "Tate's law" which is the mathematically expressed as follows:

$$W = 2\pi r\sigma \qquad (18)$$

where r is the radius of the orifice. This equation is incorrect due to two reasons :
(1). It assumed the breakaway drop is a perfect hemispherical drop; (2). It assumed the weight of hanging drop is equal to the weight of falling drop. The erroneous assumption can be revealed by observing Figure 4. In Figure 4(c), the breakaway drop can be divided to three parts : main drop , satellite drop, and residual drop. The satellite drops arise from

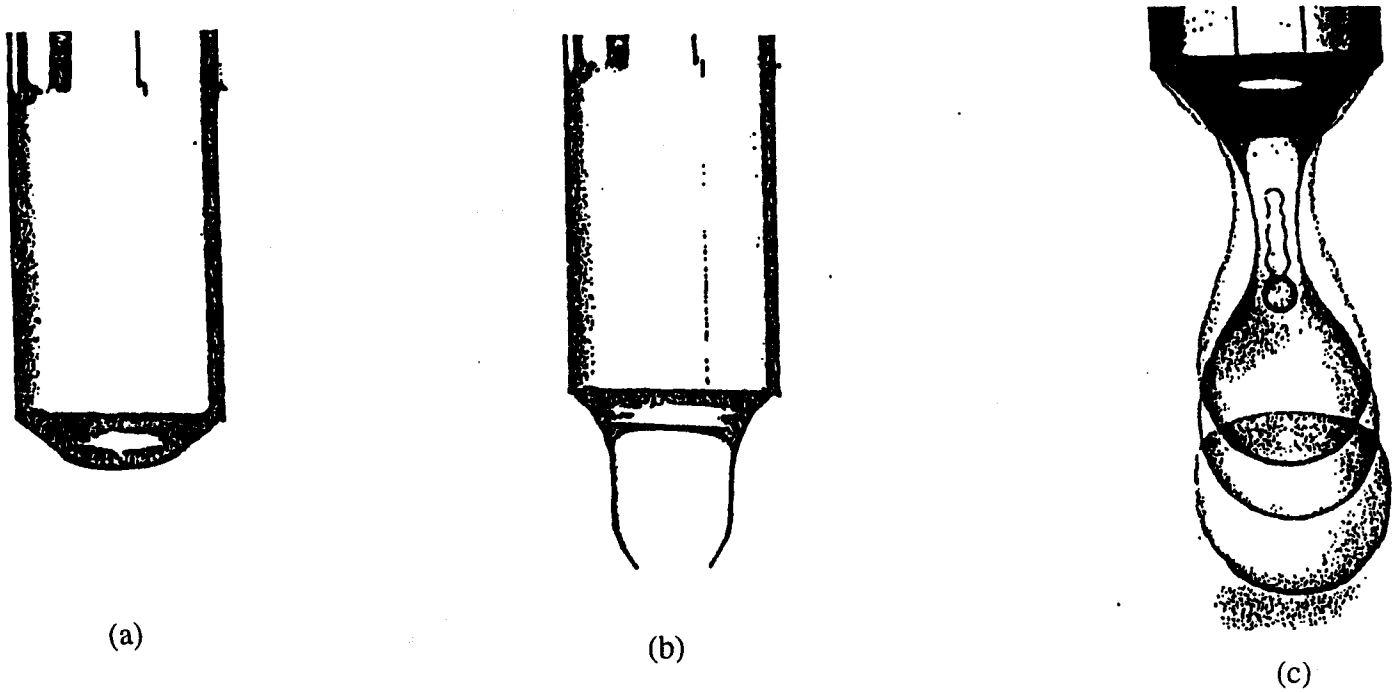

Figure 4. A drop breakaway process (after Pierson and Whitaker, 1975).

the mechanical instability of the thin cylindrical neck. In any event, it is clear that only a portion of the drop (main drop) that has reached the point of instability actually falls. As much as 40% of the liquid may remain attached to the tip (residual drop). Therefore, the radius of the main drop that was collected and weighted is not equal to the radius of tip. In fact, it is a function of $\frac{r}{V^{1/3}}$, where V is the volume of the perfect drop (Harkins and Brown, 1919). Lohnstein (1906 and 1907) also predicted that the weight of a drop is a function of r/a, where a is square root of the capillary constant**. Hence, the surface tension measured by drop weight is:

$$\sigma = \frac{mg}{2\pi r} \cdot \Psi\left(\frac{r}{V^{1/3}}\right) \tag{19}$$

or

$$\sigma = \frac{mg}{2\pi r} \cdot \Phi\left(\frac{r}{a}\right) \tag{20}$$

** The capillary constant, a, is defined as

$$a^2 = rh = \frac{2\sigma}{g(D-d)} \tag{21}$$

where r = Radius of the capillary

h = Height of liquid rises

σ = Surface tension

g = Acceleration of gravity

D = Density of the denser phase

d = Density of the lighter phase

This relationship arise because the first law of capillarity. It is being used frequently in most of the formulae for calculation surface tension. In fact, when introduce the square root of capillary constant into calculation formulae always simplifies them greatly.

The functions of Φ (r/a) and Ψ ($r/V^{1/3}$) have identical numerical values which are given in Harkins and Brown's paper (1919).

The drop weight method can be called drop volume method if the surface is calculated by the volume of drops instead of the weight of drops. The drop weight method has been extensively used over the drop volume method because of the accuracy in which measurements can be made. However, with the increased accuracy of microburets, it has become equally advantageous to use the drop volume technique.

The advantage of this method is that only a small amount of sample is needed. If carefully applied, this method can offer very high accuracy. The experimental apparatus can be inexpensive and may still provide accuracy in the order of less than one per cent. The apparatus which Harkin and Brown (1916) used, which was completely isolated from outside disturbances, temperature fluctuations, vibration, chemical contamination, evaporation, etc., was accurate in the order of one tenth of one per cent.

The method itself is convenient for studying aging effects but unfortunately it is not suitable for measuring the surface or interfacial tension of liquids or solutions that reach equilibrium slowly. However, Gunde, *et al.* (1992) used a computer-controlled device that can transfer very small (~ 10^{-2} μL/sec) liquid volume to the capillary tip. The drop formation time can be as long as 4000 seconds depending upon the diameter of the

capillary. The surface tension measured by their drop volume instrument is very close to equilibrium surface tension.

D. Maximum Bubble Pressure Method (MBPM)

The surface tension of a liquid can be determined from the maximum pressure in a bubble being formed in fine circular capillary tube that is immersed in a liquid. Since the tube is a fine capillary, from capillary raise phenomena, the liquid will rise to a height in the capillary so that the pressure at the liquid surface (meniscus) is zero. As the meniscus is pushed down to the bottom of capillary by a linearly increasing pressure, it remains in the same shape. The increasing pressure finally forces the meniscus to change to a bubble. This bubble, emerging at the end of a capillary, is stable and continuously expands with increasing gas pressure until its shape is hemisphere. At this moment, the pressure inside the bubble is the maximum pressure before it becomes unstable. The time of pressure increase from zero to maximum is called the calm stage. The time elapsed is called effective bubble age. As soon as the bubble size grows larger than hemisphere, it becomes unstable because the equilibrium pressure within it decreases as the bubble grows. Hence the bubble escapes. This process is called explosive stage and it happens within a tenth of a second. This "tenth of a second" should not be counted as part of the bubble age but can be omitted as dead time, as suggested by many researchers (Austin 1967, Kloubak 1972, Fainerman 1992).

This MBPM for measuring surface tension is over 160 years old. The method was suggested and used in 1851 by Simon. Unfortunately, his technique was not successful. Cantor was the first to produce a theory and show how it may be used accurately. Sugden (1922 and 1924) investigated MBPM thoroughly and his two papers are accepted as key references.

Surface Tension (σ)

The MBPM can be used for determining surface tension according to Laplace's law:

$$\sigma = \frac{P \cdot r}{2} \qquad (22)$$

where

σ = Surface tension [dyne/cm]

P = Pressure across the bubble interface [dyne/cm]

r = The radius of the capillary [cm]

Equation (22) is inaccurate because it assumes that the bubble is a perfect hemisphere at maximum pressure so that the radius of bubble is equal to radius of capillary. Sugden has calculated a correction factor for Equation (22) based upon Bashforth and Adam'ssolution of Laplace Equation. Sugden, (1922) tabulated the correction factor, f, as a function of the dimensionless ratio, $\frac{r}{a}$, where a is the capillary constant, as follows:

$$a^2 = \frac{2\sigma}{\Delta\rho g} \tag{23}$$

where

$\Delta\rho$ = The density difference between gas-liquid phases

After substitution, Equation (22) becomes

$$\sigma = \frac{P \cdot r}{2} \cdot f \tag{24}$$

where

$P = P_{max} - \Delta\rho g h$

h = capillary immersion depth

Sugden's correction table has very limited range (for $0 < \frac{r}{a} < 1.5$ only) it is not amendable to computerization. Bendure (1971) developed an empirical power series as a function of the dimensionless radius ratio ($\frac{r}{a}$) to represent Sugden's tabulated values:

$$f = a_0 + a_1\left(\frac{r}{a}\right) + a_2\left(\frac{r}{a}\right)^2 + a_3\left(\frac{r}{a}\right)^3 + \cdots \tag{25}$$

with

$a_0 = 0.99951$ $a_1 = 0.01359$

$a_2 = -0.69498$ $a_3 = -0.11133$

$a_4 = 0.56447$ $a_5 = -0.20156$

Since $\frac{r}{a}$ is a function of surface tension, it is necessary to use an iterative procedure until the converging surface tension values result:

Step 1. $$P = 1.3332 P_0 - \left({}^{1333.2\,h}/_{13.56} \right)$$

P = Differential pressure; $[\text{dyne}/\text{cm}^2]$

P_0 = Gage pressure; $[\mu \text{Hg}]$

h = Immersion depth; [mm]

13.56 = Density of Hg

Step 2. $$a = \sqrt{\frac{2\sigma}{(D-d)g}}$$

D = Density of liquid; $[\text{g}/\text{cm}^3]$

d = Density of air; $[\text{g}/\text{cm}^3]$

g = Acceleration of gravity; $[\text{cm}/\text{sec}^2]$

σ = Surface tension; [dyne/cm]

a = Square root of capillary constant; [cm]

Step 3. $$f = 0.99951 + 0.01359\left(\frac{r}{a}\right) - 0.69498\left(\frac{r}{a}\right)^2 - 0.11133\left(\frac{r}{a}\right)^3 + 0.56447\left(\frac{r}{a}\right)^4 - 0.20156\left(\frac{r}{a}\right)^5$$

r = Radius of capillary; [cm]

Step 4. $$\sigma' = \frac{r}{2} \times P \times f$$

Step 5. if $\sigma' = \sigma$ then stop

else let $\sigma = \sigma'$

repeat step 1 to 4

until $\sigma' = \sigma$

Sugden's table corrects two opposite forces that originated from the size of capillary (or the size of bubble). One is capillary force, which tends to push liquid into the capillary, which reduces the pressure required to produce a bubble by lowering h. The other is gravity of a bubble that increases the pressure needed to make it unstable. However, since his table only applies to $0 < \frac{r}{a} < 1.5$, for water at 20°C with surface tension of 72.75 dyne/cm, his correction only applies to capillary with radii smaller than 0.57cm. Sugden's correction table can be applied to the capillary diameter larger than 0.57cm while measuring surface tension of pure liquids. However, for solutions, because of the

rate of bubble surface expansion, bubble growth, detachment, and hydrodynamics of the rising bubble, and the liquid level displacement at high bubble formation rates is different if the capillary size is larger than 0.57cm, it is expected that the surface tension values will be different even though the bubble frequency and gas flow-rate are the same (Mysels, 1990). Therefore, Sugden's correction can not be applied to the capillary size larger than 0.57cm.

Fainerman (1994) proposed that surface tension be calculated by

$$P=\frac{2\sigma}{r}+\Delta\rho g h+\Delta P \qquad (26)$$

The extra correction value, ΔP, is attributed to the following hydrodynamic effects:

(1). Aerodynamic resistance of the capillary to the air passage;

(2). Hydrodynamic resistance of liquid against the moving bubbles due to the viscous force. The correction value can be estimated by

$$\Delta\sigma=\frac{3}{2}\frac{\mu r}{t} \qquad (27)$$

where

μ = Viscosity of the liquid

r = Radius of capillary

t = Surface lifetime

Both effects can be neglected if the size of capillary is small. How small is small? No researcher has defined "small"; however many researchers have used internal capillary diameters ranging between 0.1 and 0.2 mm.

The proceeding discussion has emphasized the importance of capillary's size (r) in MBPM. The second important parameter is the capillary immersion depth in the solution. The error caused by this factor is easy to eliminate by the experimental set-up. This will be shown later in the experimental section.

Surface Age (t)

The bubble lifetime is conveniently adjusted by gas flow-rate but the actual calculation of bubble life is obtained from the pressure trace. Bubble formation and release can be described as a series of spikes on the recording device (Figure 5). Each spike represents a single bubble while the height of the peak is the maximum pressure in the bubble. The bubble life is simply calculated as the average time interval between successive peaks.

Austin *et al.* (1967) improved the MBPM by measuring bubbling rate with a stroboscope. They divided the bubble interval into two periods. The first period is the time in which the surface-active agent is being adsorbed on the unexposed surface and surface tension varies accordingly (calm stage). The second period is the time in which the bubble grows

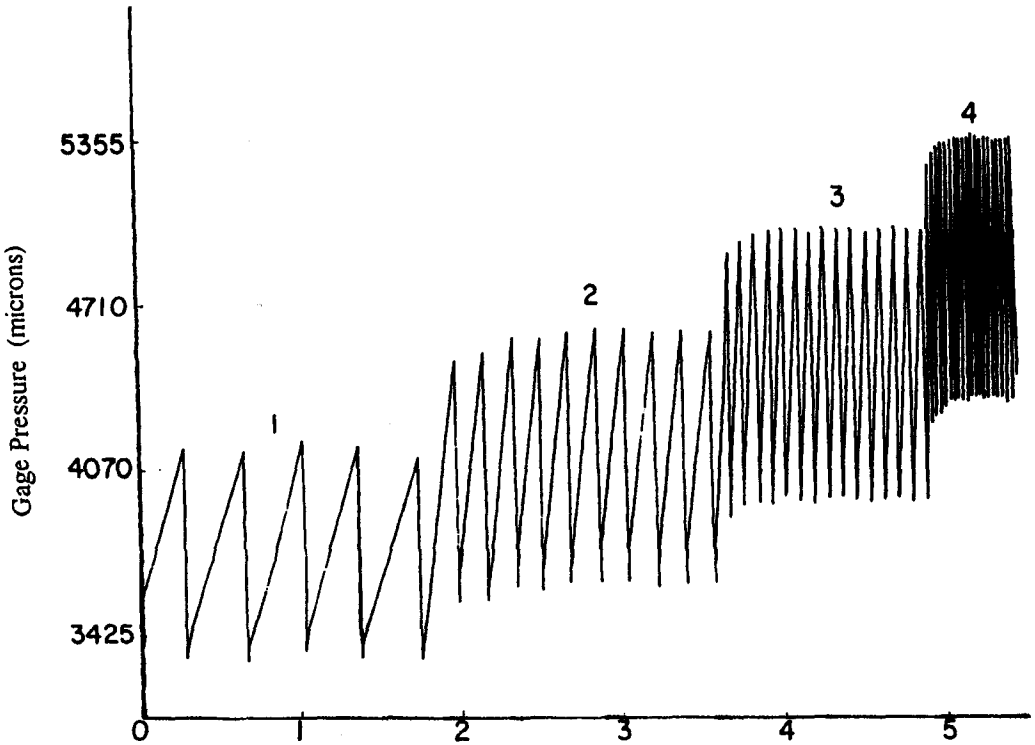

Figure 5. Bubble formation and release pattern for four adsorption times of 22.5, 13.6, 5.3, and 1.1 sec (after Bendure, 1971).

rapidly and detaches from the capillary (explosive stage). They called the second period a "dead-time" that must be subtracted from the time measured between two successive bubbles (t_b). A dead-time (t_d in msec) is given by the relation

$$t_d = 31.9 - 0.0042S \tag{28}$$

where

S = Number of bubbles per minute

Kloubek (1972) carried out a calculation to confirm that during the time dependence of surface tension determination, the surface age (t) is 10 to 20% shorter than the conventional measured bubble interval (t_b). Mysels (1989) tried to quantitatively interpret the equivalent age of the surface. He evaluated both short and long bubble intervals. He concluded that it is safe to include bubble interval in the surface age except when the bubble interval approaches dead time (t_d). Garrett *et al.* (1989) determined the true surface age with a high-speed cinematograph. The high-speed movie stills of bubble growth proved the theory of dead time. Schramm and Green (1992) identified a previously unrecognized source of error in estimating bubble surface age (Figure 6(a), 6(b), and 6(c)). They discovered that for large capillaries (the radius of their large capillary is 0.344 ± 0.02 mm), the bubble interval between two successive bubbles composed a significant decay time in addition to the dead time. Without a suitable correction, it can lead to a large error in DST interpretation.

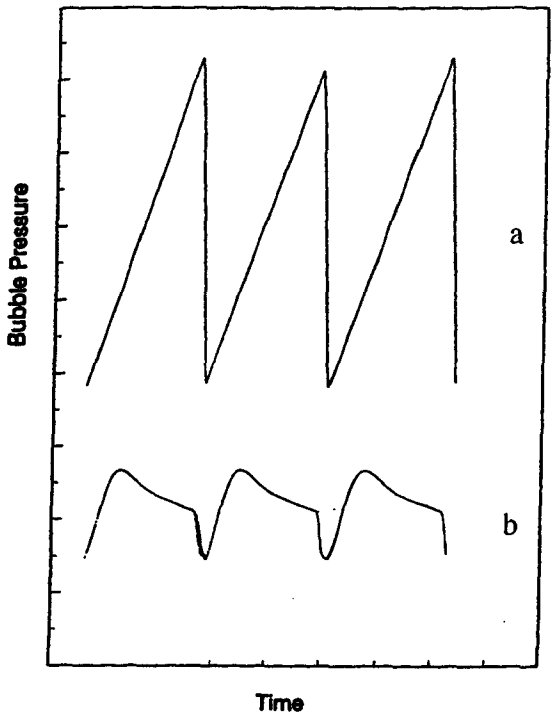

Figure 6(a) and (b). Bubble pressure-time waveforms produced
(a) at the small capillary (b) at large capillary.
(after Schramm and Green, 1992)

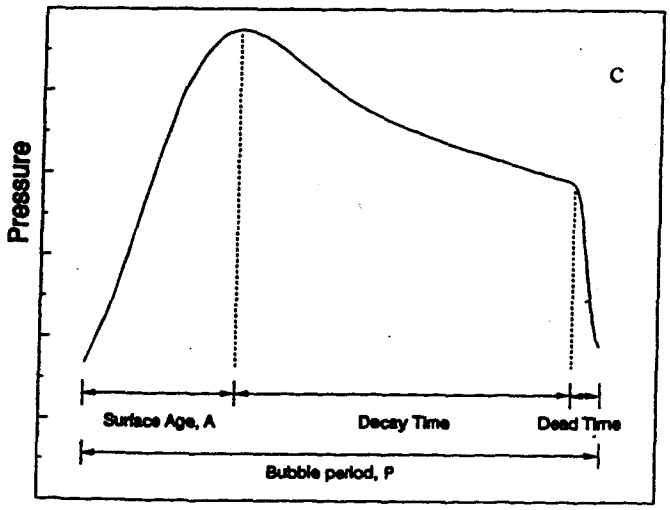

Figure 6(c). An enlarged 6(b) showing the total bubble interval is divided into 3 regions : surface age, decay time, and dead time.
(after Schramm and Green, 1992)

Fainerman *et al.* (1992 - 1995) designed an improved DST Tensiometer, MPT1 from LAUDA (Germany). This Tensiometer can be used for measuring DST in a time interval from 1 ms to 10 sec (in comparison with Austin's 10 to 200 ms). A substantial improvement in estimating surface life results from the better bubble frequency and dead-time measurement. It is interesting to compare this technique to Austin's stroboscopic technique (Equation 28). Austin claimed that he could measure surface tension at surface age up to 10 ms, or a bubble frequency of 28.6 per second. However, at high frequency of bubble formation where there is a transition (at critical gas flow-rate) from the bubble flow process to the jet flow process (Figure 7). The MBPM requires the gas flow-rate not to exceed the critical gas flow-rate, i.e., MBPM must be used within bubble regime. Because this maximum gas flow-rate can varied, the maximum bubble frequency, depending on the size of capillary, may be over 28.6 per sec. Fainerman (1992) proposed that the dead time be determined by the bubble volume that separates from the capillary and by the capillary hydraulic resistance, as follows:

$$t_d = \frac{t_b \cdot Q \cdot n}{\zeta \cdot P} \tag{29}$$

$$n = 1 + \left(\frac{3}{2}\right)\left(\frac{r}{r_b}\right) \tag{30}$$

where

t_d = Dead time

t_b = Bubble interval

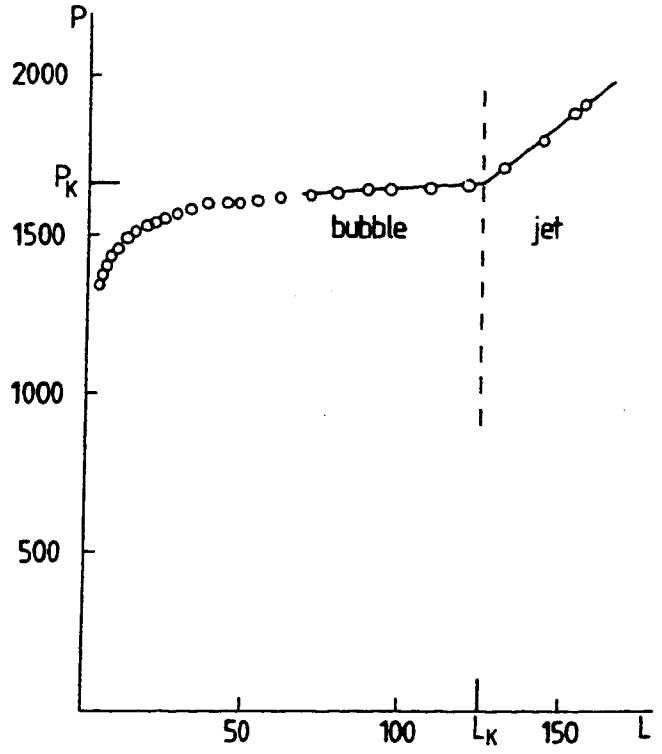

Figure 7. The bubble and jet regimes. P_k and L_k are critical pressure and flowrate points, respectively (after Makievski *et al.*, 1994)

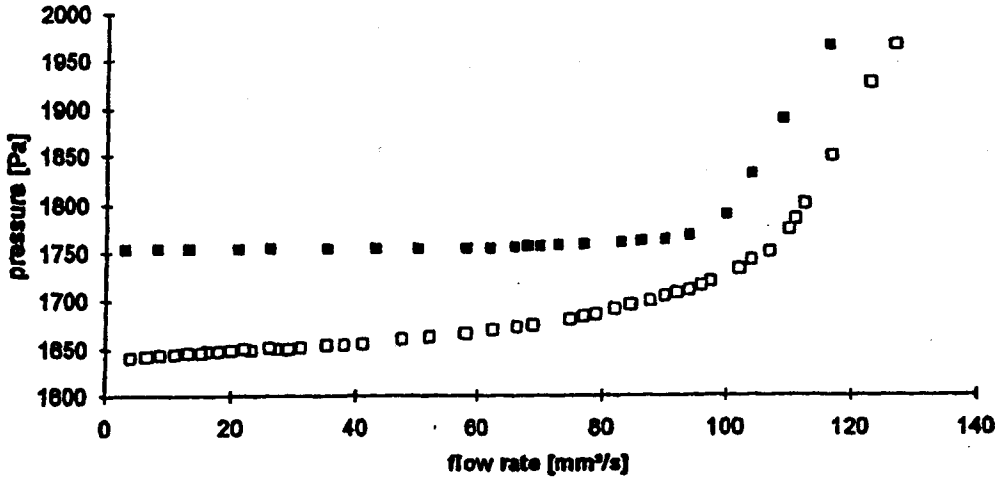

Figure 8. Dependence of pressure on air flowrate. The close symbol (■) is water, the open symbol (□) is a water/glycerine mixture (after Fainerman *et al.*, 1994).

Q = Air flow-rate

ζ = Capillary hydraulic resistance coefficient

P = Pressure in the measurement system which is connected to the capillary

r = Capillary radius

r_b = Bubble radius

After a series of simplifications, Equation (29) becomes:

$$t_d = t_b \cdot \frac{Q}{P} \cdot \frac{P_c}{Q_c} \tag{31}$$

where

P_c = Critical pressure

Q_c = Critical air flow-rate

because

$$t = t_b - t_d \tag{32}$$

After substituting Equation (31) into Equation (32), the term becomes:

$$t = t_b \left(1 - \frac{P_c \cdot Q}{P \cdot Q_c} \right) \tag{33}$$

Therefore, in order to use Equation (33), a plot showing the pressure (P) as a function of gas flow-rate (Q) is needed to obtain P_c and Q_c (Figure 8). The advantage of Fainerman's method is that much shorter bubble intervals can be evaluated in comparison with Austin's method.

Experimental Design: Main Form and Modifications

From the time of Simon's innovation of MBPM until 1932, experimental design focused on eliminating the measurement of the capillary immersion depth. The choices were either one capillary or two capillaries (Mysels, 1990). More recently many advanced lab devices have become available that can be used to measure the immersion depth accurately so that one capillary is most often used. The main components of MBPM experimental set-up are: gas supply system (at constant pressure), capillary, differential pressure detection device and bubble frequency counting device. The following section describes the components.

- Gas Supply System

The most important requirement for gas supply system is that it provides the desired gas flow-rate at constant pressure. Most researchers used compressed gas (N_2 or O_2) while some researchers used a water reservoir (Kuffner, 1961; Kragh, 1964; Austin, 1967; Masutani, 1988). Water is allowed to flow from a constant head reservoir into a water trap chamber which forces gas through the capillary. The advantage is that it is often

easier to measure liquid flow-rate than gas flow-rate. The disadvantage is that at high bubble frequency the pressure head may drift. Gas flow-rate is usually measured by displacement of a rotameter ball and, occasionally soap flow meters have been used (Yu and Shi, 1988). Mysels (1986) improved gas flow control by controlling gas pressure with a manostat instead of regulating gas volume with a rotameter. He obtained gas flow at very low rate (about $0.1\,mm^3/sec$), which extended bubble life to hours. Fainerman (1992 to 1994) used a microprocessor combined with a throttling capillary in his device. The gas flow rate was measured with the help of an electric transducer according to the pressure difference between the two ends of throttling capillary. Hallowell and Hirt (1994) used a syringe pump to supply gas at controlled rates.

- Capillary

The capillary has significant influence on bubble volume and bubble interval. According to Mysels (1986) the inside wall of capillary should be hydrophobic while the face and outside wall should be hydrophilic. If the inside wall is hydrophobic, it can prevent a receding meniscus from leaving behind a film of varying thickness, which can modify the effective radius. By keeping the face and outside wall hydrophilic the released bubble is prevented from sticking to it, which will produce irregular bubble intervals. Mysels (1986) also suggested procedures to treat the capillary so that they can be hydrophobic or hydrophilic, accordingly.

Almost all of the capillaries used in previous research are made of glass except those used by Hallowell and Hirt (1994), who used Teflon. Traditionally the capillary is vertical and pointed downward, but occasionally, it is vertical and pointed upward (Iliev and Dushkin, 1992; Roll J.B. and Myers J.E., 1964). However, Mysels (1986) used a downward but inclined capillary (45°).

- Differential Pressure Detection Device

Water manometers and differential pressure transducer are most frequently used to measure pressure. The transducers can be connected to a recording device such as an electronic recorder, oscilloscope, or computer equipped with an analog-to-digital converter.

- Bubble Frequency Counting Device

Kuffner's (1961)MBPM design could only count bubble 5 per second visually. This makes the bubble interval only 200 ms which limits the range of the measurement. Austin (1967) used a stroboscope which allowed bubble intervals as low as 10 msec to be measured (which is 28.6 bubbles per second). Garrett and Ward (1989) used high-speed cinematography to determine the true surface age. Bendure (1971) calculated the bubble interval directly from a chart recorder by averaging the time interval between successive spikes in the pressure trace. Finally, Fainerman (1992) designed a MBPM set-up with two independent systems for measuring bubble frequency: an accoustic system based on a

microphone, and an electric system composed of platinum electrodes located opposite to the tip of capillary. The accoustic system is applicable to any liquid but the electric system can only be used for electro-conductive liquids. These improvements permitted bubble measurements over the interval of 1 msec to 10 sec.

E. Oscillating Jet Method

This is one of the oldest dynamic surface tension measuring technique. The mathematical treatment was first developed by Raleigh (1879), followed by Bohr (1908) and then Sutherland (1954). From fluid mechanics, under constant pressure, a liquid jet emerges from an elliptical orifice presenting one major and one minor axis. The surface tension of the liquid tends to restore the jet to a circular shape, however, due to liquid inertia, the liquid overshoots and becomes elliptically shaped again. Consequently, the jet oscillates about its equilibrium circular section is shown in Figure 9. Regardless of the oscillation frequency, the jet stream produces stationary waves.

This simple fluid dynamics phenomena can be used for surface tension measurement because of the relationship among surface tension, jet wavelength and jet amplitude. Theoretically, the oscillation of an ideal jet is two-dimensional and its wavelength varies only with the flow rate (Addison, 1943). When surface-active agents adsorb to the jet surface, the wave amplitudes decrease due to viscous damping, and the wavelength increases due to increased surface velocity (Hansen, 1957). The lowered surface tension

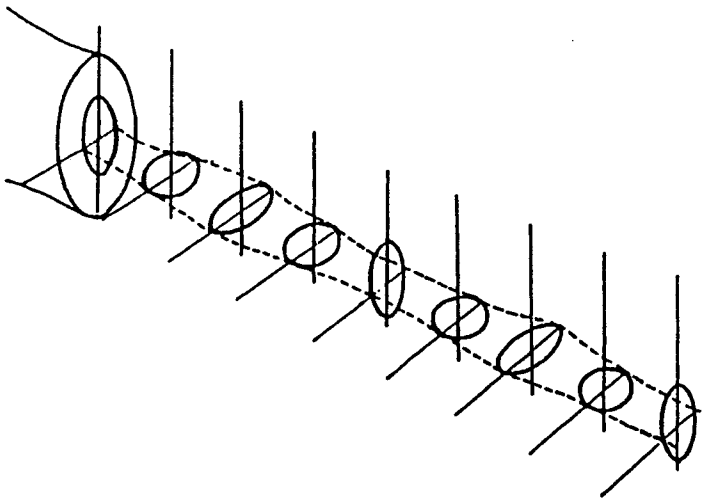

Figure 9. Schematic view of the elliptic oscillating jet (after Kubiak and Dejmek, 1993).

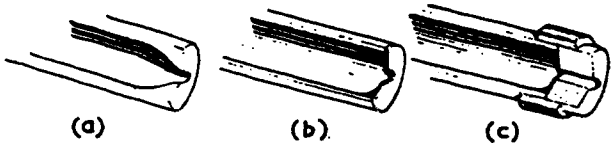

Figure 10. Orifice tubes used in oscillating jet method. (a) bell shape (b) diaphragm (c) uniform channel (after Thomas and Potter, 1975).

increases the required distance for the elliptical jet to reach equilibrium and become circular in form.

Bohr (1908) established a complete equation equating the surface tensions to wavelength, outflow rate and the minimum and maximum radii of the jet (Thomas, 1975). As mentioned earlier, for an ideal jet, the wavelength is only function of flow rate, and the jet oscillates about two axes (maximum and minimum). However, for a non-ideal jet, the wavelength will increase with wave number (Addison, 1943) even though flow rate does not change. The third dimensional oscillation is caused by superficial viscosity. Bohr included a viscosity correction for this "three-dimensional problem" (Defay, 1993). Therefore, the Bohr equation is applicable to an ideal jet. For dilute aqueous solutions with viscosities less than 10^{-2} Dyne$\cdot$sec/cm^2, the correction factor can be neglected (Thomas, 1975). The most common form for calculating surface tension is based on. Defay's (1958) simplification of the Bohr equation, as follows:

$$\sigma = \frac{4\rho D^2\left(1+\frac{37}{24}\frac{b^2}{a^2}\right)}{6r\lambda^2+\frac{5}{3}\pi^2 r^3} \qquad (34)$$

where

σ = Surface tension; [mN/m]

ρ = Density of solution; [Kg/m^3]

D = Outflow rate; [m^3/sec]

λ = Wavelength; [m]

r = Mean radii of the jet; [m] $\quad r \cong \frac{r_{max} + r_{min}}{2}$

$\frac{b}{a}$ = Amplitude; [m] $\quad \frac{b}{a} = \frac{r_{max} - r_{min}}{r_{max} + r_{min}}$

r_{max} = maximum radii of jet; [m]

r_{min} = minimum radii of jet; [m]

A jet emerging from a noncircular orifice is mechanically unstable, not only because necking will eventually cause jet breakup into droplets but also because its initial cross section is not circular (Adamson, 1976). Therefore, obtaining the maximum length of the unbroken jet is an important issue for the Oscillating Jet Method. Orifice configuration and orientation have significant effect on jet stability and data reproducibility. There are three orifice tube designs: bell-shape, diaphragm and uniform channel (Figure 10). The bell-shaped tube's walls taper over 3-5 mm to a narrow channel 0.5-2 mm long leading to the orifice. Many researchers (Bohr, 1909; Addison, 1943; Rideal and Sutherland, 1952; Defay and Hommelen, 1958) used this design and obtained irreproducible results, except Defay and Hommelen who applied the appropriate correction factor to each orifice and flow rate. Several other researchers used a diaphragm tube by piercing an elliptical hole in the end of metal plate (Burcik, 1950; Caskey and Barlage, 1971; Owens, 1969; Netzel *et al.*, 1964; Ross *et al.*, 1958; Vandergrift, 1967). An important disadvantage of this

design is that turbulence is created at the orifice entrance which requires certain distance to damp out. The distances increase with increasing Reynolds number. Erratic results are certain if the turbulence persists to the orifice exit. Hansen et al. (1958, 1959) found that although the bell-shaped orifice tube reduces turbulence, it cannot guarantee the absence of turbulence. This causes not only poor reproducibility but also may create an uncertain velocity profile at the instant of exit. Therefore, they used orifices at the end of long uniform channel (6-14 mm).

Besides the orifice tube shape, orifice size is another important factor in obtaining stable and reproducible results. Each jet shows a *vena contracta*. Theoretically, a *vena contracta* appears at a distance of 0.7 times the diameter of the orifice. The smaller the orifice diameter, the shorter distance from orifice for the *vena contracta* to form. By using smaller orifice tube diameter ensures the correctness of measurement of jet diameters and wavelength.

The Bohr equation (Thomas, 1975) was derived for a horizontal jet where the gravity effect on wavelength is negligible. However, gravity increases the length of an unbroken vertical jet stream by about 30%. Hansen et al. (1958) extended the Bohr equation for vertical jets formed by uniform-channel tubes. They included correction factors for gravitational effect and non-uniform velocity profile effect.

Like any other dynamic surface tension measurements, the definition of surface age is not obvious. Conventionally, the surface age equals the distance between the midpoint of the wavelength and the orifice divided by the mean velocity. The difficulty in creating a precise definition arises from the existence of a non-uniform velocity profile in the jet (Dfefay and Pe'tre', 1993). For a jet of a surface-active solution there are two opposing effects : 1) The jet accelerates because of the pressure gradient; 2) The jet decelerates because surface tension gradient. (Marangoni effect). Consequently, these two opposite effects result in nearly uniform velocity profile at some distance near the orifice; however, the velocity profile will never be perfectly uniform.

In practice, most investigators have assumed that the jet surface velocity is equal to the mean jet velocity. Therefore, surface age (t) is calculated by

$$t = \frac{d}{v} \tag{35}$$

and

$$v = \frac{Q}{A} \tag{36}$$

where

t = Surface age; [sec]

d = Distance between the orifice and the midpoint of the wave; [cm]

v = Mean velocity of jet; [cm/sec]

Q = Flow rate; [cm^3/sec]

A = Cross-section area; [cm^2]

This surface age is different from the proposed definition of the exact age. Hansen *et al.* (1958) showed that an exact (or correct) age must be if it is possible to inferred from surface velocity. They mathematically derived a factor for surface age in order to correct for a non-uniform velocity profile.

The oscillating jet method can provide surface tension information at very early surface age (between 1 to 100 msec). This is a big advantage for studying the adsorption kinetics of organic substances with low carbon content which have characteristics of rapid aging (i.e. equilibrium surface excess was established less than 10 msec). In spite of this advantage, the cost of equipment can be prohibitive for this method. The accuracy that can be provided depends upon the measurement of wavelength, two tube diameters, flow rate, distance between midpoint of wave and orifice diameter. Due to the nature of these parameter measurements, it is necessary to use sophisticated equipment (Kubiaak and Dejmek, 1993).

IV. Dynamic Surface Tension of Water

Theoretically, the surface tension of pure water does not change with time. For water contaminated with surfactants, the surface tension decreases as the surface life increases;

as shown in (Figure 11(a), (b), and (c)). Moreover, this phenomena exists in every dynamic surface tension measurement. Researchers attributed this phenomenon to either hydrodynamic effect or inadequate mathematical treatment.

Mysels (1989) measured dynamic surface tension of pure water by MBPM. He gave a very tentative explanation. As the bubble grows explosively, it pushes the water away from the capillary. When the bubble escapes, the water rushes back and presses against the face of the capillary and remaining bubble, thus increasing the gas pressure necessary for it to reach instability.

Pierson and Whitaker (1976) measured dynamic surface tension of pure water by the Drop-Weight Method. They hypothesized that the rising surface tension at small drop time is due to breakaway process and found there was a steady flow taking place during the drop breakaway process. They also estimated the breakaway process to occur in about 0.1 second. As the drop time approaches to 0.1 second, an additional fluid enters the main drop (refer to Drop Weight Method in Section III(C)) after it becomes unstable and before it breaks away from the tip.

Addison (1945) measured the surface tension of water using the vibrating jet method and noted a change in the surface tension during the first four wavelengths. Schmidt and Steyer (1926), using the Oscillating Jet Method, also reported that the surface tension of

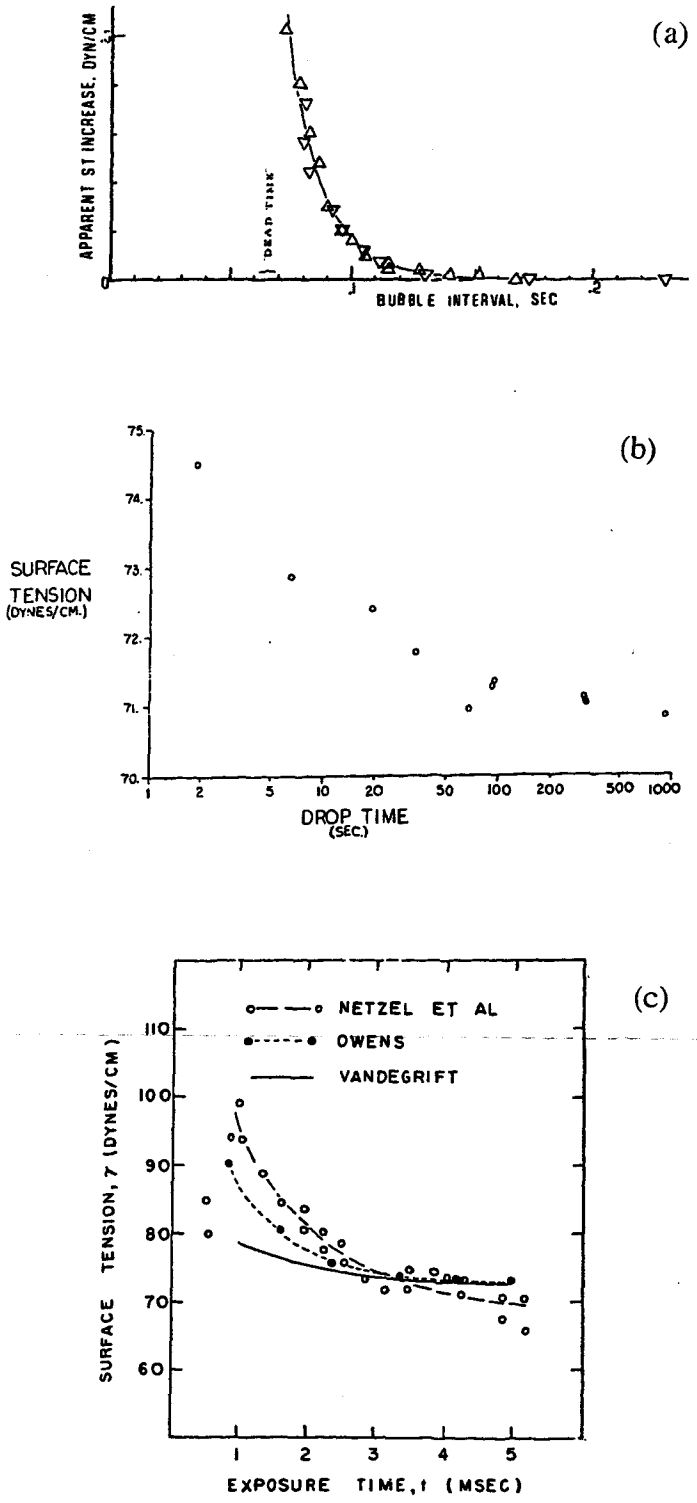

Figure 11. Dynamic surface tension of water. (a) after Mysels, 1989 (b) after Pierson and Whitaker, 1975 (c) after Barlage and Caskey, 1971.

water appears to fall from 103.6 dyne/cm to 73.7 dyne/cm within the first 5 msec. Netzel *et al.* (1964) noted that the surface tension of water at zero time appears to be of the order of 110 dyne/cm. Hansen *et al.* (1958) proposed a possible explanation for this phenomenon. They attributed the high surface tension values to the difference between the surface velocity and the mean velocity of the jet issuing from the orifice. Vandegrift (1967) concluded that water has no dynamic surface tension in the millisecond range, and that any time-dependent effect in this region is probably due to an inadequate mathematical description of the process. Caskey (1971) modified the Oscillating Jet Method by using a vertical jet stream and measured the dynamic surface tension of water. He claimed that his new improved experimental technique gave water surface tension which was dependent on exposure time and agreed closely with equilibrium values.

V. Factors Influencing Surface Tension

- Temperature

The surface tension of many pure liquids decreases approximately linearly with increasing temperature up to 30°C, and follows Le Chatelier's principle. In order to increase the interfacial area, work has to be done on the system. If the surface area is increased adiabatically, the temperature of the system will drop and the surface tension will increase to act as a constraint to further expansion. Owens (1969) examined the influence of temperature on the dynamic surface tension and found that an increase in

temperature will increase the initial rate of surface tension decrease, but had little effect at longer times.

- Viscosity

The surface tension of pure liquids that is obtained at small lifetimes is influenced by hydrodynamic effects which depend on the viscosity of the liquid. Fainerman *et al.* (1993) indicated that for a viscous liquid, the measured surface tension is somewhat higher than the real value. They believe that a viscous resistance against the displacement of the liquid meniscus causes the increase. However, this effect decreases as the lifetime increases.

- Electrolytes

As early as 1950, Burcik founded that added electrolytes affect the dynamic surface tension of different solutions in different ways (Figure12(a), (b), and (c)). In Figure 12(a), it can be seen that added anions to an anionic surfactant solution lowers its surface tension. Moreover, different anions have same influence on surface tension. For non-ionic surfactant solutions, electrolytes have no effect on their DST (Figure 12(b)). Figure 12(c) shows the influence of the valence of the added cation on the dynamic surface tension. It is clear that the effect is quite marked and the higher the valence of the cation the greater the effect. Owens (1969) re-examined these effects and concluded that electrolytes increase the dynamic surface lowering rate at longer times but have little effect on the initial rate of lowering. Oko (1971) also studied the effects of electrolytes

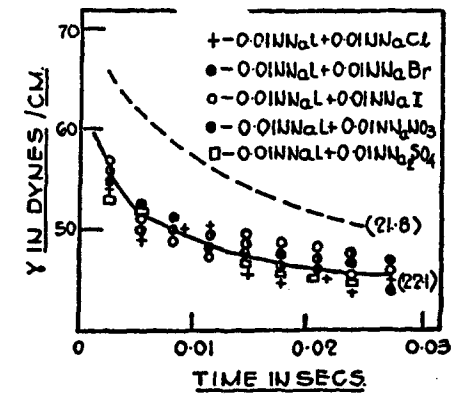

(a)

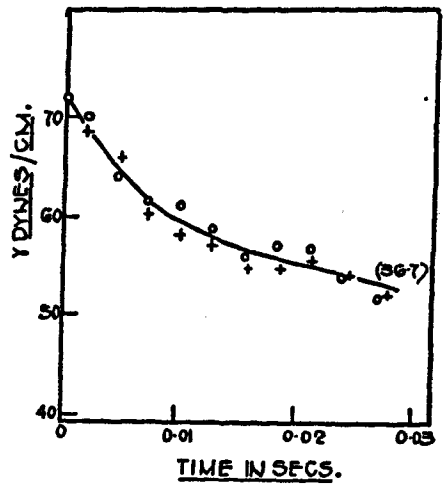

(b)

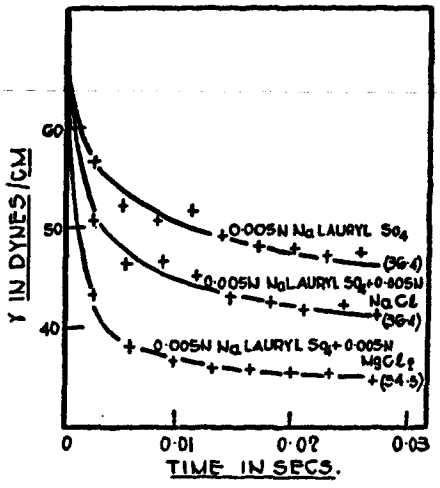

(c)

Figure 12. Electrolyte effect on DST (after Burcik, 1950-1954). (a) DST of sodium laurate (the dotted curve) and the effect of addition of several sodium salts (b) The addition of 0.03N NaCl to 0.1% Tween 20 (a nonionic surfactant) has no effect on DST (c) The influence of the valency of the added cation on DST of sodium laurate. (The number in ( ) is equilibrium surface tension)

on the micellar properties of anionic surfactant solutions. The added electrolytes lowered C.M.C. in comparison with a pure surfactant solution, and higher valence of counter ions produce greater effects. The explanation for these findings is that the potential of the surface-active ions in the interface is reduced by the presence of the electrolyte and therefore that the barrier to rapid adsorption is also decreased.

VI. Choice of Method

There are many existing techniques for surface tension measurement. Choosing the best method requires a compromise between accuracy and ease of operation. However, economy and the nature of the liquid also need to be considered. Table 1 summarizes the suitability of several methods that were discussed in Section II.

In general, the static method is not suitable if there is a new surface involved. In contrast, the dynamic method is designed to measure the surface tension change versus surface life. Just like other analytical methods, each dynamic method has detection limitations in terms of surface life, especially for very short surface life (Table 1). The range of surface lifes showed in Table 1 is only a reference operation range for each dynamic method. Two groups of experimental data are presented in Figures 13 and 14 to demonstrate that different experimental techniques may partially overlap or complement each other in their range of application (Miller *et al.*, 1994). In these two figures, the time windows of the

Table 1. Choice of Dynamic Surface Tension Measurement Method

Method	Remarks on Suitability	
	Pure liquids	Solutions
Capillary Rise	Very Satisfactory	Poor if the surface adsorption mechanism is involved
Du Noüy Ring	Satisfactory	Not good for surfactant solution
Drop Weight	Very suitable when atmospheric contamination is suspected	Good for surface age greater than 20 seconds
Maximum Bubble Pressure	Somewhat difficult to operate successfully	Good for surface age range from 1 msec to 20 seconds
Oscillating Jet	Difficult to operate and evaporation can be a problem	Good for surface age range from 3 msec to 25 msec

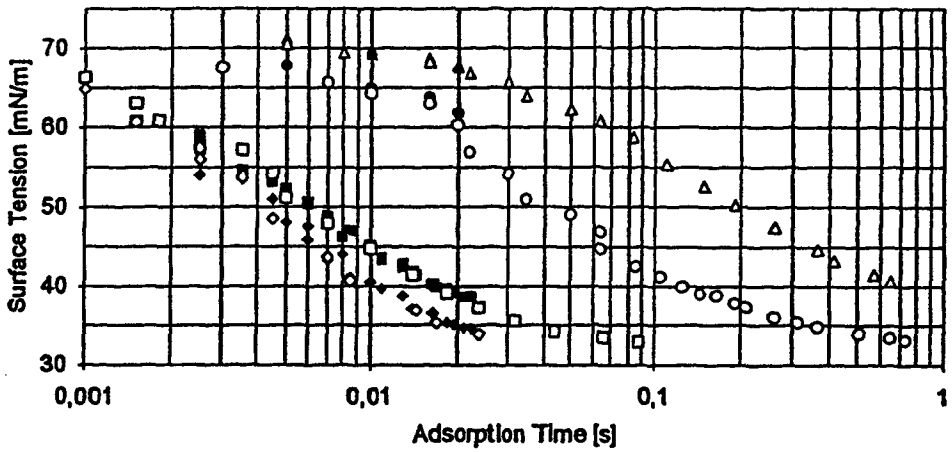

Figure 13. DST of four Triton X-100 solutions (after Miller *et al.*, 1994). The open symbol is M.B.P.M. and the close symbol is Oscillating Jet Method.

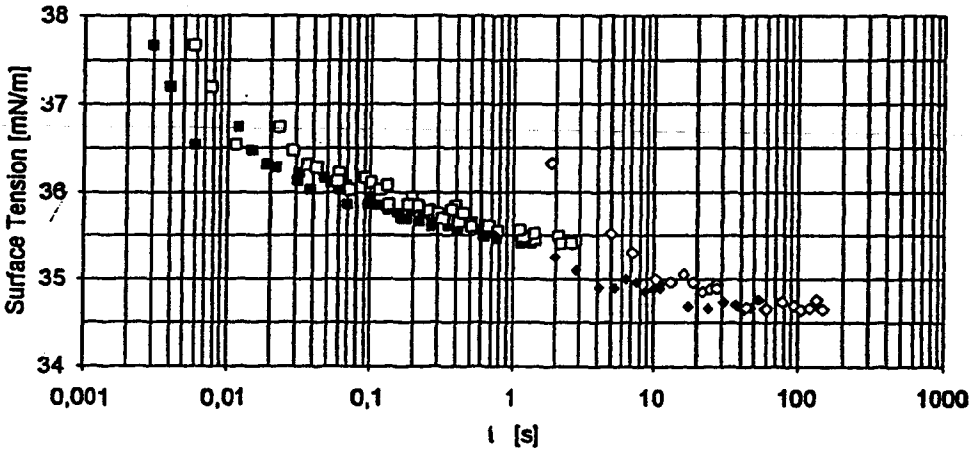

Figure 14. DST of a 0.025 mol/l pt-Bph-E010 solution (after Miller *et al.*, 1994). The open symbol is M.B.P.M. and the close symbol is Drop Volume Method.

drop volume and MBPM show only a small overlap, while the time windows of jet method overlaps completely with the MBPM.

In MBPM experiments proposed 50 or 60 years ago, the remark "somewhat difficult to operate successfully" meant problems with pressure measurement. Today pressure transducers can accurately measure the small differential pressures required for the MBPM. A stroboscopic illumination device, a microphone of high sensitivity, a computer equipped with analog-to-digital card can be used to measure high bubble frequency so that bubble surface life as low as 1 msec can be measured. Even with modern equipment there are still many problems in measuring dynamic surface tension. The major difficulty is obtaining the correct bubble pattern. The importance of bubble pattern cannot be emphasized too much when using MBPM. The bubbles must be small, slow growing and singles.

VII. Application of Surface Tension Measurement

A). Surfactant Solution Adsorption Kinetics

Interpreting dynamic surface tension measurements in terms of fundamental surfactant transport properties is crucial in judging the usefulness of a particular experimental technique. By measuring dynamic surface tension of a surfactant solution and fitting different adsorption kinetic models to the resulting data, one could calculate surfactant

diffusivity and/or micellar dissociation rate constant (Dendure 1971; Joos *et al.* 1981 and 1992; Fainerman 1992; Makievski *et al.* 1994; Filippov 1994; MacLeod *et al.* 1994).

B). Polluted Water Indication

Detergents and soaps are not the only surface-active substances. Many surfactants are generated naturally as by-products of biological activity. They can also be cultural contaminants such as petroleum products, sewage and industrial waste. Fundamentally, they can be organic or inorganic materials. When surface-active agents contaminate water, its properties, especially water surface tension, will be changed. Therefore, surface tension is useful to detect the presence pollution.

Hardy and Baylor (1975) did *in situ* surface tension measurements for the New York Bight using the Drop Spreading technique. The purpose of their work was to measure pollution dispersion from sewage sludge dumping by comparing surface tension data collected at different locations. Sridhar (1984) performed a comprehensive surface tension study on polluted and recovered polluted water, using the Du Noüy Ring Method. He concluded that the measurement of surface tension is a useful parameter in understanding the biochemical changes, and that it can also be an indication of water sanitation. Gunde *et al.* (1992) applied the Drop Volume technique to the measurement of the surface tension of secondary clarified effluents taken from sewage treatment plants in the Zurich area of Switzerland. Surface tension measurement is one of the standards for the quality of rivers and treatment plant effluents in Switzerland. The minimum value

required for river water is 65 dyne/cm and for the treatment plant effluent is 60 dyne/cm at 20°C (The surface tension of pure water at the same temperature is 72.75 dyne/cm). The purpose of their work was not only to verify that wastewater was properly treated but also to demonstrate the advantages of using Drop Volume method.

C. Critical Micelle Concentration (C.M.C.) Determination

There are many methods that can be used to determinate C.M.C. concentration, such as measuring electrical conductivity, light scattering, or refractive index versus concentration, etc. The concentration where these physical properties show a sharp change is the C.M.C. The C.M.C. is usually obtained from the intersection of two straight lines plotting the static surface tension values versus log concentration. In order to use this method, the surfactant solution must be extremely pure. Any traces of a second surface-active impurity may significantly shift C.M.C. to a lower value. Many previous investigators have suggested measuring the C.M.C. information using dynamic surface tension of surfactant solution at different concentrations, and plotting the surface tension versus log concentration (Figure15 and 16). The reason for using the dynamic surface tension is to obtain the C.M.C. information before a slowly adsorbing impurity can significantly contaminate the surface. One uses the dynamic surface tension value at relatively short times. The question is how long is a "relatively short time"? According to Mysels (1990), "it is only if two agreeing (C.M.C.) values are obtained at times differing by a reasonable factor (such as two) that one can be sure of having waited long

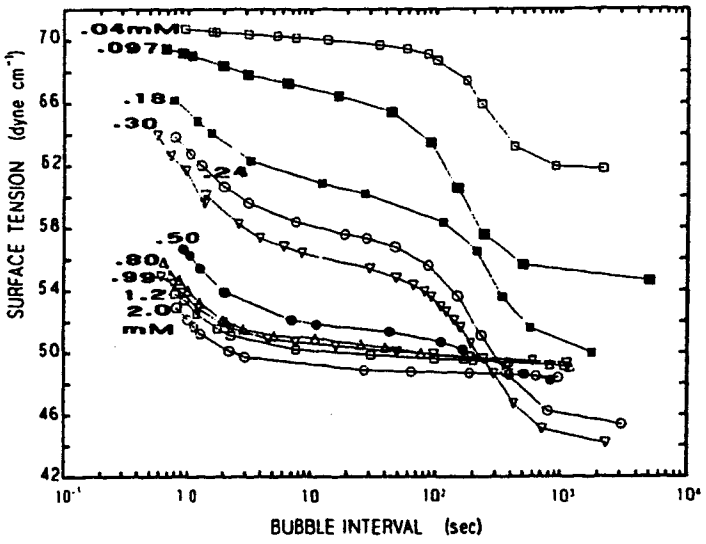

Figure 15. DST of surfactant under different concentrations (after Mysels, 1990).

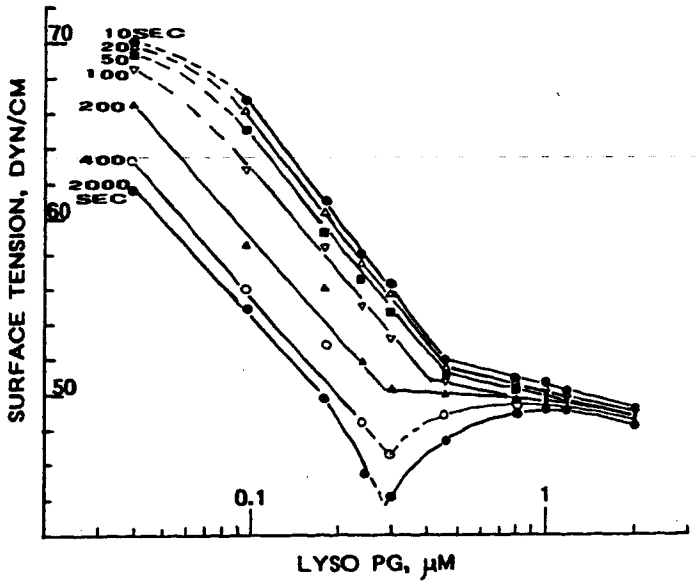

Figure 16. Replot of Figure 15 to show the variation of surface tension verses concentration at selected time (after Mysels, 1990).

enough". Therefore, in Figure 16, the C.M.C. identified by 10 to 50 sec. lines is a good choice. Unfortunately, this C.M.C. value is still not the C.M.C. of the pure surfactant and it is about 8% less than the real C.M.C. (Mysels, 1990). The above information suggests that the best way to obtain C.M.C. is to purify the surfactant and measure its static surface tension versus log concentration.

D). Surface-Active Impurities existence

Small impurities in a surfactant can cause major changes in the surface equilibrium if the impurities are strongly adsorbed. Because of the competitive adsorption of highly surface active contaminants, the equilibrium surface tension may be obtained only after hours or days (Figure 17). The contaminants in a surfactant solution may be metal ions (from water), CO_2 (from air), or homologs and long chain alcohol (from surfactant hydrolysis). Among all these, the influence of a surfactant alcohol on the surface tension is very significant (Gila'nyi, 1976). Extremely pure surfactants are required when studying adsorption kinetics or determining the C.M.C. concentrations. Therefore surfactant solution cleaning procedures are very important. Two problems exist: purification of dilution water and purification of the surfactant. Previous researchers have found that double distillated water is clean enough; however, purifying surfactants is more difficult. Mysels (1986) recommended that surfactants be purified by recrystalization, then passed twice through an adsorption column, such as Sep-Pak C_{18}, and foamed overnight.

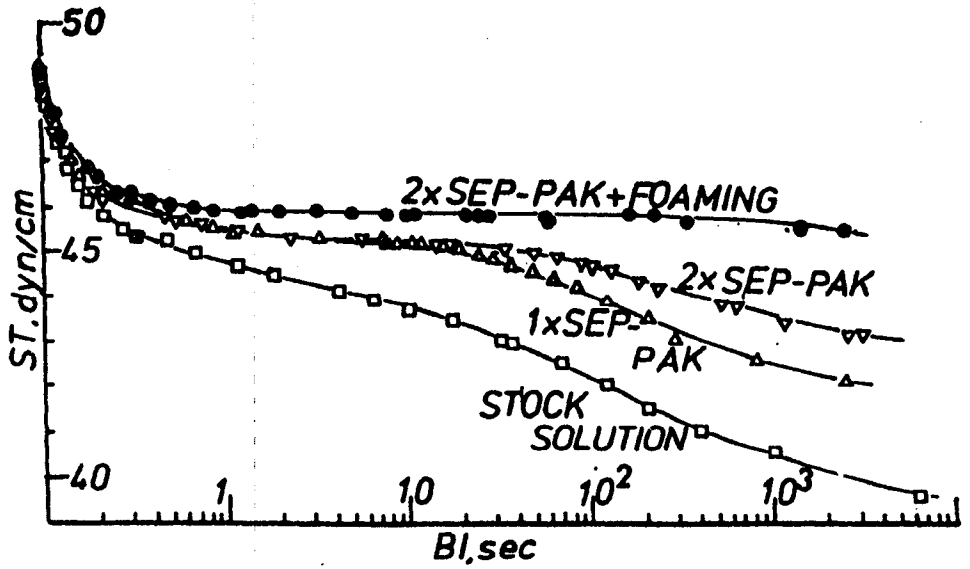

Figure 17. Surface tension of 6.2mM SDS at different stages of purification (after Mysels, 1986).

To determine purification efficiency, a criterion is needed. Previous researchers have used DST to measure the impurities. This is because following a rapid expansion of the surface, the pure components return to the equilibrium surface tension faster than a contaminated one.

The procedure to detect the presence of an impurity is the same as the technique for determining the C.M.C. (Figure 15 and 16). In the surface tension versus log concentration plot, the lines of long lifetime have a minimum, which indicates the presence of impurities. The impurity is present as free molecules or ions in the bulk surfactant solution (Mysel 1990). At low solution concentration, the impurity is much more surface active but slower adsorbing than the main component. Because of this phenomenon, the impurity will lower the surface tension below that of the pure surfactant. As the concentration increases, micelles appear in increasing amount and they begin to solubilize the impurity (the impurity is highly insoluble) or withdraw it from the surface (Mysel 1990). As a result, the rate of surface tension decrease declines until it reaches the minimum. The minimum indicates that enough micelles have formed to be in equilibrium with the maximum concentration of the impurity. After this point, the impurity is diluted by micelles, thus allowing the activity of monomer to rise. The surface tension gradually increases and approaches the surface tension of pure solution. However, it will never equal to the surface tension of pure solution.

VIII. Bubble Dynamics

Unlike cavities, which are holes in a liquid filled with air or vapor, bubbles form because of air or vapor trapped by a thin film (Brennon, 1995). Bubbles behave very much like liquid drops except their buoyancy and rise velocity are greater while their viscosity is smaller. Both bubbles and liquid drops commonly occur in many industrial and biological systems. In wastewater treatment applications, aeration with fine or coarse bubble diffusers is an important gas-liquid mass transfer process. Hence, it may be not only logical but also of practical value to understand bubble phenomena.

Bubble evolution involves three stages: 1) the growth of the bubble as it is formed prior to detachment from the orifice; 2) the acceleration of the bubble to its terminal velocity; and 3) the bubble rise at its constant terminal velocity.

(A). Mechanics of Bubble Formation and Detachment

There are many variables involved in bubble formation and detachment such as the orifice diameter, the gas flow rate, the gas inlet construction, and the physical properties of the gas and the liquid, etc. (Hughes 1955, Velentin 1967). Among all those variables, the gas flow rate is the most important factor for determining bubble formation and detachment.

The simplest mechanics of bubble formation is that in which the bubble is formed very slowly at the open end of a tube immersed vertically in a liquid. In this case volumetric gas-flow rate is very slow and the bubble will grow until its buoyancy exceeds the surface tension of liquid, when it detaches. This is a static bubbling region, which is defined by bubbles forming singly (singlet) at the orifice over a given time interval. In fact, this phenomenon is

basis of surface tension measuring technique (Maximum Bubble Pressure Method). At the low gas-flow rate, the bubble behavior is well predicted (including its steady-state terminal velocity which will be discussed later). At the low gas flow rate, the volume of the bubble remaines relatively constant, but the frequency of formation increases as the gas-flow rate is increased. Only in this flow regime can the bubble volume be calculated (or estimated) by dividing gas-flow rate by bubble frequency. However, the bubble diameter can be approximated by following equation (Velentin, 1967)

$$d_b = \left[\frac{6 d_0 \sigma (\cos\theta) f\left(\frac{d_0}{a}\right)}{\Delta\rho g} \right]^{1/3} \qquad (37)$$

where

d_b = Bubble diameter

d_0 = Orifice diameter

σ = Surface tension of liquid

$\Delta\rho$ = Density difference of liquid and gas

g = Acceleration due to gravity

$f\left(\frac{d_0}{a}\right)$ = Bubble shape factor. For spherical bubble this factor equals 1

a = Capillary constant. $\qquad a^2 = \frac{2\sigma}{\Delta\rho g}$

θ = Contact angle of water on the surface area around the orific. (Lin; 1993 and 1994). If this area is perfectly wetted by liquid, then $\theta = 0$.

From the above equation, it is clear that when surface tension decreases (e.g., in the presence of surface-active agent) the bubble size decreases. At high liquid viscosity, bubbles are prevented from breaking-up at the orifice so that the bubble grows larger than it would be in a low viscosity liquid.

As the gas-flow rate increases, the bubbles begin to from in pairs (doublet), which means two bubbles form simultaneously at a given time interval. As the flow rate continues to increase, the bubbles are formed in groups of three (triplets), four, or five in a single time period. The time period depends on the number of bubbles in the group and the gas flow rate. In this flow regime multiple bubble formation is not always reproducible. A condition that yields groups of four bubbles when repeated under the same condition that might yield groups of three bubbles. Regardless of the numbers of bubbles in a group, the volume of each bubble is approximately the same.

As gas-flow rate passes a critical value the formation of bubbles becomes irregular, at which time it is difficult to obtain bubble volume by simple calculation. Davidson and Harrison (1963) derived an equation for bubble volume as a function of gas flow-rate in this region. In this flow regime, the bubble frequency levels off at a constant value and that the bubble volume increases in proportion to the gas-flow rate. This phenomenon can be explained by the fact that at high flow rates bubble formation is hindered by the presence of preceding bubbles. This means that at critical flow rate the bubble frequency is so high that the present bubble touches the preceding bubble. As soon as flow rate passes the critical value the present bubble either swallows the preceding bubble or the bubble volume increase so that it

will rise faster (Davidson 1956, Leibson 1956, Velentin 1967). As a result, the bubbles become as large as necessary to accommodate the supplied quantity of gas so that two succeeding bubbles do not touch each other.

Although the bubble frequency in this region is constant, it is dependent upon orifice diameter, and varies from 15/sec. for a large diameter orifice to 45/sec for small capillaries (Velentin 1967). The critical gas-flow rate also varies with orifice diameter.

(B). The Acceleration of a Bubble to its Terminal Velocity

This is second stage of bubble evolution. The driving force of the acceleration is the net force between buoyant force, drag force and inertial force. Bubble formation and terminal velocity have been well-studied, but the bubble acceleration phenomenon is not well investigated. However, it is known that the motion of a bubble rising from an orifice is unsteady. Clift (1978) and Varty (1991) suggested the following governing equation:

$$\underset{\left[\begin{array}{l}\text{rate of change}\\ \text{of bubble momentum}\end{array}\right]}{\rho_b V \frac{dU_b}{dt}} = \underset{\left[\begin{array}{l}\text{buoyancy}\\ \text{force}\end{array}\right]}{\Delta\rho g V} - \underset{[\text{drag force}]}{F_D} \qquad (38)$$

Jiang *et al.* (1993) studied the variation of bubble rise velocity with distance above the nozzle for different bubble sizes. They found that

- The bubble rise velocity accelerates very rapidly as soon as it leaves the nozzle and then the acceleration decreases until a terminal velocity is reached. Therefore, the acceleration distance is very short. For example, for a bubble diameter in the range of 2 - 4 mm, the bubble reaches terminal velocity after about 40 mm of ascent (Shorter 1995).

- The smaller bubbles rise more slowly than the larger bubbles, and they reach their terminal velocities closer to the nozzle than larger bubbles.

(C). Bubble Rise Terminal Velocity

From fluid mechanics, the total force of the fluid on a solid sphere can be represented as follows: (Bird 1960):

$$[\text{total force}] = \underset{(1)}{[\text{gravitational force}]} + \underset{(2)}{[\text{buoyant force}]} + \underset{(3)}{[\text{form drag}]} + \underset{(4)}{[\text{friction drag}]}$$

Form drag results from a normal force while friction drag results from tangential force. Both drag forces are associated with fluid movement. Unlike drag forces, gravitational force and buoyant force are forces exerted even if the fluid is stationary. A sphere will accelerate only if the driving force (the sum of gravitational force and buoyant force) is not equal to zero. Its velocity and direction depends on the sum of driving force and drag force (It is initiated by motion). However, as soon as the net force is zero the sphere moves at constant maximum velocity (i.e. terminal velocity).

Terminal velocity can be calculated if the drag force is known. To determine drag force the flow regime or Reynold number (Re) must be known (Peavy *et al.* 1985, Bird *et al.* 1960). The following regime have been defined:

$Re < 0.1$	creeping flow
$Re < 1.0$	laminar flow
$1.0 < Re < 10^4$	transitional flow
$Re > 10^4$	turbulent flow

Case I. For $Re < 0.1$

$$\text{drag force} = 6\pi\mu r v_\infty \tag{39}$$

where

μ = Viscosity of fluid

r = Radius of sphere

v_∞ = Terminal velocity of sphere

This is known as Stoke's law and it is only valid for creeping flow around a solid sphere.

Case II. For all other flow regimes

$$\text{drag force} = C_D \cdot A_P \cdot \rho_W \cdot \frac{v_\infty^2}{2} \qquad (40)$$

where

A_P = Cross-sectional area of the bubble, perpendicular to the direction of movement

ρ_W = Density of water

v_∞ = Terminal velocity of the bubble

C_D = Coefficient of drag, which changes with different flow regimes.

$$C_D = \frac{24}{Re} \qquad \text{(laminar)} \qquad (41)$$

$$= \frac{24}{Re} + \frac{3}{Re^{1/2}} + 0.34 \qquad \text{(transitional)} \qquad (42)$$

$$= 0.4 \qquad \text{(turbulent)} \qquad (43)$$

Fluid particles (both liquid drops and gas bubbles) differ from solid particles in that internal circulation and particle deformation exist, which both affect drag and terminal velocity.

1. Internal Circulation of Bubbles

In the beginning of the Bubble Dynamics section, bubbles were defined as air trapped by a thin film. Therefore, the bubble surface is not formed by the relativity immovable lattice structure like a solid sphere, but is formed by two extensible layers of molecules. The inner layer is composed of gas molecules and outer layer is composed of molecules of the fluid in

which the bubble is immersed. Because of the extensible nature of the interface, the effect of external shearing forces produced by motion can be felt inside the bubble (Figure 18). Thus, by transferring the shear force across the interface the gas inside the bubble can be set in motion (Garner and Hammerton, 1954).

This internal circulation results in a significant change on bubble surface boundary condition as compared with solid sphere. Due to the no-slip theory, the boundary velocity of a solid particle is always zero. However, the interior circulation of a bubble induces a finite velocity on both sides of the bubble interface, and as result, the drag of a bubble moving in a liquid is smaller and the terminal velocity is higher than velocity of a solid sphere of the same size.

2. Bubble Size and Shape

In a dynamic situation the bubble interface will adopt or conform to the forces acting upon it. Under different flow conditions a bubble will assume different shapes. Bubble deformation has a significant influence on the drag coefficient as well as the terminal velocity. Barnhart (1969) correlated bubble shape with Reynold's number and found:

i) $Re < 300$

- Bubble diameter is very small ($d_p < 0.1$ cm).
- Bubble shape is spherical and behaves as a rigid sphere.
- Bubble rise is characterized as rectilinear or helical with a constant terminal velocity.

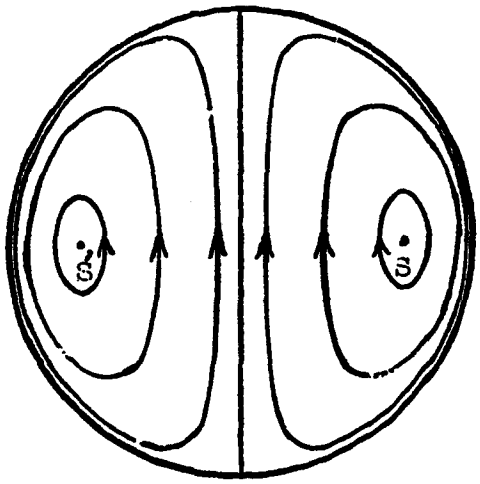

Figure 18. Cross section of the internal flow pattern of a bubble (after Langston, 1964). Note that both S , and S′ are the stagnation points.

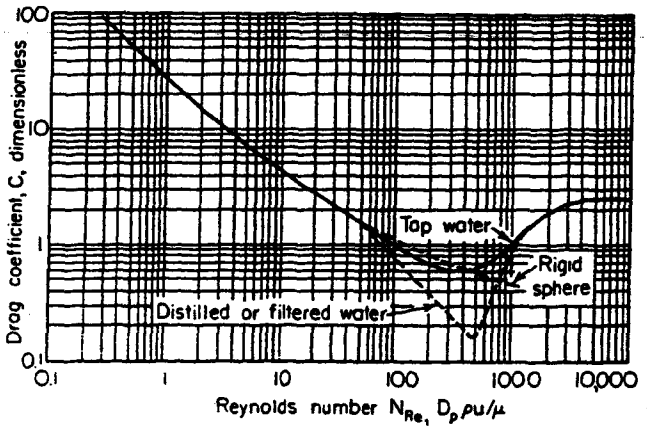

Figure 19. Drag coefficient for air bubbles rising in water at room temperature (after Haberman and Morton, 1954).

ii) $300 < Re < 4000$

- Diameter is medium size ($0.2\ cm < d_p < 1.5\ cm$).
- Bubble shape is ellipsoidal or oblate spheroid.
- Bubble rise is characterized as a rectilinear, rocking motion.

iii) $Re > 4000$

- Bubble are spherical caps.
- Bubble terminal velocity is constant with a constant drag coefficient of 2.6.
- Bubble rise is characterized as rectilinear.

Haberman and Morton (1954) calculated drag coefficients for air bubbles in water which are shown in Figure 19.

3. Surfactant Effects

Earlier it was noted internal gas circulation can reduce the drag coefficient below that of a solid sphere. However, it has been found by numerous investigators (Haberman 1954; Levich 1962; Garner 1954; Rodrigue 1996) that only a small concentration of surface-active agents will radically change bubble motion in the spherical and ellipsoidal regimes by reducing internal circulation. The reason that the surfactant reduces internal circular motion is that surfactants have a strong tendency to adsorb on the bubble interface. Those adsorbed surfactant molecules sweep around the front of the bubble to the rear and accumulate at the bottom of the bubble. The resultant distribution of surfactant concentration then leads to a

surface tension gradient which opposes the flow along the interface, and even causes it to cease if the surface tension gradient is sufficiently large (Marangoni Effect). At high surfactant concentration, the surface tension gradient disappears and the interface is mobile again (Andrews, 1988). Therefore, the surfactant effect is less pronounced for more concentrated surfactant solutions.

Rodrigue *et al.* (1996) concluded that at small bubble volumes the effect of surfactant on internal circulation is negligible. The reason for this is that small volume bubbles behave as rigid spheres and obey Stokes law. Therefore the addition of impurities to the system does not contribute to a further reduction in the bubble velocity. Haberman and Morton (1953) also found that trace impurities have negligible effect on both small and large bubbles (as shown in Figure 20). Table 2 summaries the discussion in Section (A), (B), and (C).

IX. Aeration

A. Mass Transfer

Mass Transfer occurs when a component in a mixture migrates in the same phase or from phase to phase because of a concentration gradient between two points. There are two models for mass transfer - molecular diffusion and mass transfer. In many cases the models are equivalent. The diffusion model is more fundamental and is appropriate when concentrations are measured, or when they are a function of both position and time. This model is often used in chemistry. In contrast, the mass transfer model is simpler and

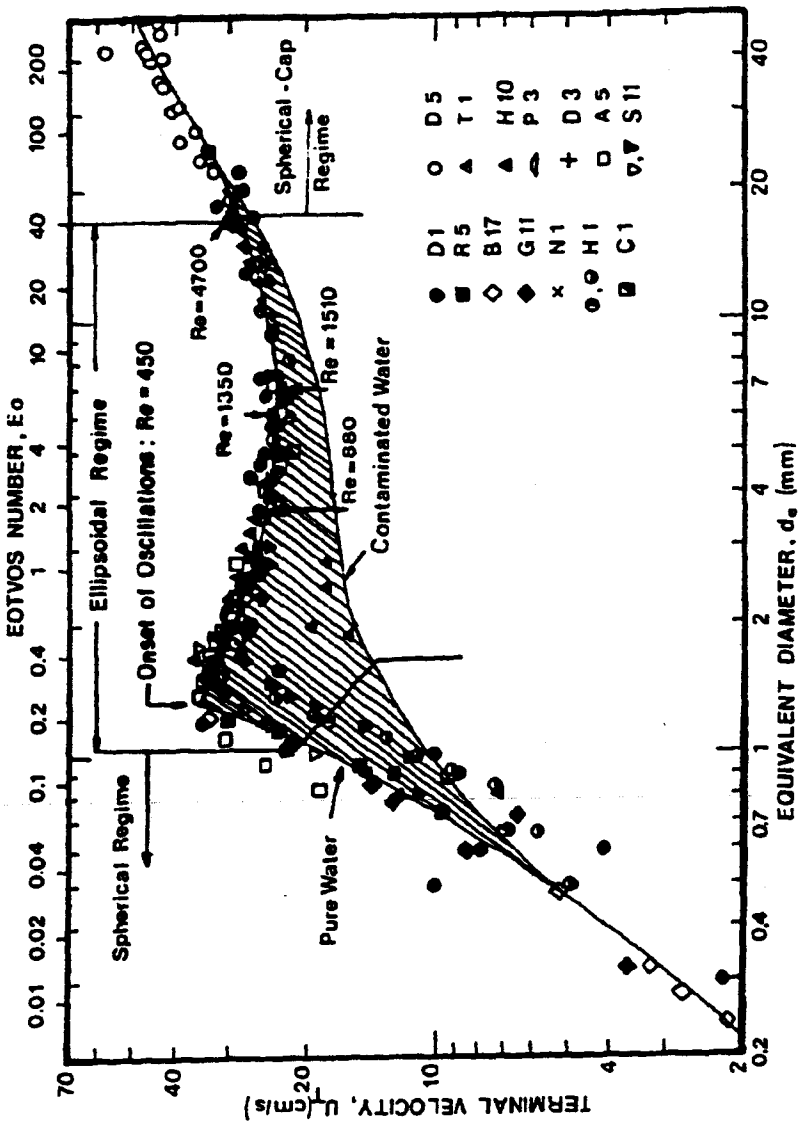

Figure 20. Terminal velocity of air bubbles in water at 20 °C (after Gaudin, 1957).

Table 2. Summary of Bubble Dynamics

Bubble formation and detachment (buoyancy equals surface tension)	Static bubbling region (low gas flow rate): 1) Bubble volume is constant but bubble frequency is increased as flow rate is increased. 2) Bubble diameter is independent of gas flow rate. However, it is a function of orifice diameter, surface tension and viscosity. 3) Bubble volume can be calculated by dividing gas-flow rate with bubble frequency. 4) Surface-active agents will decrease bubble size.
	Transition bubbling region : 1) Bubbles formed in groups of two, three, etc. at a given time interval. 2) The volume of the bubbles are the same regardless the number of bubbles in a group.
	Chain bubbling region (high gas flow rate): 1) Bubble frequency is constant but bubble volume increases in proportion to the gas-flow rate. 2) The value of bubble frequency depends on orifice size. 3) The critical gas-flow rate varies with orifice size, liquid properties and liquid surface tension.
Bubble acceleration	1) The acceleration distance from the nozzle is very short 2) The smaller bubbles reach their maximum velocities closer to the nozzle than larger bubbles. 3) The acceleration phase is very short and it is thought that contaminants do not have time to accumulate in order to influence velocity significantly.
Steady-State Bubble Rising (driving force equals drag force)	1) Because of the nature of internal circulation, the drag of bubbles moving in liquid is smaller and terminal velocity is higher than solid sphere. 2) Bubble size and shape depend on Reynold's number: $Re < 300$ Bubble diameter is less than 0.1 cm with spherical shape. $300 < Re < 4000$ Bubble diameter is in between of 0.2 and 1.5 cm. Bubble shape is ellipsoidal or oblate spheroid. $Re > 4000$ Bubble diameter is greater than 1.5 cm and are shaped spherical caps 3) The presence of surfactant decreases the bubble rise velocity. 4) The surfactant effect is less pronounced for the more concentrated surfactant solution. 5) For very small and very large bubbles the effect of surfactant is negligible.

more approximate, and is especially useful when only average concentrations are known. Therefore, the mass transfer model is used more often in engineering. Thus, the choice between the mass transfer and diffusion models is often a question of preference rather than precision.

Molecular diffusion occurs in stagnant fluids or fluids in laminar flow. The rate of molecular diffusion is very slow. As a result of this slow diffusion rate, a large concentration change occurs across two points. The flux caused by molecular diffusion can be written as Fick's law:

$$J^*_{AZ} = - D_{AB} \frac{dC_A}{dZ} \qquad (44)$$

where

J^*_{AZ} = The molar flux of component A in the Z direction due to molecular diffusion; $\left[Kg \cdot mol\, A \Big/ Sec \cdot m^2 \right]$

D_{AB} = The molecular diffusivity of the molecule. A in B; $\left[m^2 \Big/ Sec \right]$

C_A = The concentration of A; $\left[Kg \cdot mol\, A \Big/ m^3 \right]$

The concentration profile can be predicted by integrating the following equation:

$$\frac{\partial C}{\partial t} = D\frac{\partial^2 C}{\partial Z^2} \qquad (45)$$

where

$\frac{\partial C}{\partial t}$ = Rate of concentration changing

$\frac{\partial C}{\partial t} = 0$ steady state diffusion

$\frac{\partial C}{\partial t} \neq 0$ unsteady state diffusion

The mass transfer model is also called the convective mass transfer model. For a fluid to be in convective flow usually requires the fluid to be flowing through another immiscible fluid or by a solid surface.

Case I.

When a fluid is in turbulent flow and is flowing past a solid surface, large eddies move rapidly in a random fashion. This phenomenon forces the solutes in the eddies to move rapidly from one part of the fluid to another, which, transfers relatively large amounts of solute. This turbulent diffusion or eddy transfer is quite fast in comparison to molecular diffusion. The flux caused by this convection can be written as follows:

$$J_A^* = -(D_{AB} + \varepsilon_M) + \frac{dC_A}{dZ} \qquad (46)$$

where

J_A^* = The flux of A; $\left[\text{Kg}\cdot\text{mol A}/\text{Sec}\cdot\text{m}^2\right]$

ε_M = The eddy diffusivity; $\left[\text{m}^2/\text{Sec}\right]$

(The value of ε_M is a variable. It is near zero at the surface and increases as the distance from the surface increases).

Integrating equation (46) between point 1 and 2 :

$$J_{A1}^* = \frac{D_{AB}+\varepsilon_M}{Z_2-Z_1}(C_{A1}-C_{A2}) \tag{47}$$

If J_{A1}^* is replaced with N; the following equation results:

$$N = k_c(C_{A1}-C_{A2}) \tag{48}$$

and

$$k_c = \frac{D_{AB}+\varepsilon_M}{Z_2-Z_1} \tag{49}$$

where

N, J_{A1}^* = The flux of A from the surface A1

k_c = Mass-transfer coefficient; $\left[\text{m}/\text{Sec}\right]$

C_{A1}, C_{A2} = Concentration of A at point 1 and 2, respectively; $\left[\text{Kg} \cdot \text{mol A}/\text{m}^3\right]$

Z_1, Z_2 = The distance of the transfer, which is often unknown.

There are many definitions of the mass transfer coefficient (Cussler, 1984). This arises because the concentration (driving force) can be measured using so many different units such as partial pressure, mole, mass fractions, molarity, etc. The mass transfer coefficient can be found experimently. Alternatively, we can estimate the mass transfer coefficient using published correlations.

The mass transfer rate of a convective flow across a solid with a fixed area can be derived by performing the following mass balance :

$$\frac{dC}{dt} = k_c \cdot \frac{A}{V} \cdot (C_1 - C_2) \tag{50}$$

$$= k_c a \cdot (C_1 - C_2) \tag{51}$$

where

$\frac{dC}{dt}$ = The rate of concentration change

A = The interfacial area normal to mass transfer

V = Liquid volume

C_1, C_2 = Concentration at points 1 and 2, respectively.

$a\left(=\frac{A}{V}\right)$ = Volumetric interfacial area

The difficulty in determining $\frac{A}{V}$ is overcome by lumping it with mass transfer coefficient and using $k_c a$ as one parameter.

There are three mass transfer regions (Figure 21):

- Sublayer region. It is a very thin film near the surface. Most of the mass transfer occurs as molecular diffusion.
- Transition or Buffer region. There are some eddies present and the mass transfer is a sum of turbulent and molecular diffusion.
- Turbulent region. Most of the transfer is in convective mass transfer mode. The concentration difference between two points is very small since the eddies tend to keep the fluid concentration uniform.

Case II.

The mass transfer of solute A from one fluid phase (Example: water) by convection and then through a second fluid phase (Example: liquid coated on solid particles in a packed

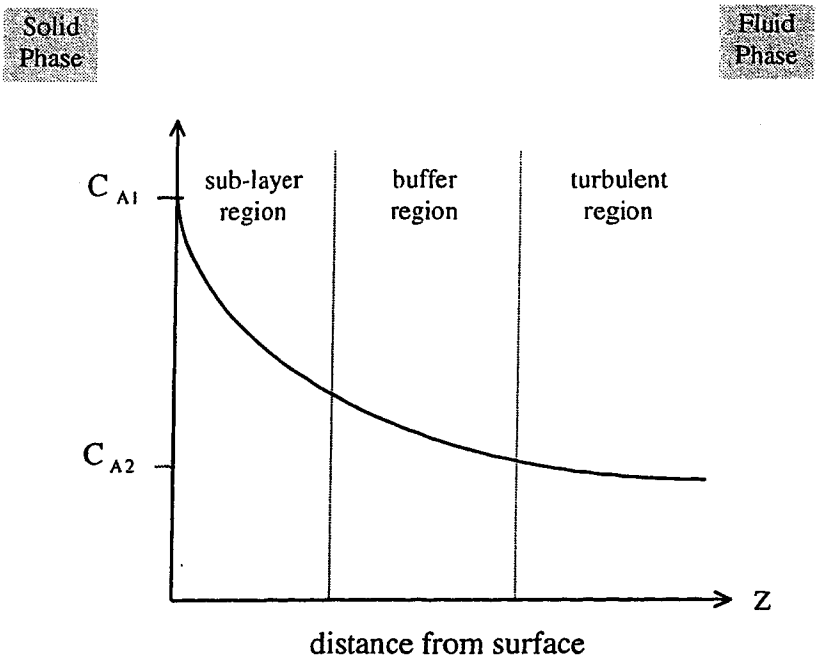

Figure 21. Three mass transfer regions.

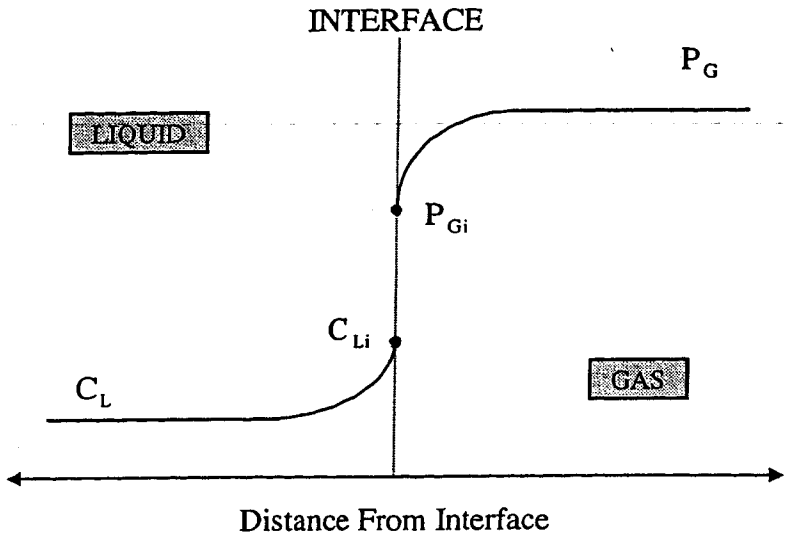

Figure 22. Concentration profile of two-phase mass transfer.

bed, liquid drops, or bubbles) by convection. (Note: These two phases are essentially immiscible.)

To analyze this kind of diffusion problem requires assuming that changes in concentration are limited to a small part of the system's volume near its boundaries. This requires that the fluids on both sides of interface be well mixed except near the interface. A characteristic of this group of mass transfer problems is that the interfacial area between the phases is usually not well defined, and a concentration gradient will exist in each phase to initial mass transfer. At the interface, equilibrium usually does not exist in the thin film (Figure 22).

We can write the flux on both phases as follows:

$$N_L = k_L (C_{Li} - C_L) \tag{52}$$

and

$$N_G = k_G (P_G - P_{Gi}) \tag{53}$$

where

N_L = The flux on the liquid side,

N_G = The flux on the gas side,

k_L = Liquid mass transfer coefficient, and

k_G = Gas mass transfer coefficient

Although both k_L and k_G can be estimated by experimental correlation, both C_{Li} and C_{Gi} are very difficult to measure. In order to solve this problem, the overall mass transfer coefficient and driving force are derived based on two assumptions: (1) the flux on both sides of interface is equal, and (2) the equilibrium relationship across the interface between pressure and concentration (in dilute system) can be expressed by Henry's Law, as follows:

$$P_{Li} = H \cdot C_{Li} \tag{54}$$

where

H = Henry's law coefficient (a type of partition coefficient); $\left[cm^3 \cdot atm / mol \right]$

P_{Li} = Liquid side of interfacial pressure; [atm]

C_{Li} = Liquid side of interfacial concentration; $\left[mol / cm^3 \right]$

We now write the flux across an interface:

$$N = K_L \left(C^* - C_L \right) = K_G \left(P_G - P^* \right) \tag{55}$$

where

K_L = Overall liquid side mass transfer coefficient

$$K_L = \frac{1}{\frac{1}{k_L} + \frac{1}{k_G \cdot H}}$$

K_G = Overall gas side mass transfer coefficient

$$K_G = \frac{1}{\frac{1}{k_G} + \frac{H}{k_L}}$$

C^* = Hypothetical liquid concentration that would be in equilibrium with the bulk gas.

P^* = Hypothetical gas pressure that would be in equilibrium with the bulk liquid.

When the Henry's coefficient is large, the above equation becomes:

$$N = K_L (C^* - C_L) \qquad (56)$$

The physical meaning of equations (55) and (56) is that the overall mass transfer resistance across an interface is the sum of the resistance in each phase. However, when mass transfer rate is much less in the liquid phase than in the gas phase (i.e. the Henry's coefficient is large), the overall mass transfer resistance is approximately equal to the

liquid side resistance. In this case the liquid side mass transfer resistance will be the rate limiting step.

There are several simple physical theories providing the relationship between the mass transfer coefficient and the diffusivity when the fluid is under forced convection:

Two Film Theory

Lewis and Whitman (1924) are credited with the simplest theory for interfacial mass transfer. This theory assumes that a stagnant thin film exists near every interface despite the turbulent mixing in the bulk phase. The solute near the film diffuses across this idealized hypothetical film slowly in steady state mode (Figure 23).

From the previous discussion, the steady-state flux across this thin film can be written and calculated using both diffusion and mass transfer coefficients. By equating both fluxes we obtain the result, which relates K and D; as follows:

$$K = \frac{D}{l} \qquad (57)$$

where

K = Mass transfer coefficient,

D = Molecular diffusivity, and

l = Thickness of film (unknown)

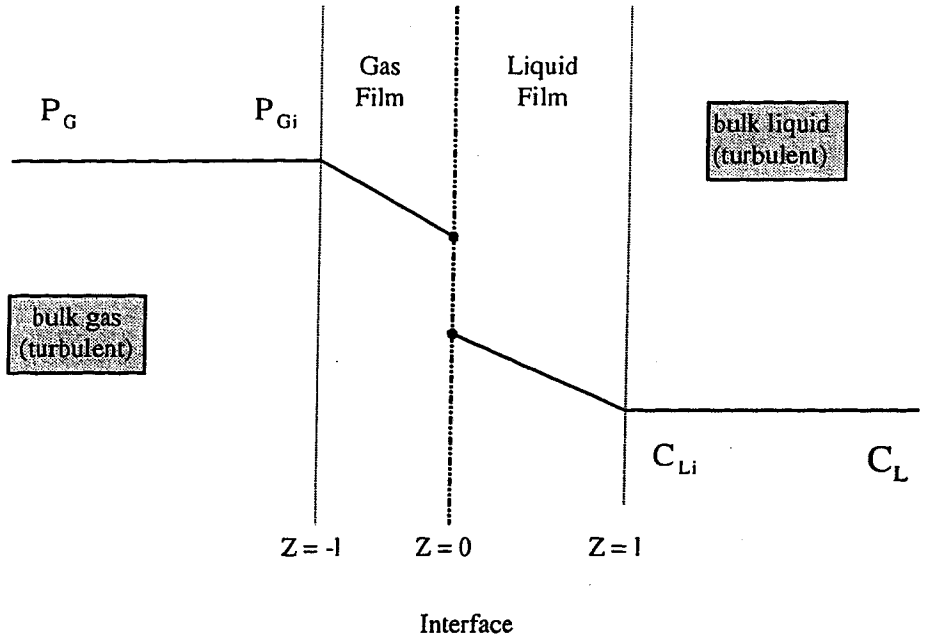

Figure 23. Concentration profile of two-film theory.

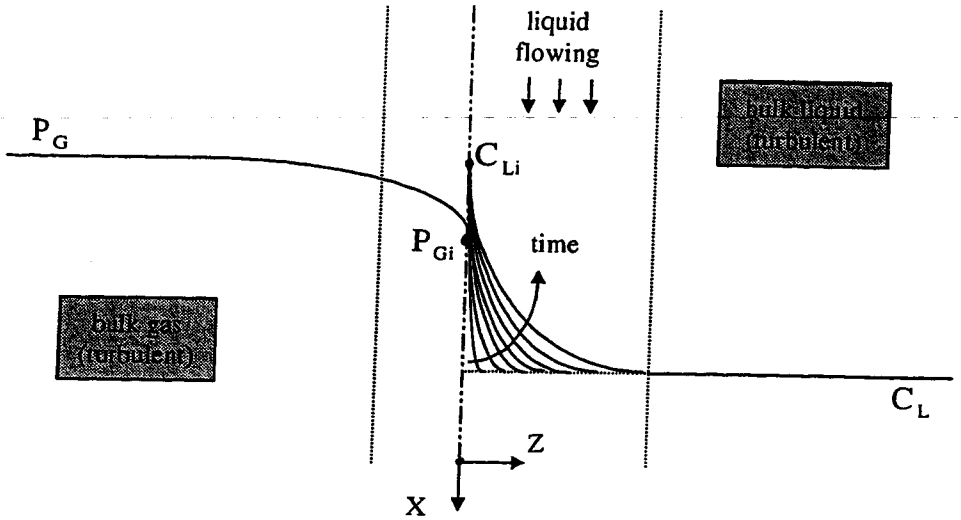

Figure 24. Concentration profile of penertration theory.

This model predicts that the mass transfer coefficient is directly proportional to the diffusion coefficient $(K \propto D)$. The model does not provide sufficient information to predict K from D. The film thickness is almost never known without measuring K and D. This raises the question of what value is this theory?

This theory is valuable for two reasons:

- It provides simple physical insight about how resistance to mass transfer might occur near an interface, and
- It often predicts very well the change of K due to chemical reaction (Cussler, 1984).

Penetration Theory

The main differences between two-film theory and Penetration Theory are (Figure 24):

1) Penetration Theory assumes the liquid film is very thick. The diffusion across this thick film is similar to diffusion across semi-infinite slab. Unsteady state diffusion exists;
2) Penetration Theory also assumes this thick film is continuously refreshed by flow.

Under these two assumptions, penetration theory relates the mass transfer coefficient to diffusion coefficient with a new parameter--contact time (or exposure time).

$$K = 2\sqrt{\frac{D}{\pi t_c}} \qquad (58)$$

where

$t_c \quad (=\frac{L}{v_{max}}) \quad =$ Contact time

L = The total length the fluid has traveled in x-direction; (Figure 24).

v_{max} = Maximum velocity of flowing liquid in liquid film.

By examining equation (58), penetration theory indicates $K \propto D^{1/2}$. This theory provides a better physical description of mass transfer at interface than two-film theory. However, it also creates a new unknown parameter--contact time. Just like the film thickness l in two-film theory, the contact time, t_c, may not be known *a priori.* This is especially in complicated situations.

Surface-Renewal Theory

Penetration theory is part of surface-renewal theory. It is derived in the way as penetration theory but under a different physical model (Dankwerts, 1951). The surface-renewal model assumes there are two regions near interface. In the interfacial region, mass transfer occurs by means of the penetration theory. However, the liquid is in turbulent motion and eddies tend to continually expose fresh surface to the gas by sweeping away liquid film which is in contact with the gas for varying lengths of time and mixing it into the bulk region (Figure 25).

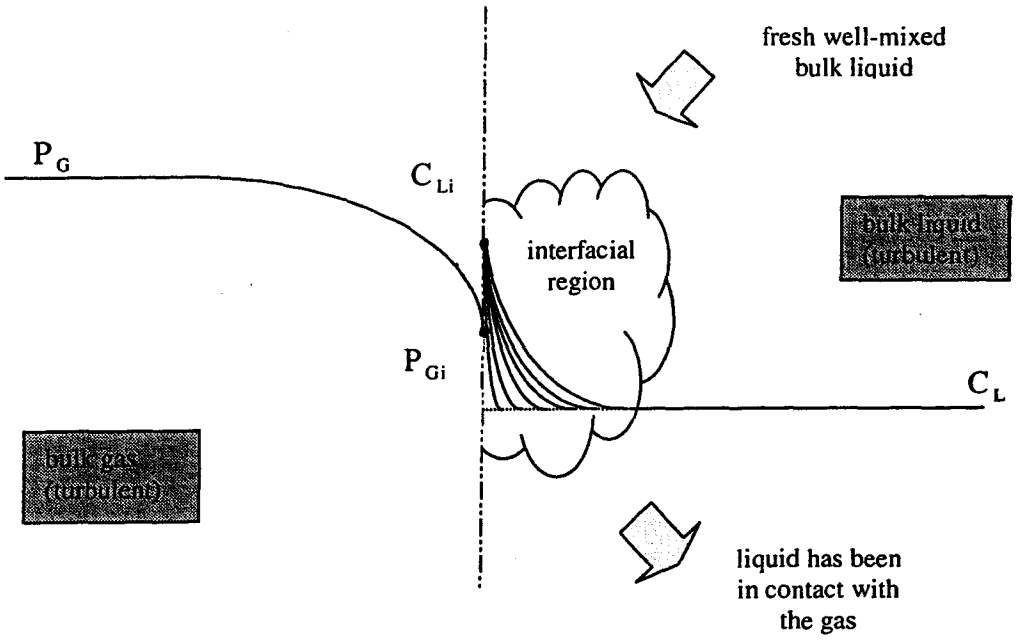

Figure 25. Concentration profile of surface-renewal theory.

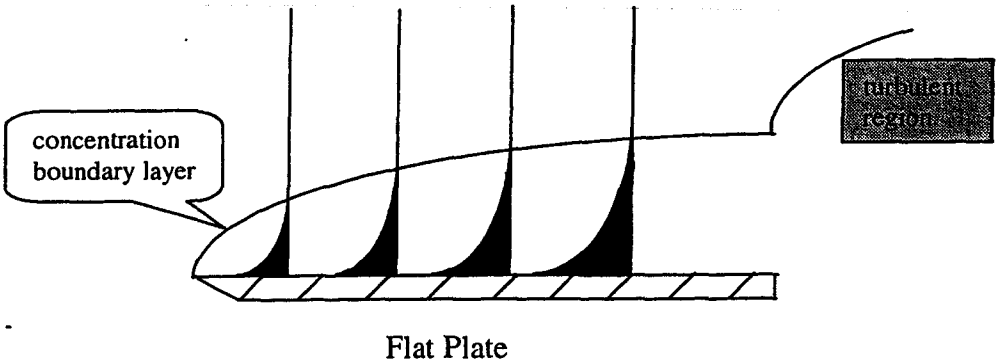

Figure 26. Concentration profile of boundary layer theory.

The mathematical expression of this theory is:

$$K = \sqrt{\frac{D}{t}} \tag{59}$$

or

$$K = \sqrt{D \cdot r} \tag{60}$$

where

t = An average residence time for an element in the interfacial region.

r $(=\frac{1}{t})$ = The frequency of a surface element renewal in unit time.

As in the penetration theory, surface-renewal theory also predicts $K \propto D^{1/2}$, and the theory also introduces a new unknown variable, r. However, the value of the surface-renewal theory is that it extends theory to more realistic conditions. None of above theories are completely satisfactory because each introduces an unknown parameter.

Boundary Layer Theory

Boundary layer theory provides more complete and specific descriptions of mass transfer near the interface (boundary). The theory applies to an exact physical situation of a specific case instead of a model that tries to explain many cases. Although the mathematical calculations are long, it may give the best results for a specific situation.

The most common physical situation used to demonstrate boundary layer theory is fluid flowing across a flat plate (Figure 26). The flow is disrupted by the drag caused by the plate, which creates a velocity boundary layer near the plate surface. The solute dissolves from the plate and creates a concentration gradient in the boundary layer. The mathematical derivation of this case can be found in any mass transfer book. The significant result is that boundary layer theory predicts that $K \propto D^{2/3}$ which is a value midway between the $K \propto D$ of two film theory and $K \propto D^{1/2}$ of penetration theory. This prediction has been experimentally verified for laminar flow and turbulent flow.

B. Oxygen Transfer from Air Bubbles in Water

The most common application of gas transfer is the field of wastewater treatment is in the transfer of oxygen in the biological treatment of wastewater. Because of the low solubility of oxygen, an aeration device is needed to transfer sufficient oxygen to meet the requirements of aerobic waste treatment. In wastewater treatment plants, aeration is most frequently accomplished using air dispersed by fine pore diffusers at depths from 15 to 25 feet. These bubbles serve to provide dissolved oxygen for the maintenance of biological activity as well as to furnish turbulent agitation for the suspension of the organic sludge contained in the aeration tank.

1. Oxygen Transfer Model

The oxygen transfer process can be considered to occur in three steps (Mancy and Okun, 1965):

i. Oxygen molecules are initially transported to the gas-liquid interface. This transport rate is very rapid.

ii. Oxygen molecules pass through the finite thickness of liquid film by molecular diffusion. There are many diffusion models for describing this transfer phase such as two-film theory, penetration theory and surface renewal theory.

iii. Oxygen molecules are mixed in the body of liquid by diffusion and convection.

The oxygen transfer rate is almost always controlled by second step, which is the rate of molecular diffusion. In a quiescent liquid, an undisturbed liquid film exists so that the two-film theory can be used to model oxygen transfer. However, in real situations the laminar flow films may never truly exist. At increased turbulence levels, the surface film is disrupted and liquid surface is constantly replenished by bulk liquid. Therefore, surface renewal theory is the most correct choice for describing oxygen transfer (Eckenfeller and Ford, 1968), but because of the difficulty in identifying the unknown parameter, r, and its limited additional ability, two film theory is most often used. Many of the problems with currently accepted method for estimating oxygen transfer result because of the restrictive assumptions in two film theory.

The basic model for oxygen transfer in a dispersed gas-liquid system is given by

$$\frac{dC}{dt} = \hat{k}_L a (C_S - C) \qquad (61)$$

where

$\frac{dC}{dt}$ = The rate of oxygen concentration changes in aeration basin

$\hat{k}_L$ = Overall volumetric mass transfer coefficient in clean water

C_s = Dissolved oxygen saturation concentration

C = Dissolved oxygen concentration

However, Equation (61) applies only to a particular point in an oxygen transfer system. In general, the total rate of oxygen transfer is of interest. Conventionally, the total oxygen transfer rate is expressed in terms of an apparent average volumetric mass transfer coefficient and oxygen saturation concentration in infinite time

$$OTR = K_L a (C^*_\infty - C) \cdot V \qquad (62)$$

where

OTR = Oxygen Transfer Rate occurring in the liquid volume V; $[Mt^{-1}]$

$K_L a$ = Apparent spatial average volumetric mass transfer coefficient in clean water; $[t^{-1}]$

C^*_∞ = Average dissolved oxygen saturation concentration approached at infinite aeration time; $[ML^{-1}]$

C = Average dissolved oxygen concentration; $[ML^{-1}]$

V = Liquid Volume of the aeration system; $[L^{-1}]$.

In diffused aeration, air bubbles are formed at an orifice. They break off, rise through the liquid, and finally burst at the liquid surface. Oxygen transfer occurs during each phase of the bubble's life:

i) Bubble formation. As the bubble emerges from the surface, the absorption rate is very high. The air-water interface is continuously replenished during bubble formation which results in a high surface renewal rate until the bubbles reache full growth. It is estimated 20-25% of the total transfer occurs during bubble formation (Barnhart, 1969).

ii) Bubble ascent. The amount of oxygen transferred during ascent depends upon the mean surface area of all the bubbles in ascent, the bubble retention time, and the concentration gradient. The effective film thickness and the rate of surface renewal are thought to vary with the bubble velocity relative to the liquid velocity. Furthermore, in aeration tanks where the liquid is in motion, the transfer process is complicated by eddy currents which result in irregular bubble movement. Nevertheless, when the bubble reaches its terminal velocity, the transfer rate is constant as it rises through the liquid.

- Bubble size and velocity

Bubble size has profound influences on oxygen transfer rate (Barnhart, 1966) which are shown in Figure 27. The influences can be subdivided into total interfacial area, terminal velocity, and internal circulation. From the oxygen transfer model, it is clear that the smallest bubble provides largest total interfacial area and the greatest transfer rate. Also, from bubble dynamics, small bubbles act as solid spheres so that they rise slowly in the bubble column, which provides longer contact time for transfer. However, if the bubble is too small the internal circulation is essentially absent due to the interfacial monolayer on the bubble surface, which acts as a viscous membrane. This internal circulation is necessary for enhanced mass transfer within the bubbles. As a result, very small bubbles actually hinder the specific rate of oxygen transfer. For the highest transfer efficiency the bubbles should be of such a size that when they reach the surface they contain little or no oxygen.

If the bubbles are too large, they rise to surface so quickly that there is insufficient time for oxygen transfer to take place. If they are too small they may have lower transfer coefficients. For these reasons, Barnhart (1969) proposed that maximum mass transfer occurs at a bubble diameter of 2.2 mm. Motarjemi and Jameson (1978) also confirmed that K_L reaches a maximum when the bubble diameter is about 2 mm. Moreover, they also concluded that that a bubble will lose internal circulation if the diameter of bubble is less than 0.15 mm. This is approximately one-half the diameter Hammerton and Garner (1953) proposed. They found that bubbles circulate freely at diameters greater than 0.3 mm.

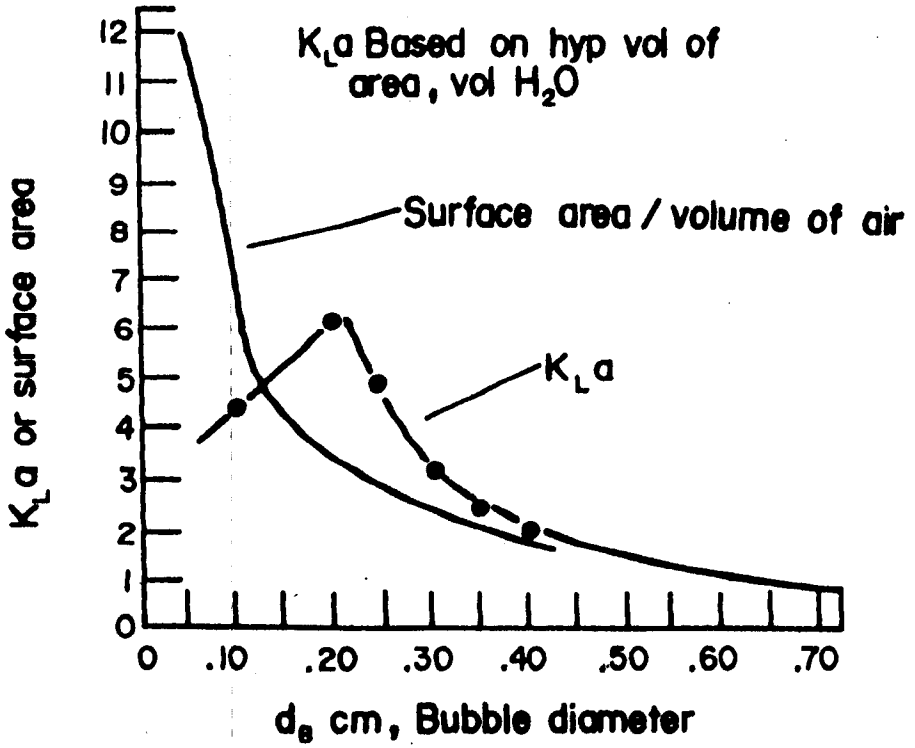

Figure 27. Effect of bubble size on mass transfer (after Barnhart, 1966).

- Air flow rate

  The per cent of oxygen adsorbed per foot of water column height decreases with increasing air flow rate. The reduction in the oxygen absorption rate is due to the fact that larger bubbles are generated at greater frequencies for the higher air flow rates, thus resulting in a larger number of bubbles over the vertical of water column. The entrainment of liquid in the wakes of the ascending bubbles creates an upward liquid motion, or so-called "Chimney" effect. This effect increases in intensity with increasing air flow-rate and results in a reduction of the lateral diffusion of dissolved oxygen. The reduction will be less pronounced when the number of orifices per unit of floor area increases.

iii) Bubble burst. Oxygen transfer takes place at the surface of the aeration basin as oxygen enriched bubbles burst. The disturbance of the free water surface by the bursting bubble is responsible for this re-aeration from the surface. However, this phase of oxygen transfer is very small (Carver, 1955; Pasveer, 1956; and Downing, 1960).

2. Factors Affecting OTR in Aeration System

The volumetric mass transfer coefficient $K_L a$ is an important design parameter as well as an indication of the aeration system performance. Its value can be obtained by a clean water test (discussed later) under standard conditions (20°C, 760 mm Hg barometric pressure and zero dissolved oxygen concentration). However, the $K_L a$ for an aeration

system operating in a wastewater treatment plant is very much different from the $K_L a$ obtained from a clean water test because there are many factors affecting mass transfer. Therefore, before this $K_L a$ can be used for design purposes, it generally requires "correction" for the influence of those factors. The most important factors are water temperature (θ factor), water characteristics (α and β factors) and surfactants.

i) Effect of temperature (Theta factor)

The influence of temperature on the oxygen transfer coefficient is defined in Equation (4). The value of θ reported in the literature range from 1.008 to 1.047, and is influenced by geometry, turbulence level, and type of aeration device (Stenstrom and Gilbert, 1981). The wide diversity of reported θ values suggests that no single temperature correction technique can be applied to all methods. To minimize correction error it is desirable to perform the clean water test at temperatures as close as possible to the design application temperature. The clean water test standard recommends that 1.024 be used for θ, unless experimental data for the particular aeration system indicate conclusively that the value is significantly different from 1.024.

ii) Effect of water characteristics (Alpha and Beta factors)

Alpha factors The α factor is defined in Equation (2). It is very difficult to accurately determine alpha factor (Gilbert, 1979) because the α factor varies with many process conditions including wastewater quality, intensity of mixing or turbulence, suspended

solids concentration, method of aeration, tank geometric scales, bubble size, degree of treatment, etc. Above all the cited effects, the effect of aeration method is particularly important. For a detail review of the effects of alpha factor, reference to Stenstrom and Gilbert's review paper (1981) is highly recommended.

The alpha factor ranges from approximately 0.2 to greater than 1.0 (Doyle and Boyle, 1985). In selecting an α factor for design purpose, one should remember that a possible range of α values should be considered in estimating the transfer rate under process conditions, and not just a single value (Doyle and Boyle, 1985; Huang and Stenstrom, 1985).

The α factor cannot be measured using small lab devices and scaled up to large devices. Ideally, the α factor would be measured by conducting full-scale oxygen transfer tests with clean water and process water, but normally this is impractical. However, the general conditions for α factor testing should resemble the condition for the proposed full system as closely as possible.

A goal of developing a standard α factor testing procedure is to make α dependent only on wastewater properties and not on basin geometry or aeration type. The British have been adding 5 mg/L anionic surfactant to test waters in order to simulate the contaminants in wastewater and to minimize the effects of trace contaminants in tap water. The

resulting values from this procedure appear to be less dependent on aerator type and thus result in reduction of design error caused by improper alpha factor testing.

Beta factors.

The β factor was defined in Equation(3). Although the β factor is more consistent than those reported α factor, it is still affected by a large number of variables and process conditions such as suspended solids and dissolved solids, etc. Above all, it is certain that high dissolved solids will significantly reduce the saturation dissolved oxygen concentration. The beta factor can be measured using the Winkler method or calculated from a total dissolved solids measurement (Bass and Shell, 1977).

iii) Effect of Surface-Active Agents

Traces of surface-active contaminants may have a profound effect on the behavior of bubbles. Even though the concentration of impurities may be so small that there is no measurable change in the bulk fluid properties, a contaminant may cause extend resistance to transfer and may reduce internal circulation. Moreover, accounting for the influence is complicated by the fact that both the amount and nature of surface-active agents are important, and often unknown in wastewater. Surface-active agents can affect oxygen transfer in two ways, changing the interfacial area (a) and the liquid mass transfer coefficient (K_L).

Changing the interfacial area (a)

The surface-active agents reduce liquid surface tension and the size of primary bubbles, which results in increasing interfacial area for oxygen transfer. Moreover, they also may prevent bubbles from coalescing (Zlokarnik, 1978; Keital and Onken, 1982; Drogaris *et al.*, 1983; Gurol *et al.*, 1985). However, researchers also found that coalescence is totally inhibited up to a certain concentration level (concept of total coalescence inhibition). As the concentration of surface-active agents increases beyond the critical concentration, the bubbles coalescence depends on gas flow-rate or contact time between two bubbles. High gas flow rate promotes bubble coalescence. If a bubble's contact time is longer than its coalescence time, the bubble tends to coalesce.

Changing the liquid mass transfer coefficient (K_L)

Two theories are used to explain the effect of surface-active agents on the K_L : the barrier effect (or Molecular effect) and the hydrodynamic effect. In the barrier theory, the presence of a surface-active agent at the bubble surface creates additional resistance to oxygen transfer (Springer and Pigford, 1970). In addition, sometimes, the interaction of surface contaminants with the species being transferred also reduces the mass transfer. However, in comparison with hydrodynamic effects, the barrier effect is insignificant (Llorens *et al.*, 1988).

The hydrodynamic effect includes two opposing phenomena. As mentioned earlier, bubbles have moving interfaces and a strong internal gas circulation. Surface-active contaminants have a strong tendency to adsorb on the bubble-water interface that decreases the mobility of the interface because of the increasing drag arising from "viscous" bubbles. In extreme cases, the mobility may be inhibited completely. Also, in the presence of a surfactant the internal circulation tends to compress the adsorbed contaminant into the rear surface of the bubble (Figure 28). As a result, the motion of the interface is enhanced through the action of local surface tension gradients caused by small differences in concentration along the interface (Marangoni Effect).

The overall hydrodynamic effect on oxygen transfer depends on surfactant concentration. As low surfactant concentration, the oxygen transfer rate is reduced because of decreasing internal circulation. As the concentration increases, the effect is more serious. However, when the bubble surface is completely covered by surfactant, internal circulation resumes because of the lack of surface tension gradient. Therefore, the K_L will increase instead of decreasing (Abdrews *et al.*, 1988; Lee *et al.*, 1980).

C. Aeration System Testing

There are two methods for determining the oxygen transfer capacity of any aeration system: The non-steady state clean water test and the process water test which are conducted in operating treatment plants. For an activated sludge aeration basin, the

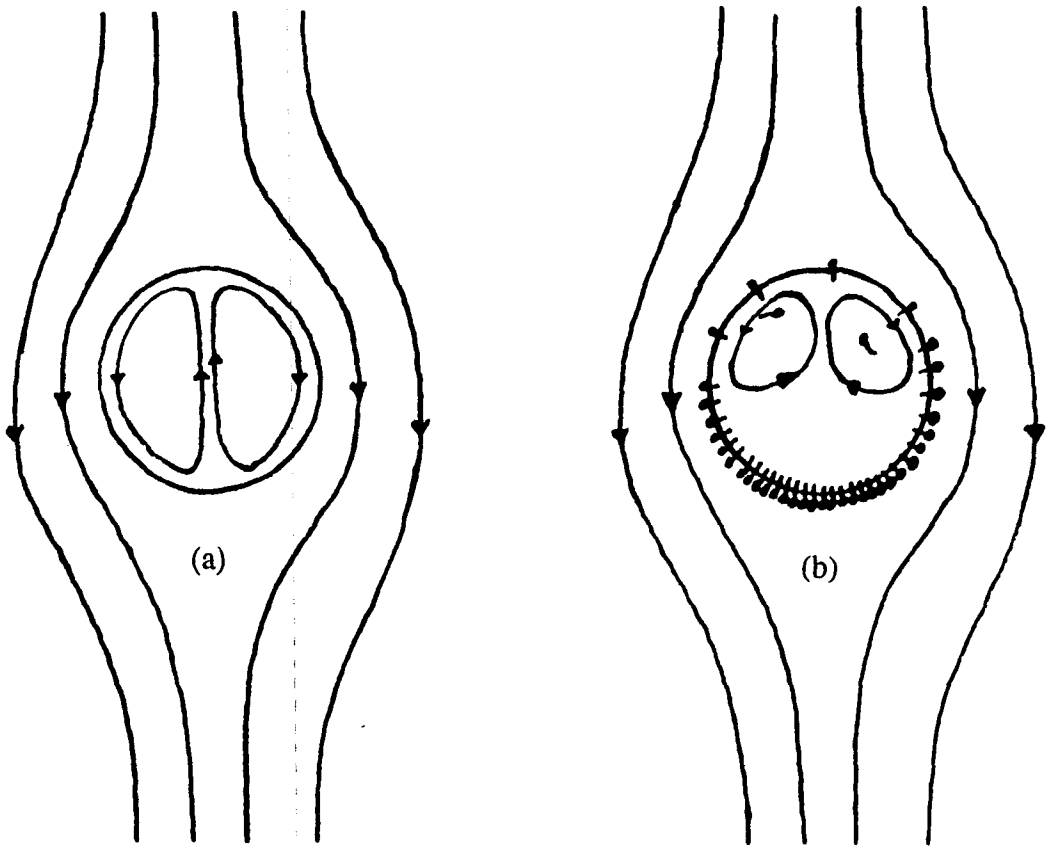

Figure 28. Circulation within a rising drop (bubble). (a) unhindered circulation (b) the adsorbed surfactant reduces the circulation pattern. (after Linton and Sutherland, 1957)

process water test is conducted after a wastewater treatment plant is placed in operation and a suspension of microbial solids is developed. The fundamental mathematical models for both methods are similar and are based on the same basic assumptions. Theoretically, both tests should give the same result; however, this is not readily achieved and the reasons will be discussed later.

Process Water Test

The mathematical model for steady state testing is:

$$\frac{dC}{dt} = K_L a \left(C_\infty^* - C\right) - R \qquad (63)$$

where

$\frac{dC}{dt}$ = Rate of change of DO concentration

$K_L a$ = Overall transfer coefficient under process conditions

C_∞^* = DO saturation concentration under process conditions

R = Respiration rate or oxygen uptake rate of biological organisms

C = Dissolved oxygen concentration at time t

This technique has been successfully used to measure oxygen transfer rate when steady state conditions are established for organic load, mixed liquor suspended solids concentration, and dissolved oxygen. After the aeration basin is at steady state, the

aeration, raw sewage, and recycle flows are turned off. Waiting for the DO drop to zero, then start up the aeration and flows again. The value of C at different time and points in the aeration tank were taken until a stable value of C is obtained. This value should be at least equal to 3 mg/l but below 5 mg/l (Kalinske, 1978). The result is shown in Figure 29. This plot can be transformed to plot dC/dt versus C if dC/dt is calculated for different value of t. This new plot is a straight line (Figure 30) whose slope is $K_L a$. This comes about by transforming Equation (63) to the following form:

$$\frac{dC}{dt} = \left(K_L a \cdot C_\infty^{\ *} - R\right) - K_L a \cdot C \qquad (64)$$

Obviously, the intercept of this straight line at C= 0 is equal to $\left(K_L a \cdot C_\infty^{\ *} - R\right)$. Therefore, R can be calculated after determining the proper value of $C_\infty^{\ *}$ under process condition.

The advantage of this technique is that $K_L a$ is determined without the need to measure R, or even to estimate the value of $C_\infty^{\ *}$. However, the problems encountered in this technique are:

- Difficulties in establishing steady state in treatment plants.

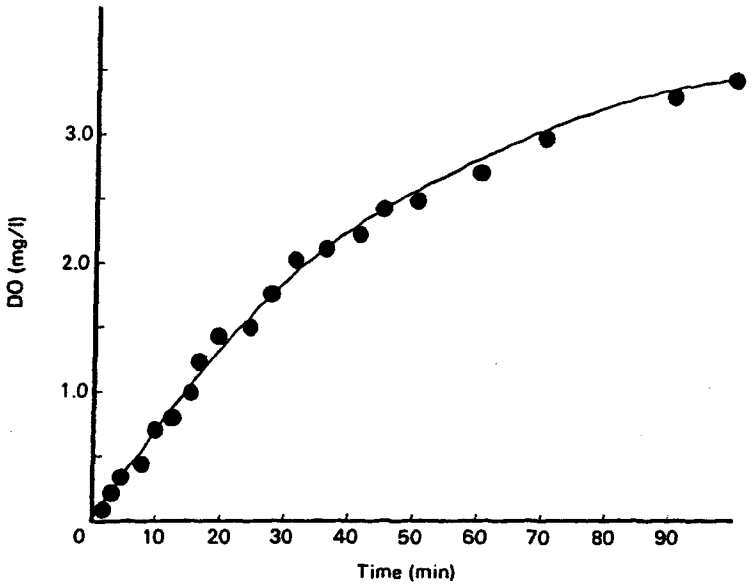

Figure 29. Reaeration of activated sludge basin under process conditions. (after Kalinske, 1978)

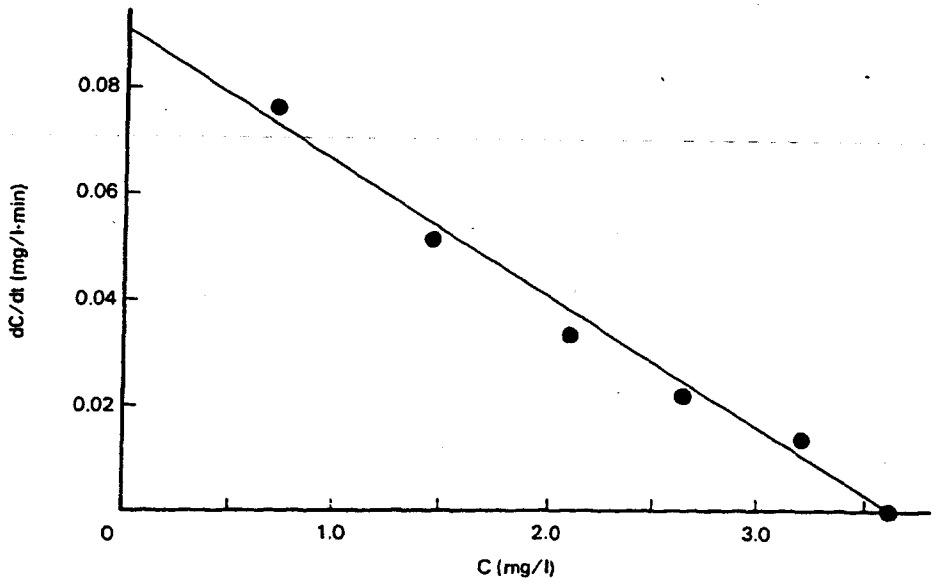

Figure 30. Replot of Figure 29. (after Kalinske, 1978)

- In order to compare and evaluate various designs of aeration systems, it is necessary that their performance be determined for standard conditions. The data obtained from steady state test is difficult to convert to standard conditions because it requires knowledge of the *in situ* value of α .

For other steady state testing technique, the difficulties encountered are the measurement of oxygen uptake rate by the activated sludge and the selection of dissolved oxygen concentration (McKinney and Stukenberg, 1978; ASCE, 1993). The conclusion is that the steady state test has greater potential for error than the non-steady test. Therefore, the non-steady state clean water test appears to be the best method for evaluating aeration equipment performance.

Non-Steady State Clean Water Test

The mathematical model for non-steady state test is:

$$\frac{dC}{dt} = K_L a \left(C_\infty^* - C\right) \qquad (65)$$

The purpose of this clean water test is to measure the Oxygen Transfer Rate (OTR) by an aeration system operating under given gas rate and power conditions. The test procedure is well defined in Standard-Measurement of Oxygen Transfer in Clean Water (1993). It is based upon the removal of dissolved oxygen (DO) from the clean water volume by

sodium sulfite (Na_2SO_3) followed by re-oxygenation to near saturation level. The DO concentration is monitored during the re-aeration period. The data obtained at each determination point (e.g. probe location) are then analyzed by non linear regression method (next section) in order to estimate the apparent volumetric mass transfer coefficient, $K_L a$, and steady-state DO saturation concentration, C^*_∞.

The primary result of this test is expressed as the SOTR:

$$SOTR = K_L a \cdot C^*_\infty \cdot V \qquad (66)$$

The SOTR is a hypothetical mass of oxygen transferred per unit of time at zero dissolved oxygen concentration, water temperature of 20°C, and barometric pressure of 1.00 atm (standard conditions), under specified gas rate and power input. From the SOTR result, OTR can be easily calculated by applying, α, β, and θ corrections:

$$OTR = \alpha \left(\frac{\beta \cdot C^*_{\infty,t} - C_L}{C^*_{\infty,20}} \right) \theta^{T-20} \cdot SOTR \qquad (67)$$

where

C_L = Desired value of DO concentration under normal operation

t = Subscript indicating temperature

D. Parameter Estimation

The purpose of the parameter estimation procedure is to determine the best estimates of the three model parameters, $K_L a$, C_∞^* and C_0 so that the model given by Equation (65) best describes the variation of DO with time at each sampling point in the aeration tank. A number of methods have been used for this purpose. The reasons for having different methods for data analysis are:

- The integration form of Equation (65) can be expressed in logarithm and exponential forms (Equation 72 and 73).
- The oxygen saturation concentration at infinite time (C_∞^*) is not constant in most aeration systems. It may vary with the depth of the aeration tank and the gas flow-rate.

Three basic approaches have been used to estimate the parameters (Bass and Shell, 1977; Campbell *et al.*, 1976; Schmit *et al.*, 1978) :

Differential Method (Direct Method)

The Equation (65) can be rewritten as:

$$\frac{dC}{dt} = K_L a \cdot C_{\infty}^{*} - K_L a \cdot C \tag{68}$$

or

$$\frac{\Delta C}{\Delta t} = K_L a \cdot C_{\infty}^{*} - K_L a \cdot \overline{C} \tag{69}$$

which

$$\overline{C} = \frac{C_i + C_{i+1}}{2} \tag{70}$$

$$\frac{\Delta C}{\Delta t} = \frac{C_{i+1} - C_i}{t_{i+1} - t_i} \tag{71}$$

The experiment data, fitted curve, and error structure (residual of the data set) are shown in Figure 31. Inspection of Figure 31 clearly demonstrates that the observed values of $\Delta C/\Delta t$ are scattered about the fitted curve and the residuals do not have uniform variance.

The advantage of this method is that a value of C_{∞}^{*} is not required; it is calculated from the data. However, the main problem with this method is that it magnifies the noise in the data because differentiating DO concentration creates larger error than using the concentration itself. This error is especially disturbing if the concentration data are noisy. This method is rarely used today.

2) Nonlinear Regression Method (Best Fit Exponential Method)

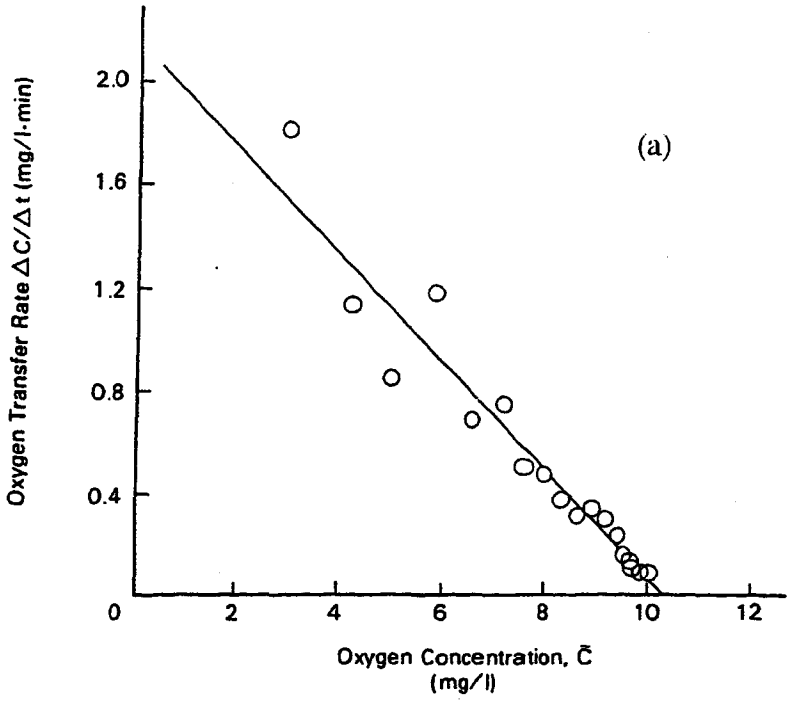

Figure 31(a). Experimental result of differential method.
(Data of Gilbert and Chen, 1976; Plot of Brown, 1978)

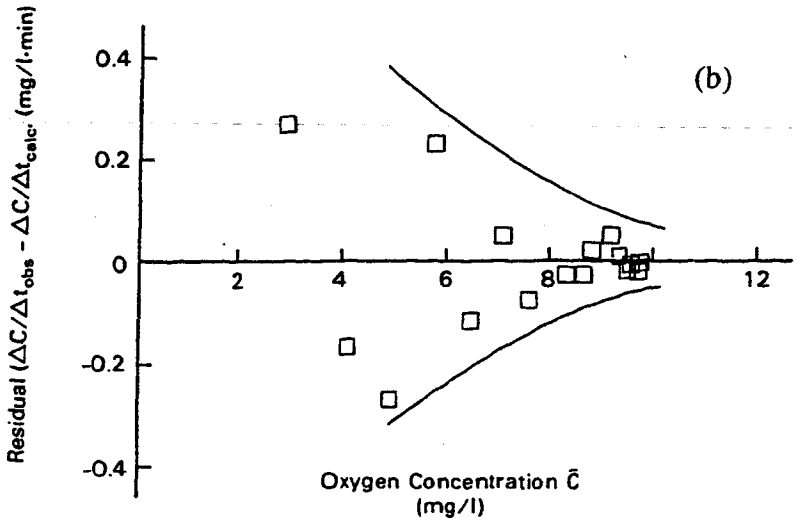

Figure 31(b). Error structure of differential method.
(Data of Gilbert and Chen, 1976; Plot of Brown, 1978)

This method is to use the exponential form of Equation (65):

$$C = C_{\infty}^{*} - \left(C_{\infty}^{*} - C_0\right) \cdot e^{(-K_L a \cdot t)} \qquad (72)$$

to estimate $K_L a$. The dissolved oxygen concentration is plotted versus time (Figure 32).

The advantage of this method is the same as Differential Method, and there is no need to assume a value of C_{∞}^{*} to compute $K_L a$. Since C_{∞}^{*} is estimated from the data, no error is introduced by incorrectly estimating C_{∞}^{*} from any sources. The disadvantage is that the error structure in concentration is not uniform, but is larger for low values of C than at high values (Figure 32(b)). However, this can be improved by fitting data to square of concentration versus time instead of concentration versus time (Davies, 1967).

In order to estimate $K_L a$, it is necessary to compute a nonlinear least squares fit by programming technique. There are user-oriented FORTRAN and BASIC programs available from American Society of Civil Engineering which will give the least square estimates, standard deviations of $K_L a$, values and residuals. ASCE also provides a TURBOPASCAL (version 4) program which can be used with a portable or lap-top computer capable of performing graphics. It requires very little memory and does not use a math coprocessor (ASCE, 1994). A program written for a programmable calculator is also available (Stenstrom *et al.*, 1981). A newer modification programming is written in

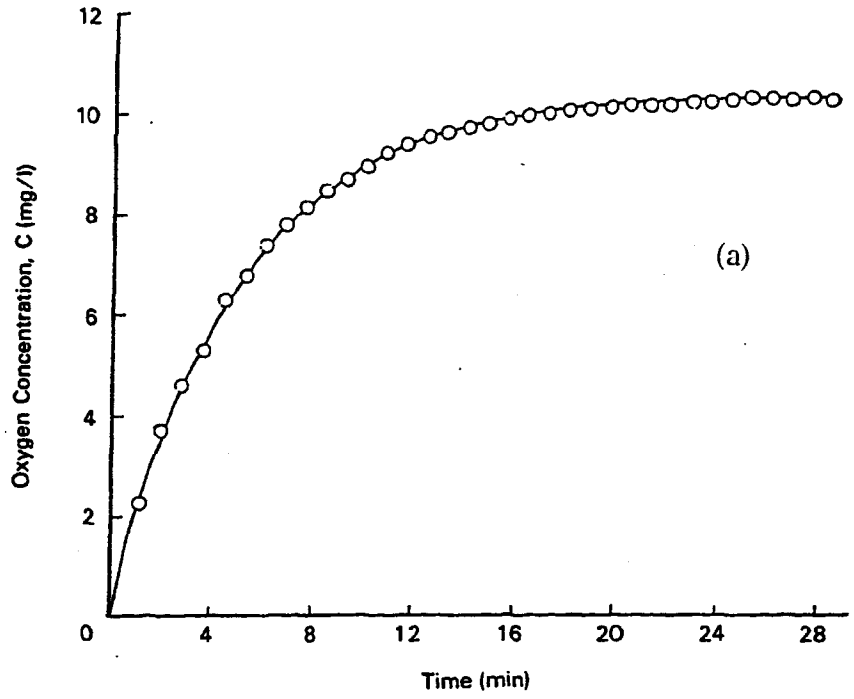

Figure 32(a). Experimental result of best-fit exponential method.
(Data of Gilbert and Chen, 1976; Plot of Brown, 1978)

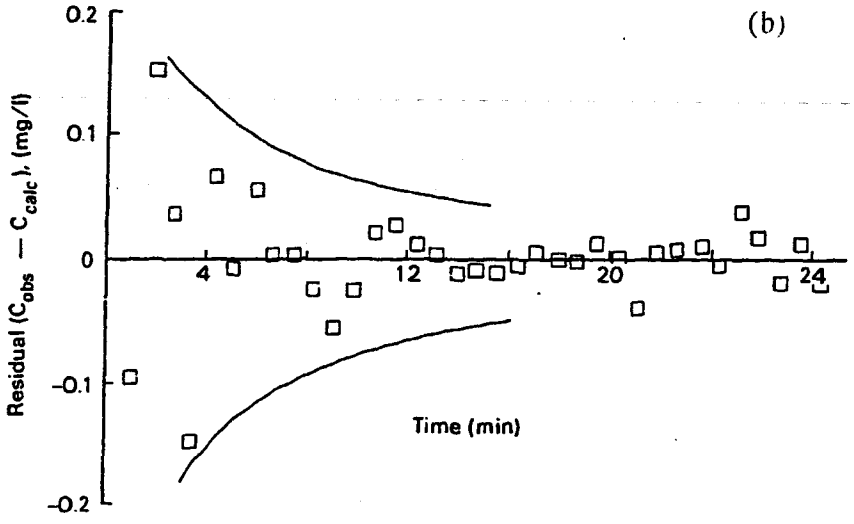

Figure 32(b). Error structure of best-fit exponential method
(Data of Gilbert and Chen, 1976; Plot of Brown, 1978)

Microsoft Visual Basic with a Windows interface (Lee, Ma, and Stenstrom from UCLA Civil and Environmental Engineering Department). The Internet address for this program is http:// fields.seas.ucla.edu/andy.

3) Log-Deficit Method

The Equation (65) is integrated and rearranged to the following logarithmic form:

$$\ln\left(C_{\infty}^{*} - C\right) = \ln\left(C_{\infty}^{*} - C_{0}\right) - K_{L}a \cdot t \qquad (73)$$

Figure 33 shows an example of using this technique. The error structure of this method has increasing by large errors as the deficit decreases. This can be improved by truncating the lower end of data set, but may result in failure to recognize an incorrect value of C_{∞}^{*}.

The mass transfer coefficient $K_{L}a$ can be estimated using simple linear regression if C_{∞}^{*} is known. In other words, this method requires *a priori* knowledge of C_{∞}^{*}. There are 5 *a priori* models of estimating C_{∞}^{*}. They all involve the use of the saturation values of dissolved oxygen, C_S (handbook values). The value of C_S is determined from handbook and is corrected for barometric pressure and temperature (Campbell, *et al.*, 1976).

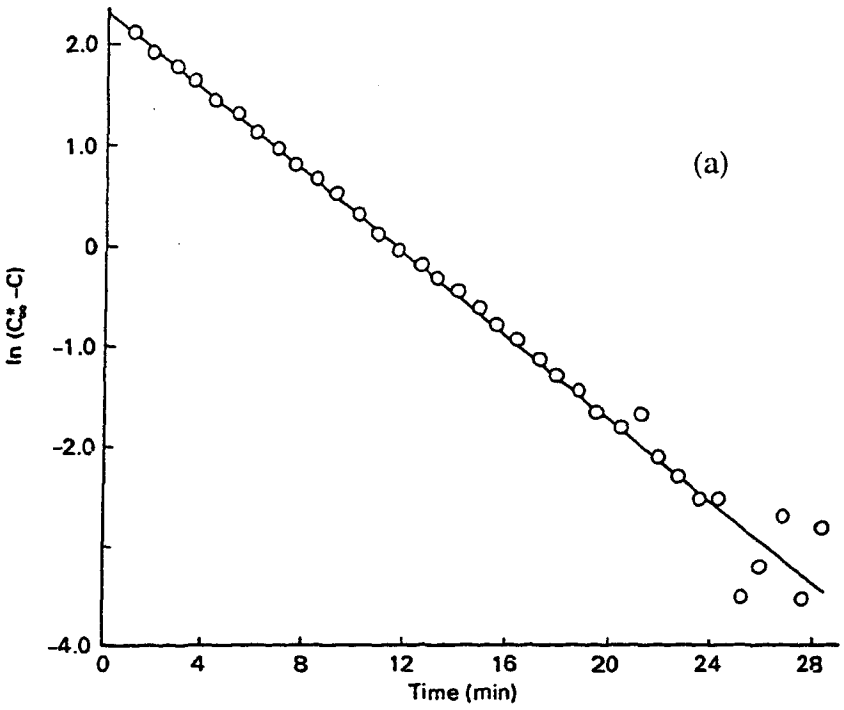

Figure 33(a). Experimental result of log-deficit method.
(Data of Gilbert and Chen, 1976; Plot of Brown, 1978)

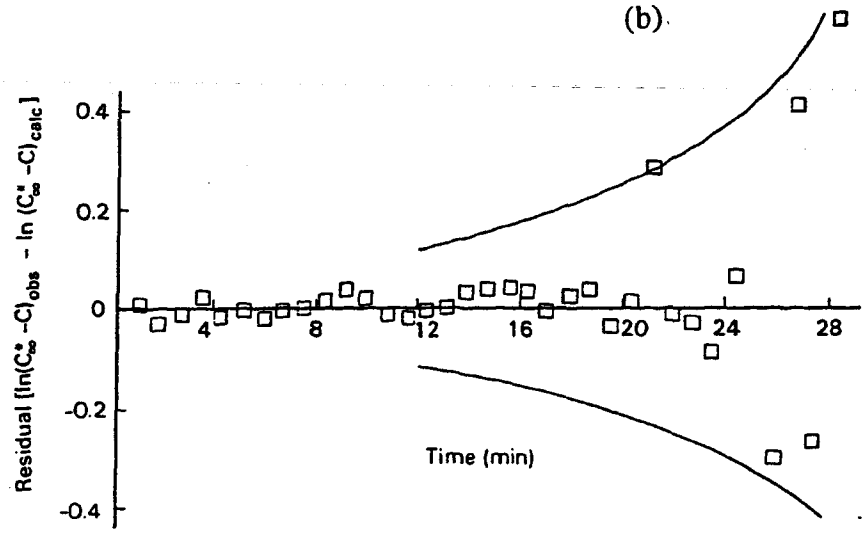

Figure 33(b). Error structure of log-deficit method
(Data of Gilbert and Chen, 1976; Plot of Brown, 1978)

i) Surface saturation model:

$$C_{\infty}^{*} = C_S \tag{74}$$

ii) Bottom Saturation model:

$$C_{\infty}^{*} = C_S\left(1+\frac{\gamma h}{P}\right) \tag{75}$$

iii) Mid-depth model:

$$C_{\infty}^{*} = C_S\left(1+\frac{1}{2}\frac{\gamma h}{P}\right) \tag{76}$$

iv) Mid-depth corrected model:

$$C_{\infty}^{*} = C_S\left(1+\frac{1}{2}\frac{\gamma h}{P}+\frac{O_r}{2O_i}\right) \tag{77}$$

v) Log-mean model:

$$O_r = \frac{O_i(1-E)}{(1-O_i)+O_i(1-E)}\times 100 \tag{78}$$

and

$$\ln C_{\infty}^{*} = \frac{\ln\left(C_S+\frac{\gamma h}{P}\right)+\ln\left(C_S\cdot\frac{O_r}{O_i}\right)}{2} \tag{79}$$

where

γ = Specific weight of water per feet, (=0.433)

P = Barometric pressure; [Psia]

h = Diffuser depth; [ft]

O_i = Inlet oxygen mole fraction in air, (=20.95%)

O_r = Exit oxygen mole function in air; [%]

E = Fractional oxygen transfer efficiency (0 to 1.0)

Many researchers have reviewed the advantages and disadvantages of each parameter estimation technique. All of them agree that the non-linear regression method is the most desirable of all three methods. The log-deficit method is the second choice.

MATERIALS AND METHODS

I. Static Surface Tension Measurement

A. Surface Tension Apparatus for Capillary Rise Method

The capillary apparatus used for capillary rise method is from Fisher Scientific (Catalog No. 14-818). This apparatus consists of a 250 mm borosilicate glass capillary tube, graduated from 0 to 10 cm in 1-mm increments. A larger outer tube opens at one end and with a glass side-arm opening near the top. A one-hole rubber stopper holds the capillary inside the outer tube. The capillary radius was determined in the lab by measuring the surface tension of pure benzene in a thermostat-controlled bath at two temperatures: 20 °C and 40 °C. The depth (arbitrary number was picked) of immersion should be adjusted at each temperature such that the meniscus in the capillary is kept at the same point on the scale. The value of σ (surface tension of benzene) and ρ (density of benzene) may then be obtained by (from insert):

$$\sigma = 30.607 - 0.12732 \cdot T \qquad (80)$$

and

$$\rho = 0.8995 - 0.0010818 \cdot T \qquad (81)$$

where

T = Temperature (°C)

The radius of capillary can be calculated from the Equation (15) and it is 0.35 mm. This procedure must be repeated for every new capillary tube before it can be used.

It is important that this glass capillary be kept extremely clean so that the sample has zero contact angle. The following steps are taken to clean capillary before each use:

- Clean apparatus thoroughly with chromic acid.
- Rinse with tap water (three times) and with distilled water (three times).
- Rinse with methanol to get rid of water.
- Dry the apparatus by blowing air through it.

B. Fisher Surface Tensiomat (Model 21) for Du Noüy Ring Method

Essentially, the tensiomat is a torsion-type balance. A platinum-iridium ring of precisely known dimensions is suspended from a counter-balanced lever-arm. The arm is held horizontally by torsion applied to a taut stainless steel wire, to which it is clamped. Increasing the torsion in the wire raises the arm and the ring that carries with it a film of the liquid in which it is immersed. The force necessary to pull the ring free from this surface film is measured.

In order to obtain precise surface tension with this instrument, the following precautions must be followed:

- The glass vessels (example: Petri dishes) with a diameter of at least 4.5 cm are

required to avoid wall effects.

- The glassware is cleaned by chromic acid, tap water, distilled water, and dried. If any residual oil from the previous sample remains, the glassware should be rinsed with either petroleum naphtha or benzene followed by methyl ethyl ketone before rinsing with chromic acid.
- The ring is cleaned by dipping it into benzene (to remove hydrocarbon), then acetone (to remove the benzene). Finally, the ring is flashed in a flame (lighter was used) untill red. This procedure is to remove residual hydrocarbons.

This tensiomat measures static surface tension either by a manual or semi-automatic procedure. The semi-automatic procedure was used in order to increase reproducibility. Both procedures determined the "apparent surface tension". The apparent surface tension was converted to absolute values by following relationships:

$$\sigma = P \times F \tag{82}$$

where

σ = Absolute surface tension, [dyne/cm]

P = Apparent value indicated on the dial; [dyne/cm]

F = Correction factor

$$F = 0.7250 + \sqrt{\frac{0.01452\,P}{C^2(D-d)} + 0.04534 - \frac{1.679r}{R}} \tag{83}$$

R = Radius of the ring (R/r = 53.7936868)

r = Radius of the wire of the ring

D = Density of the lower phase (samples)

d = Density of the upper phase (air)

C = Circumference of the ring (=6.005 cm)

II. Dynamic Surface Tension Measurement (DST)

Maximum Bubble Pressure Method is the only method used for DST measurement in this study. Although there are two Bubble Pressure Tensiometers available on the market (Bubble Pressure Tensiometer BP2 from KRUSS USA, North Carolina and Maximum Bubble Pressure Tensiometer Model MPT-1 Landa from Brinkmann Instruments, Westbury, N Y), we constructed a MBPM instrument (Figure 34) similar in function to most of other researchers' instruments. The following section describes the instrument.

Building air (50 psig) was reduced to 20 psig using a pressure regulator and passed through a dessicator (DRIERITE; Gas Purifier; Model L68GP; W.A. HAMMOND DRIERITE Co.). The purpose of this step is to eliminate the water vapor, which causes the pressure fluctuations. A second regulator was used to reduce the pressure to 5 psig. Air flow-rate was monitored with a rotameter (Cole Parmer; 0 - 7 ml/min direct reading), and was split into three lines.

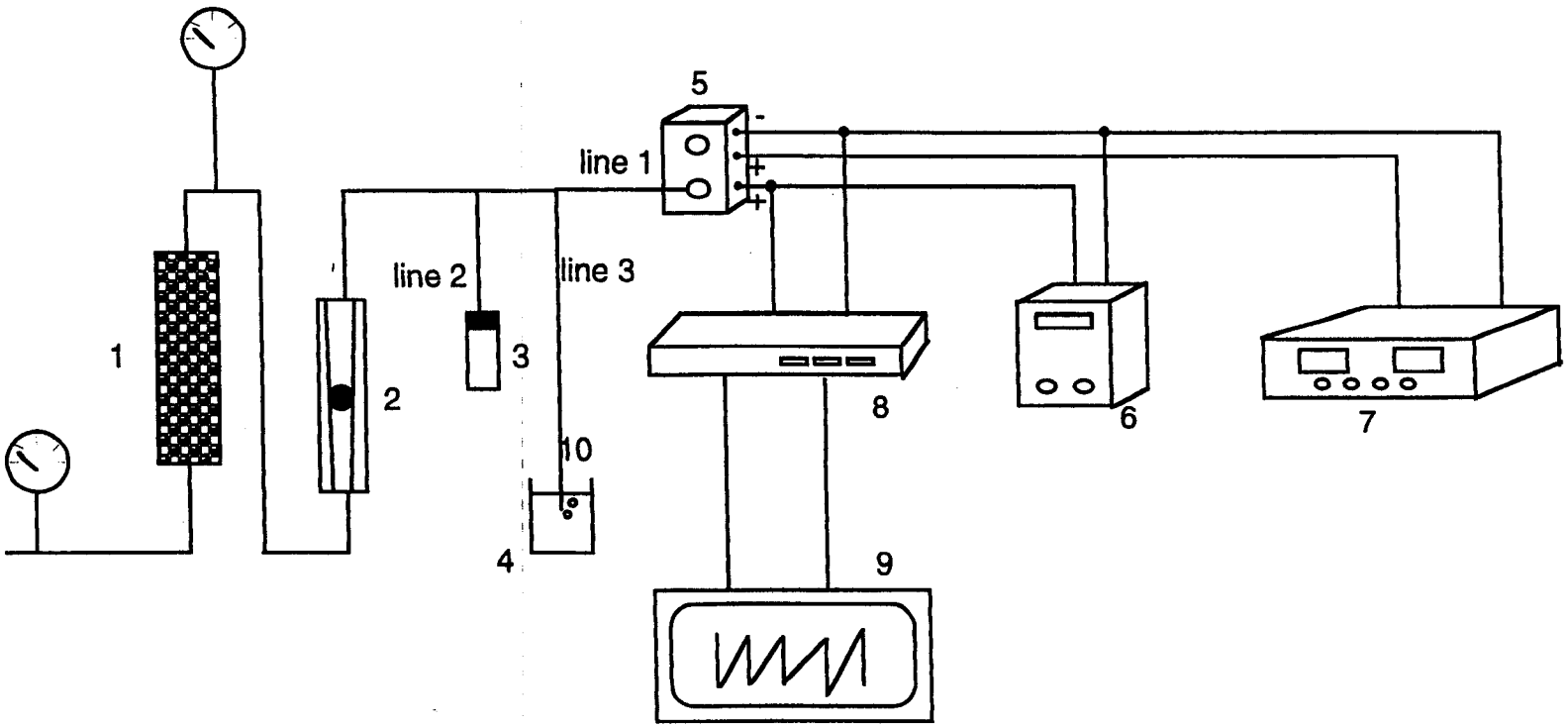

1. dessicator 2. rotameter 3. 40 ml vial 4. beaker 5. pressure transducer
6. voltameter 7. HP power supply 8. A/D convertor 9. laptop 10. capillary

Figure 34. The set-up of Maximum Bubble Pressure Method.

Line 1 goes into pressure transducer (Setra Systems, Inc.; model 264 D-10 in WC with output 0 - 5 VDC). The pressure transducer senses differential pressure and converts this pressure difference to a proportional high level analog output for both unidirectional (0 - 10 volts) and bi-directional pressure ($\pm$ 5 volts) ranges. The analog output is fed to a data acquisition system (IOtech, DaqBook/216 model, 16-bit 100 kHz Data Acquisition System with Enhanced Parallel Port (EPP)) through channel 00. This data acquisition system is software driven by DaqView3 (with Windows drivers) which was loaded an IBM PS/2 model L40 SX Notebook computer. To operate this pressure transducer, a 12 to 24 VDC unregulated power is required. A HP 6205B Dual DC Power Supply (0 - 40V/0.3 A; 0 - 20v/0.6 A) was used. A voltmeter is also connected to the transducer for the purpose of visually monitoring the system's pressure change

.

Line 2 is connected to a 40 ml vial. This vial serves as a gas chamber that helps maintain constant pressure.

Line 3 is connected to a fused silica needle syringe (Hamilton 1701 RNFS 10 μL GASTIGHT syringe with a 0.23 mm ferrule. Part No. 87404 and 30949). Instead of using Hamilton fused silica needle (O.D. = 0.23 mm), a pyrex round capillary tubing (0.15 mm I.D. x 0.25 mm O.D. x 100 mm long, from Wilmad Glass) is used. The only reason for this replacement is price. The syringe is attached to an adjustable caliper so that the capillary can be lowered until it just touches the solution surface and then

immersed a specific distance. Air with constant pressure is released through the submerged glass capillary (I.D. = 0.15 mm) tip forming bubbles in an aqueous solution.

The experimental procedure begins with pressure accumulation to overcome the friction of capillary and static head that depends on the capillary's I.D. and immersion depth. The time required to form the bubble ranges from one-half minute to 10 minutes. This idle time depends on air flow-rate. As soon as bubbles appear and the bubble pattern is correct (Note: the bubble pattern must be a singlet; otherwise, change with new capillary and restart.), the data acquisition can be started using the DaqView. All the data are collected and surface tension is calculated using a program written in Visual Basic. The bubble frequency is calculated using Fourier Transforms using Mathcad Plus 6.0. Finally, surface tension (dyne/cm) versus bubble life (sec) is plotted using KaleidaGraph.

III. Bubble Size, DST, and $K_L a$ Measurement

The glass beaker (aeration container) in Figure 34 was replaced by a 2 cm × 2 cm × 1 ft square pyrex tube (Wilmad Glass, Inc.). An upward capillary (I.D. = 0.15 mm) and a MI-730 micro-oxygen electrode (Microelectrodes, Inc.) were contained inside of this glass tube (Figure 35). This modification was used to measure oxygen transfer rate, dynamic surface tension, and bubble sizes, simultaneously. Bubbles formed in the solutions were photographed using a SONY Video camera recorder Hi8 (10,000 shutter speed, F1.8

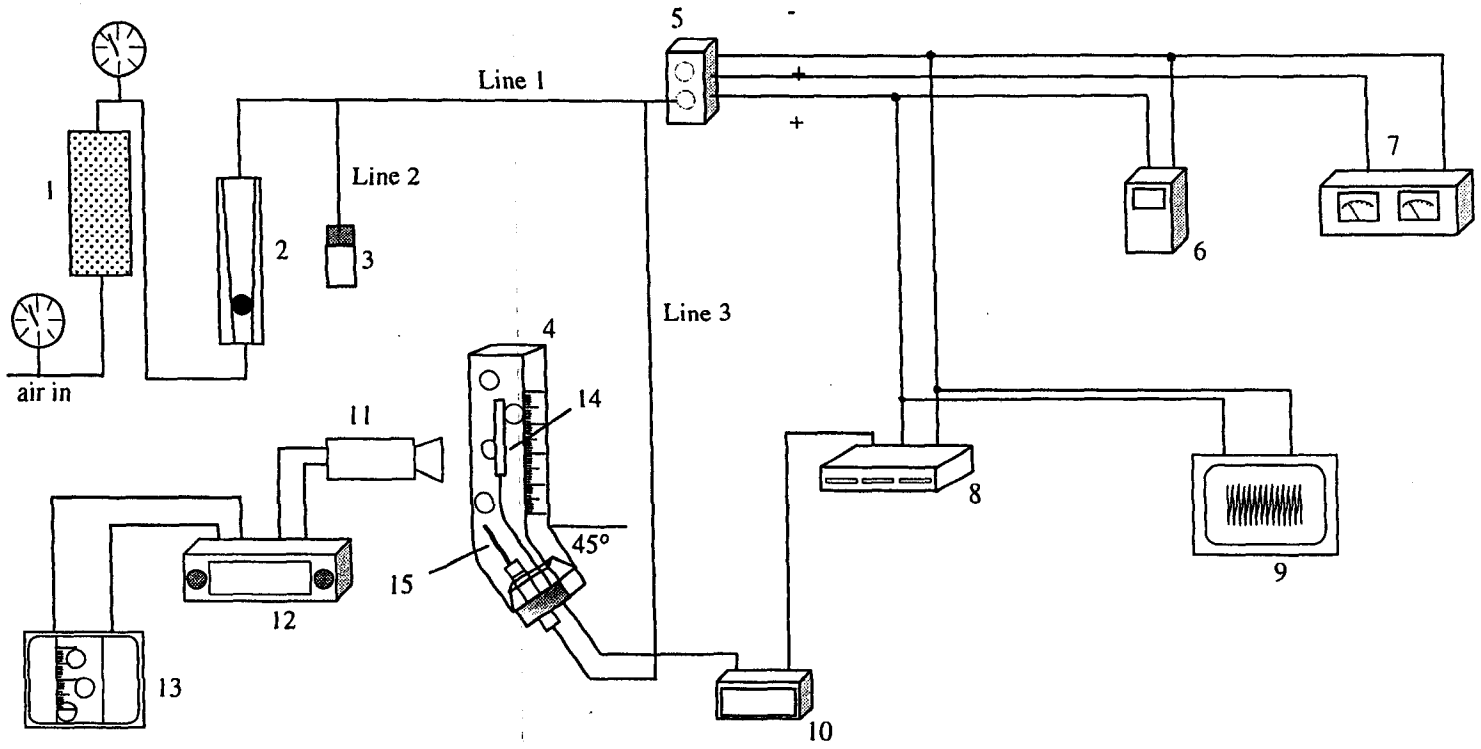

Figure 35. Device for measuring bubble life, dynamic surface tension, and oxygen transfer rate, simultaneously.

1.dessicator 2. rotameter 3. 40 ml vial 4. glass tube 5. pressure transducer
6. voltameter 7. HP power supply 8. A/D convertor 9. laptop 10. micro DO meter
11. vedio camera 12. VHS 13. TV monitor 14. micro DO probe 15. Glass capillary

aperture, +18db Gain). A ruler with a 0.01 cm graduations was taped on the side of glass tube and was used as a reference during photography. Bubble diameters were measured visually on 19" TV monitor. Theoretically, the upward capillary position has advantage of generating more regular bubbles. In practice, positioning the capillary in an upward position allows steady bubble growth until buoyancy is equal to gravitational force. As a result, the bubble life at high flow-rate is much longer in comparison with bubble produced in a downward capillary orientation at the same gas flow-rate (Figure 36). Because of the nature of this research, the DST at short bubble life (high flow-rate) is more interesting than at long bubble life, so that the upward capillary orientation with some modification was used.

Lin *et al.* (1994) conducted a series of experiments to investigate the effect of the tilt angle of an orifice plate against water surface on the bubble volume. Assuming that the surface of orifice plate is extremely hydrophilic and gas flow-rate is below the critical value, the bubble volume reduces as tilt angle increases:

Tilted Angle	0°	30°	45°	60°
Bubble volume (ml)	0.011	0.0091	0.0066	0.0056

The reason for this volume reduction is because of the buoyancy of a tilted bubble has a force component (Figure 37) which tends to destabilize bubble growth, causing early bubble detachment. A modification was applied to the MBPM set-up according to Lin's

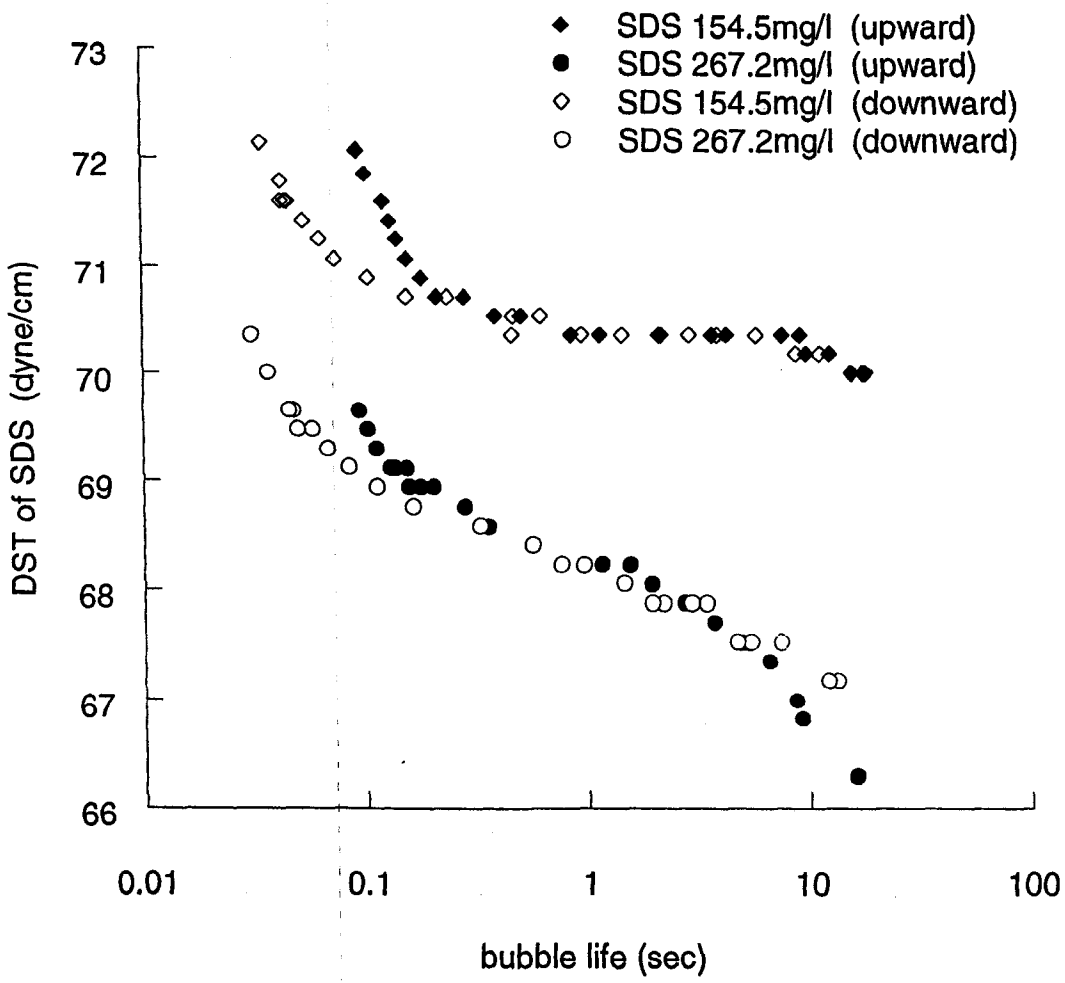

Figure 36. Comparison of DST measured with capillary pointed upward and downward.

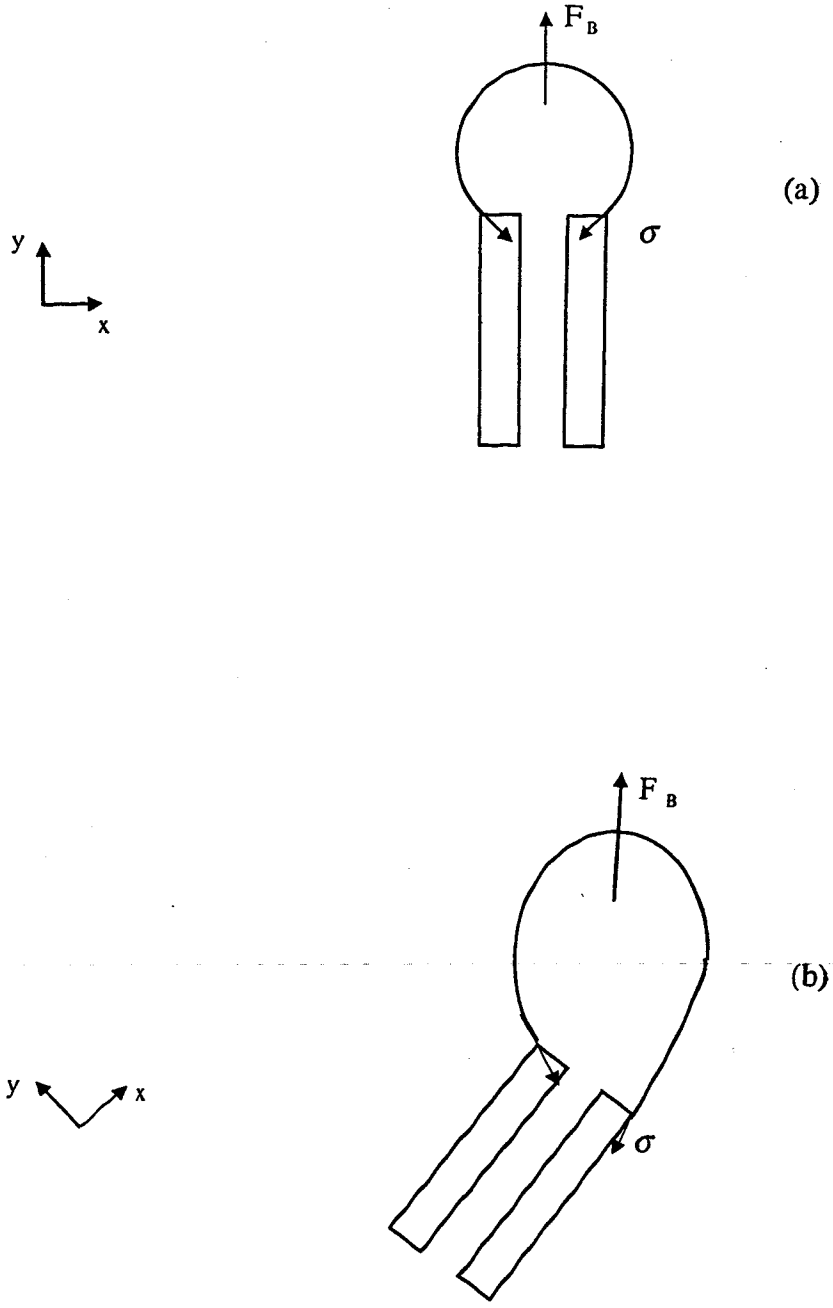

Figure 37. Force balance of bubble formed on capillary tip which is a) 0° b) 45° to solution surface.

findings. A stainless steel needle (Hamilton, point style 3 Luer tip needle with I.D. 0.13 mm) which was bent at a 45° angle, relative to the solution surface, and pointed upward. This was the first modification used to reduce bubble volume and bubble life at high flow-rate. However, the disadvantage of this modification was solution often trapped in the elbow of bent needle, producing an irregular and unpredictable bubble pattern. Therefore, a second modification was to bend the glass pyrex tube at 45° angle, relative to the solution surface using a straight glass capillary. The DST measured with this modified MBPM is shown in Figure 38. The bubble life at high flow-rate was reduced to milliseconds with this modification. Consequently, the bubble life is not only a function of gas flow-rate (before the critical value) but also a function of the angle between capillary orfice and water surface.

IV. Chemicals and Water

Several different type of water were evaluated:

- NANO Water (Barnstead NANOpure Infinity ultrapure water system; resistivity is 18 megohms-cm)
- Tap water (Conductivity = 450 to 500 umhos/cm)
- Primary, secondary and Tertiary effluents from Tapia Treatment Plant, Las Virgines, California. The effluents were collected and used the next day. They were preserved

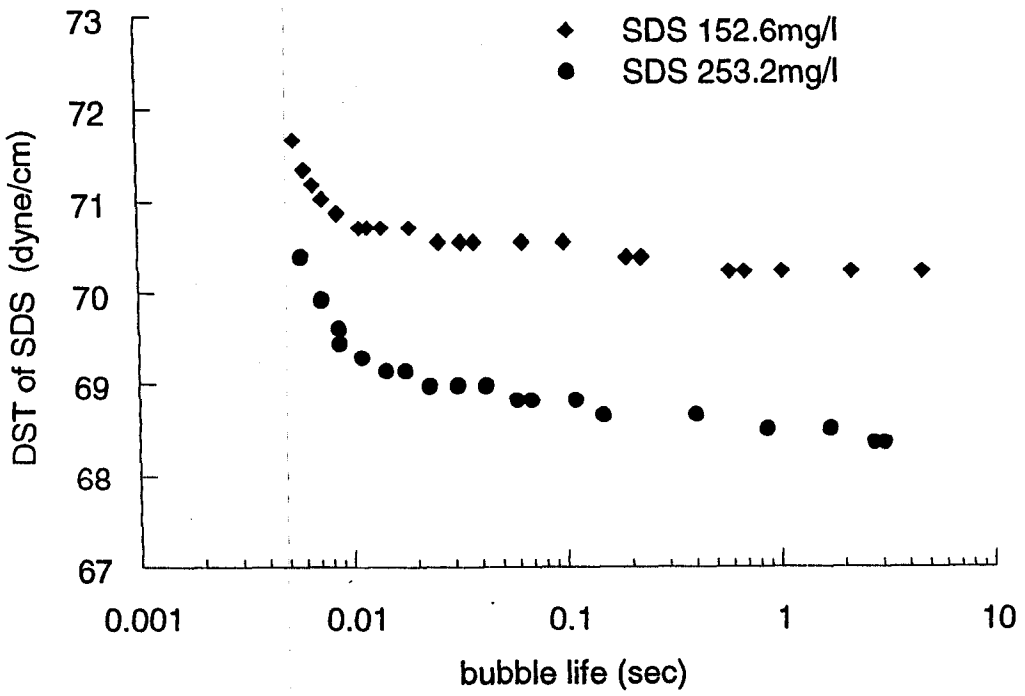

Figure 38. DST of SDS with capillary point upward and 45° to solution surface.

by sodium azide and kept at temperature 0°C. Right before analysis, all effluents were filtered by MSI Micron membrane filter (0.22μ).

The following surfactants were used:

- Dodecyl Sodium Sulfate (DSS; $CH_3(CH_2)_{11}OSO_3Na$; F.W.=288.38)

  Fisher ⇒ Assay 99.7%

  Millinckrodt ⇒ 95%

  Signma ⇒ Lauryl Sulfate Sodium salt

  Approximately 95% based on total alkyl sulfate content

  Aldrich ⇒ 70% Dodecyl Sulfate, Sodium salt,

  ~25% Tetradecyl Sulfate, Sodium salt

  ~5% Hexadecyl Sulfate, Sodium salt.

- Iso-Amyl Alcohol ($(CH_3)_2CHCH_2CH_2OH$; F.W.=88.15; from Fisher Scientific)

RESULTS AND DISCUSSSIONS

I. Comparison of Capillary Rise Method with Du Noüy Ring Method

The Capillary Rise Method is the easiest way to measure static surface tension, but cleaning the glassware is very tedious and labor intensive. The benefit of using this method is its improved accuracy over the Du Noüy Ring Method (Table 3). The Du Noüy Method has the reputation of being difficult to apply and poor reproducibility. It is still frequently used because of its simplicity. As early as 1919, researchers noticed more precise results when measuring pure liquids, as compared to more scattered results for solutions, especially surfactant solutions. The "low reproducibility" of Du Noüy Method is apparent when measuring the surface tension of surfactant solutions. The poor reproducibility should be expected for this method because of effects of adsorption equilibrium on the measurement of surfactant solutions.

It is well known that the prerequisites for correctly determining the surface tension by the ring method are (i) the diameter of container must be large enough to eliminate wall compression effects, (ii) the ring must be absolutely hydrophilic. Lunkenheimer and Wantke (1981) made several suggestions (a, b, and c) for improving precision of the Du Noüy Method, and Table 4 shows the improvement of using these suggestions.

a. Fill the sample container as close to the rim as possible. This reduce hydrophilic wall expansion effect (refer to literature review section).

Table 3. Surface Tension Of Pure Liquid And Binary Mixture Measured With Capillary Rise Method And Du Noüy Ring Method. (Temp. = 20 °C)

Substances	σ* (dyne/cm)	Capillary Rise Method		Du Noüy Ring Method	
		σ (dyne/cm)	% error	σ (dyne/cm)	% error
Tap Water	72.75	71.95	-1.02	74.18	+1.96
Acetone	23.70	23.62	-0.34	24.44	+3.12
Benzene	28.85	28.06	-2.74	29.97	+3.88
Acetic Acid	27.80	27.91	+0.40	28.86	+3.81
14.92% (w/w) NaCl in Water	77.65	76.88	+0.99	75.63	-2.60
30.81% (w/w) Acetic Acid in Water	43.60	44.50	+2.06	45.95	+5.39

* Value from CRC Handbook of Chemistry and Physics, 75th Edition.

Table 4. Surface Tension Of SDS With Du Noüy Method

Substances	Apparent σ (dyne/cm) Temp. = 18.5 °C (4 repeatitions)				Absolute σ † (dyne/cm)	Standard Deviation
DI Water	76.75	76.81	76.82	76.81	71.97	±0.032
SDS From Sigma (100.28 mg/l)	66.67	66.63	66.58	66.64	61.58	±0.037
SDS From Aldrich (100.58 mg/l)	63.78	63.63	63.75	63.64	58.48	±0.076
SDS From Millinckrodt (100.33 mg/l)	59.75	59.79	59.59	59.73	54.57	±0.087
SDS From Fisher Sci. (100.14 mg/l)	73.75	73.77	73.78	73.69	68.65	±0.040

† Absolute σ = Apparent σ x Correction Factor (F)

$$F = 0.7250 + \sqrt{\frac{0.01452\,P}{C^2 \cdot (D-d)} + 0.04534 - \frac{1.679\,r}{R}}$$

R : Radius of the ring
r : Radius of the wire of the ring
D : The density of the lower phase
d : The density of the upper phase
C ; The circumference of the ring

b. It is necessary to thoroughly disturb the surface of the surfactant solution with a pasteur pipet each time before lowering the ring into solution.

c. The time interval between the end of disturbing and the beginning of measurement should be 20 - 40 minutes.

Figure 39 shows a comparison of the capillary rise and improved Du Noüy methods. Surface tensions measurements from both methods are quite similar. Each data point in Figure 39 is an average value of four repetitions. The error bar of each method is so small that is not visible for many points. From literature review, the surface tension of surfactant depends on parameters like temperature, concentration, and purity. Therefore, the surface tension shown in Figure 39 cannot be exactly compare with literature values. However, Miles (1943) measured surface tension of pure SDS at room temperature and his results (Figure 39) had similar value as of this study.

II. Dynamic Surface Tension (DST)

The MBPM for DST measurement was selected for this research. It has been the most thoroughly investigated and has the greatest application to mass transfer measurements. The technique can be in corporate into a bubble column for simultaneous measurement of DST and mass transfer.

The surface tension calculation procedure was mentioned in earlier (Section III (D)) and a computer program was written for this procedure. The bubble frequency is obtained by applying Fourier transform function to DST function. From literature review, there are many different ways to detect bubble frequency. The advantage of using software

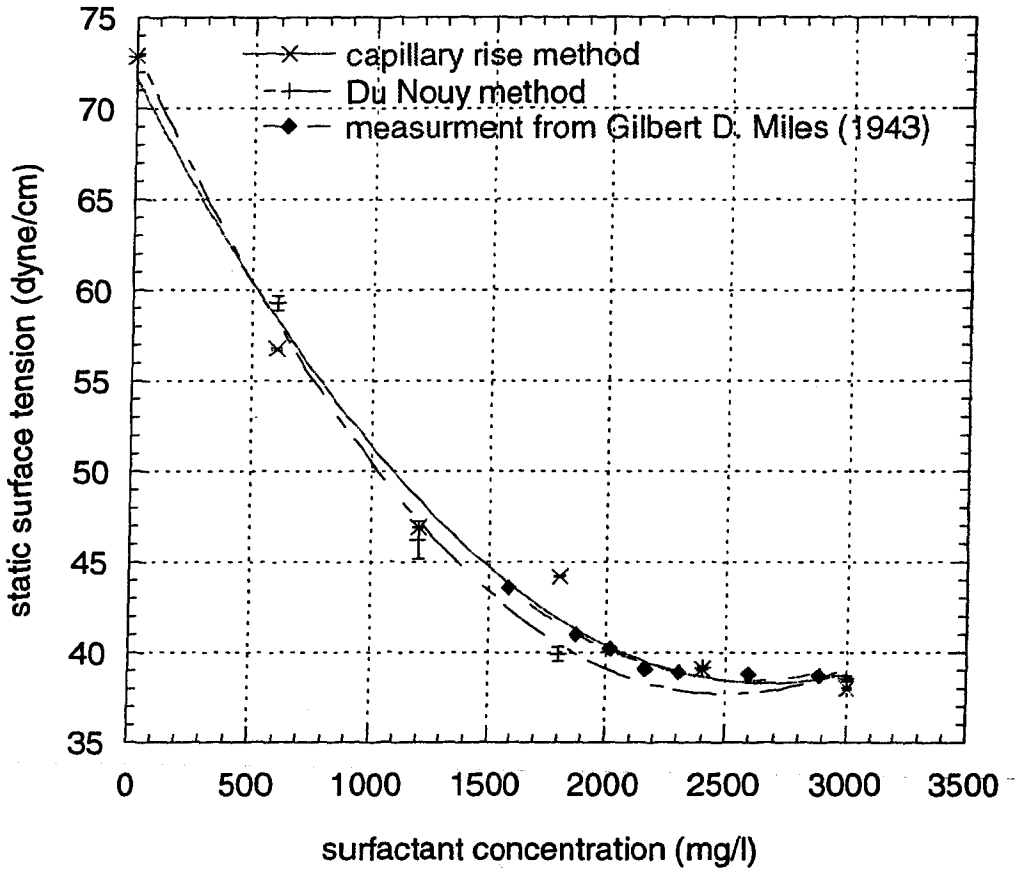

Figure 39. Comparison of Capillary Rise Method with Du Nouy Ring Method. (Surfactant: Dodecyl Sodium Sulfate)

transformation instead of hardware devices is not only reduced costs but also ease of use.

A. Validation of Bubble Frequency Calculation

To demonstrate the accuracy and precision of the bubble frequency calculation procedures, two issues needed to be validated: the sampling rate of data acquisition device, and the FFT (Fast Fourier Transform) calculations from MathCad.

The IOtech DaqBook 216 offers various sampling rates, which can be controlled by DaqView. The choice of sampling rate must conform to Shannon's Sampling Theorem (Bernardin, 1993). The sampling theorem establishes a minimum rate at which an analog signal must be sampled. According to this theorem, sampling at any rate faster than two times the maximum frequency of the signal produces a valid representation of the signal. Therefore it is necessary to investigate the relationship between sampling rate and bubble frequency at different flow-rates.

A video camera and VHS tape recorder (TOSHIBA OSP) were set up to record the bubbling process while the DaqBook was acquiring the system pressure changes. Afterwards, the videotape was played back in slow motion, and the bubbles were visually counted. The data acquired by DaqBook were used to calculate the bubble frequency using the FFT (Figure 40).

The results (Table 5) indicate that bubble frequency calculated by Fourier Transform is the same as by VCR except more accurate. The extremely high sampling rate at low gas

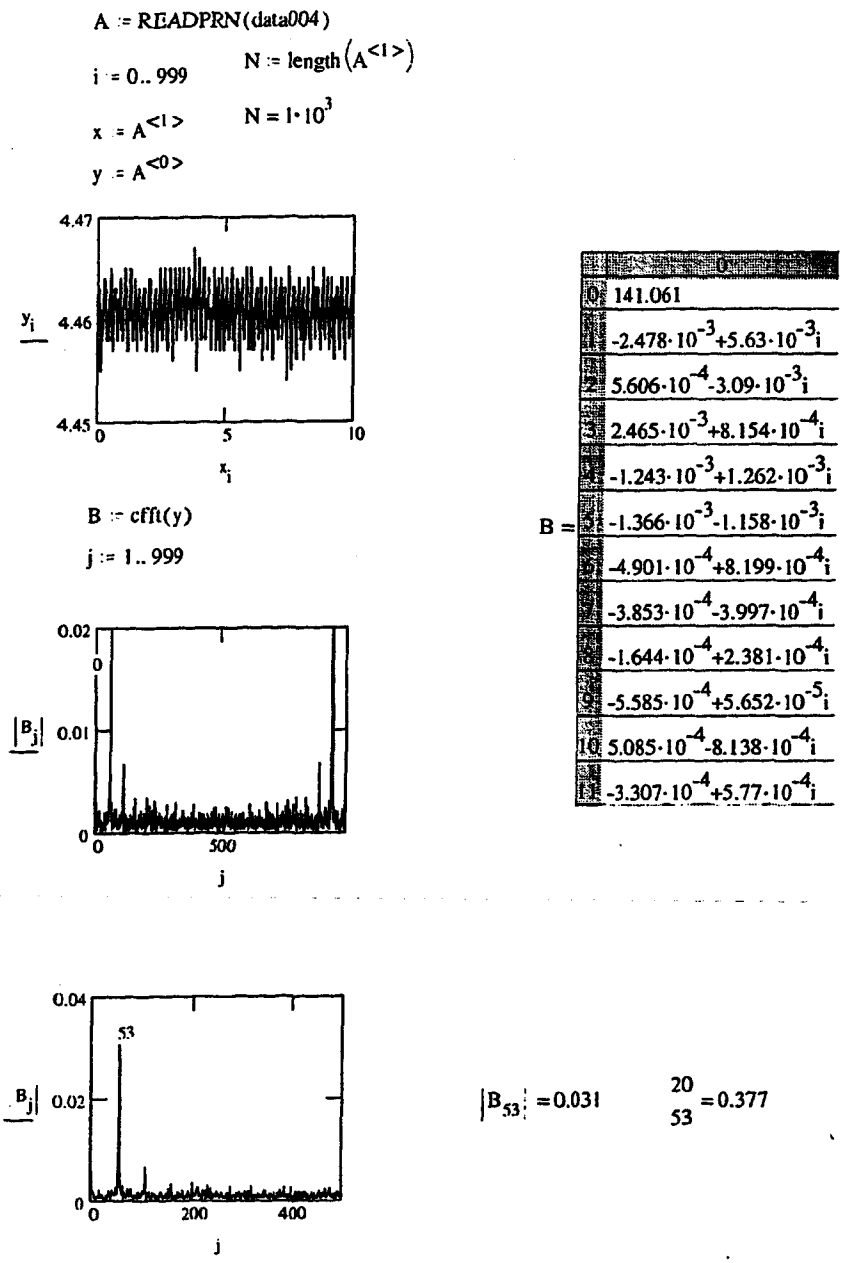

Figure 40. A FFT page from MathCad.

Table 5. Bubble frequency obtained by different sampling frequency

Gas flow rate = 0.8 ml/min

Sampling frequency (#/sec)	Total sampling time (sec)	Bubble frequency from VCR (#/sec)	Bubble frequency from FFT (#/sec)
20	60	5.0	4.727
50	24	5.0	4.738
100	20	5.0	4.750
200	15	5.0	4.733
500	10	5.0	4.740
1000	5	5.0	5.200

Gas flow rate = 1.7 ml/min

Sampling frequency (#/sec)	Total sampling time (sec)	Bubble frequency from VCR (#/sec)	Bubble frequency from FFT (#/sec)
20	60	11.0	9.717
50	24	11.0	10.262
100	20	11.0	10.250
200	15	11.0	10.267
500	10	11.0	10.260
1000	5	11.0	10.260

flow-rate, which results in a very short period of observation, due to many restrictions, introduces error and should be avoided. The extremely low sampling rate at high flow-rate also introduces error and should be avoided. In conclusion, a sampling rate of 250/sec and 500/sec providing an observation period from 10 to 60 seconds works best for low and high flow-rate, respectively.

B. Surface Tension of Tap Water and D.I. Water

The DST experiment was carefully performed under constant room temperature and pressure. However, there are still many factors that can result in erroneous results. For example, the length of capillary may be cut differently each time, or the inside diameter of glass capillary may vary within each lot. Also room vibration (there are 3 pumps, 1 air conditioner and 2 hoods operating each day) may cause early detachment of bubble. Therefore, the DST set-up is calibrated by water each day (Water surface tension is 72.75 dyne/cm at 20° C). After calibrated by water, it is important to use the same capillary for all samples. The following sensitivity analysis confirms this importance:

- ± 0.48% error by every ± 1 mm error immersion depth
- ± 6.66% error by every ± 0.01 mm error capillary I.D.
- ± 5.00% error by every ± 1 mm error capillary length

As mentioned in the literature review, it is very important to use only singlet bubble patterns. Using the singlet bubble pattern reduces complexity and increase accuracy and

reproducibility. A singlet bubble pattern is not always obtained with any experimental set-up. The controlling factor is the length of capillary (Mysels, 1986). Mysels used a capillary length 40 mm to avoid a bubble train pattern appear. However, if the length is too long, then the 'dead time' during the explosion of the bubble becomes excessive. Capillary length between 25 - 40 mm always produced a singlet bubble pattern in this study. For each millimeter capillary length increase (for capillary I.D. = 0.15 mm and gas flow rate = 1 ml/min) the system pressure increases 0.056 in. W.C. Since the experimental set-up is calibrated at the beginning of each experiment, this pressure drop will not affect the results as long as the capillary length is not changed during the experiment. The other minor controlling factor is the cleanliness (or smoothness) of the inside of the capillary tube. Carefully examine the capillary with magnify, discard the capillary has particulate and/or water drops inside.

The choice of source water for calibration is dependent on the sample matrix. It can be tap water (for example, during clean water aeration testing, tap water is matrix) or D.I. water for the surfactant standards. It is interesting to know the surface tension difference between these two sources of water. Repeated measurements were performed over four days for both water sources (Figure 41). The standard deviations for D.I. water and tap water are ± 0.41 and ± 0.30, respectively. It is concluded, the surface tension difference between two water sources is not statistically significant. The water surface tension obtained with this set-up indicates surface tension value about +3.35dyne/cm higher than CRC value (+4.6% error). This error could originate from capillary diameter. The

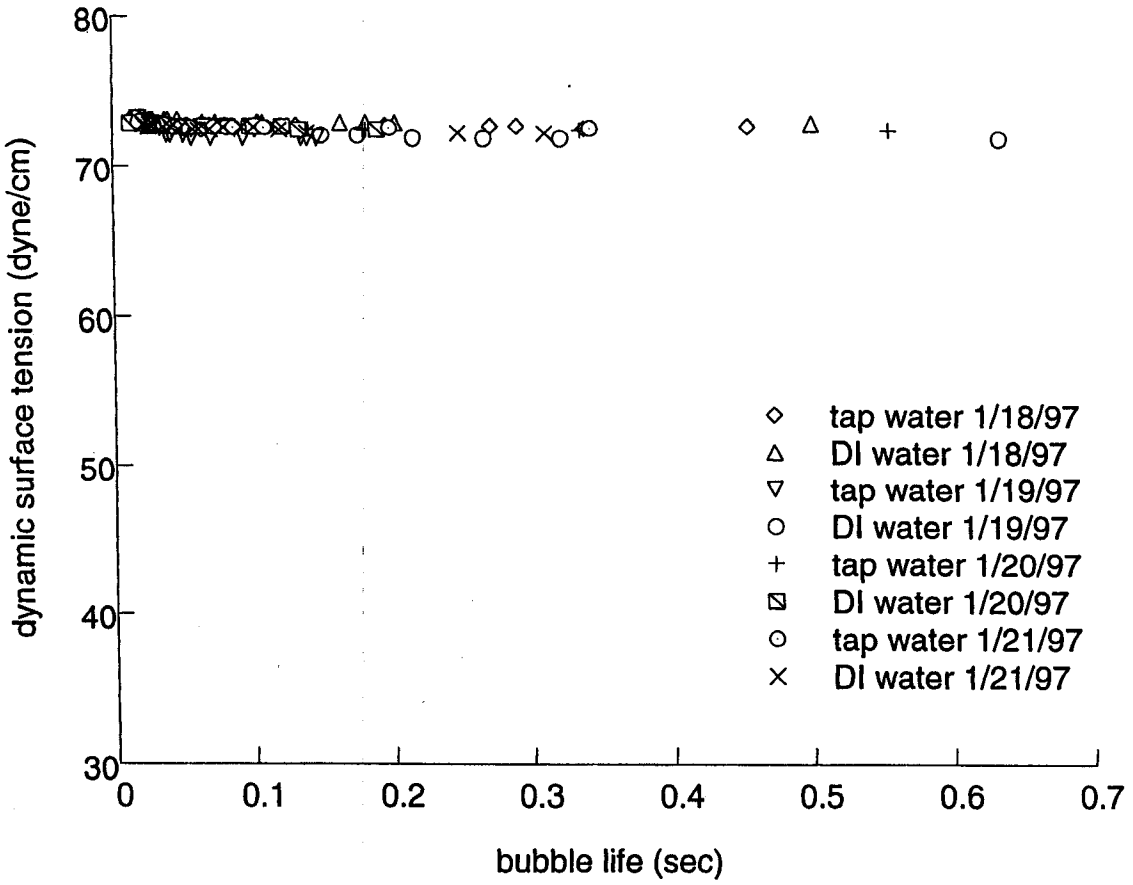

Figure 41. DST of D.I. water and tap water.

manufacturer's nominal capillary I.D. is 0.15 mm. However, it could vary slightly, the capillary tubes are not manufactured in high precision. To overcome this systematic error, a correction procedure was developed and applied to all measurements:

1. Measuring water and samples surface tension as routine at lab temperature.
2. Calculating capillary "true" internal diameter using reported surface tension value for water.
3. Applying the calculated capillary I.D. for all other surface tension calculations.

C. Validation of Experimental Set-up

According to Laplace Equation, the accuracy of DST is related to the pressure difference between two ends of capillary tube. The pressure difference (ΔP) consists two parts:

$$\Delta P = \Delta P_1 + \Delta P_2 \qquad (84)$$

where

ΔP_1 = Pressure difference for overcoming liquid surface tension

ΔP_2 = Pressure difference for compensating the friction

and

$$\Delta P_2 = \begin{cases} \frac{l}{r^2} \cdot Q & \text{laminar flow} \\ \frac{l}{r^{1.25}} \cdot Q^{1.75} & \text{turbulent flow} \end{cases} \qquad \begin{matrix} (85) \\ (86) \end{matrix}$$

where

l = Length of capillary

r = Internal radius of capillary

Q = Gas flow-rate

The surface tension is a static force while friction is a dynamic force. Therefore, when the flow-rate changes, the dominate force also changes. This can be demonstrated as shown in Figure 42. In this figure, when gas flow-rate is below a critical value, ΔP is controlled by ΔP_1. After a critical value, the ΔP is totally controlled by ΔP_2. A correct set-up should reveal the same relationship between pressure difference and gas flow-rate. In order to verify the constructed device, a set of experiments were performed. Figure 43 shows the results, and compare well with Figure 42. Yu and Shi (1988) performed their experiments at 25°C and using 0.106 mm I.D. capillary. This study was performed at 20°C using a 0.15 mm I.D. capillary. The overall pressure drop is smaller because of the larger capillary. The similarity of the results validates the experimental set-up.

Later in this research it will be desirable to measure dilute surfactant solutions, which are similar to the concentrations found in wastewater. DST measurements for concentrated solutions are easier to measure than for dilute solutions because the high concentration tends to mask spurious effects. To validate my experimental set-up, high concentration surfactant solutions were chosen for two reasons: 1) there are literature results that can be used for comparison 2) it is easier to predict the behavior of high concentration surfactant

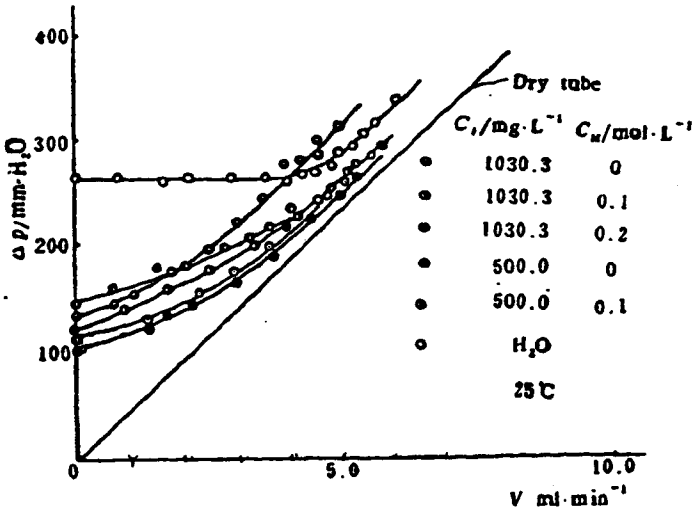

Figure 42. Plot of pressure difference versus gas flowrate (after Yu and Shi, 1988).

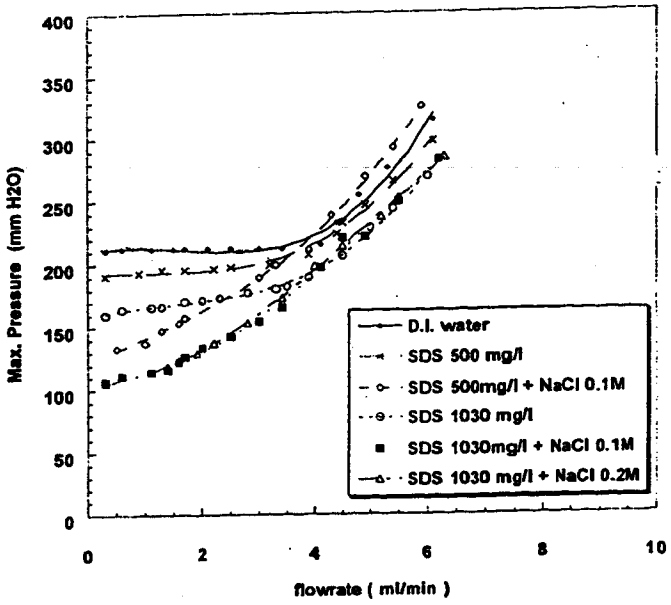

Figure 43. Maximum bubble pressure versus gas flowrate at different Sodium Dodecyl Sulfate concentrations.

solutions. Figure 44 shows Kloubek's (1972) results for various concentrations of SDS, which compare well with my results shown in Figure 45.

D. Equilibrium Surface Tension from MBPM versus Du Noüy Ring Method

From the literature review, we already know MBPM is not a good choice for measuring equilibrium surface tension of surfactant solution. However, from the surfactant kinetic studies we know that if the surfactant is pure then its surface tension falling rate (decrease in surface tension with respect to time) will be large and equilibrium surface tension can be reached within a short time (< 0.5 sec). Therefore, for pure surfactants, if highly accurate results are not required, the equilibrium surface tensions obtained by MBPM are sufficiently accurate. However, it is dangerous to extrapolate the equilibrium surface tension from DST plot without knowing the existence of impurities in surfactant.

Experiments were carried out with SDS, which was obtained from four different manufacturers in four different purities (refer to the Chemical Section). The equilibrium surface tension was measured by the Du Noüy Ring Method and MBPM for two concentrations. Figure 46 shows the discrepancy between these two methods. It becomes very significant when the surfactant contains more impurities. We already know that the impurities are also surface-active substances except they are highly active but slow adsorbing in comparison with primary surface active agent. It may take hours for the impurities reach equilibrium. Physically, the conventional MBPM (i.e. using gas flow-rate regulation by adjusting a flow meter) can not be used at such long bubble life. Several researchers (Kuffner, 1961; Kragh, 1964) suggested MBPM at constant pressure

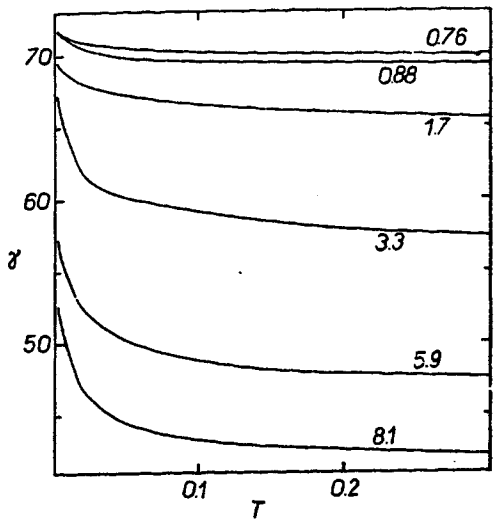

0.76 mM ~ 220 mg/l
0.88 mM ~ 250 mg/l
1.70 mM ~ 500 mg/l
3.3 mM ~ 1000 mg/l
5.9 mM ~ 1700 mg/l
8.1 mM ~ 2340 mg/l

Figure 44. DST of SDS at different concentrations (after Kloubek, 1972).

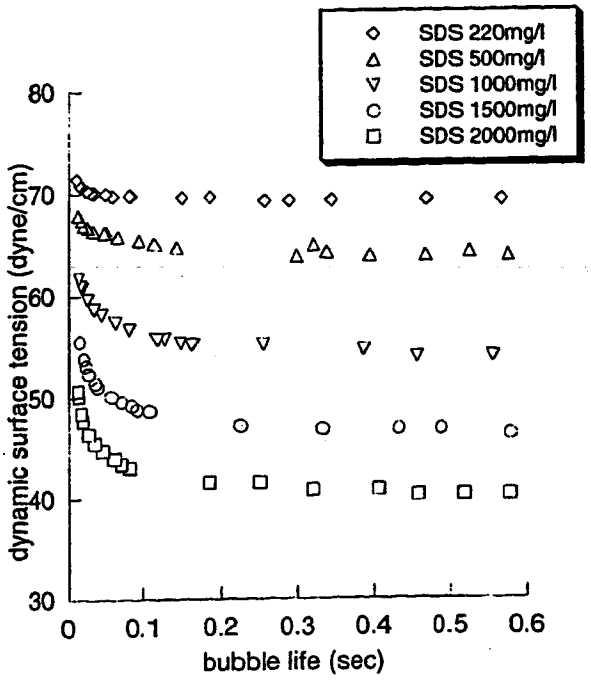

Figure 45. DST of SDS at similar concentration levels as Figure 43.

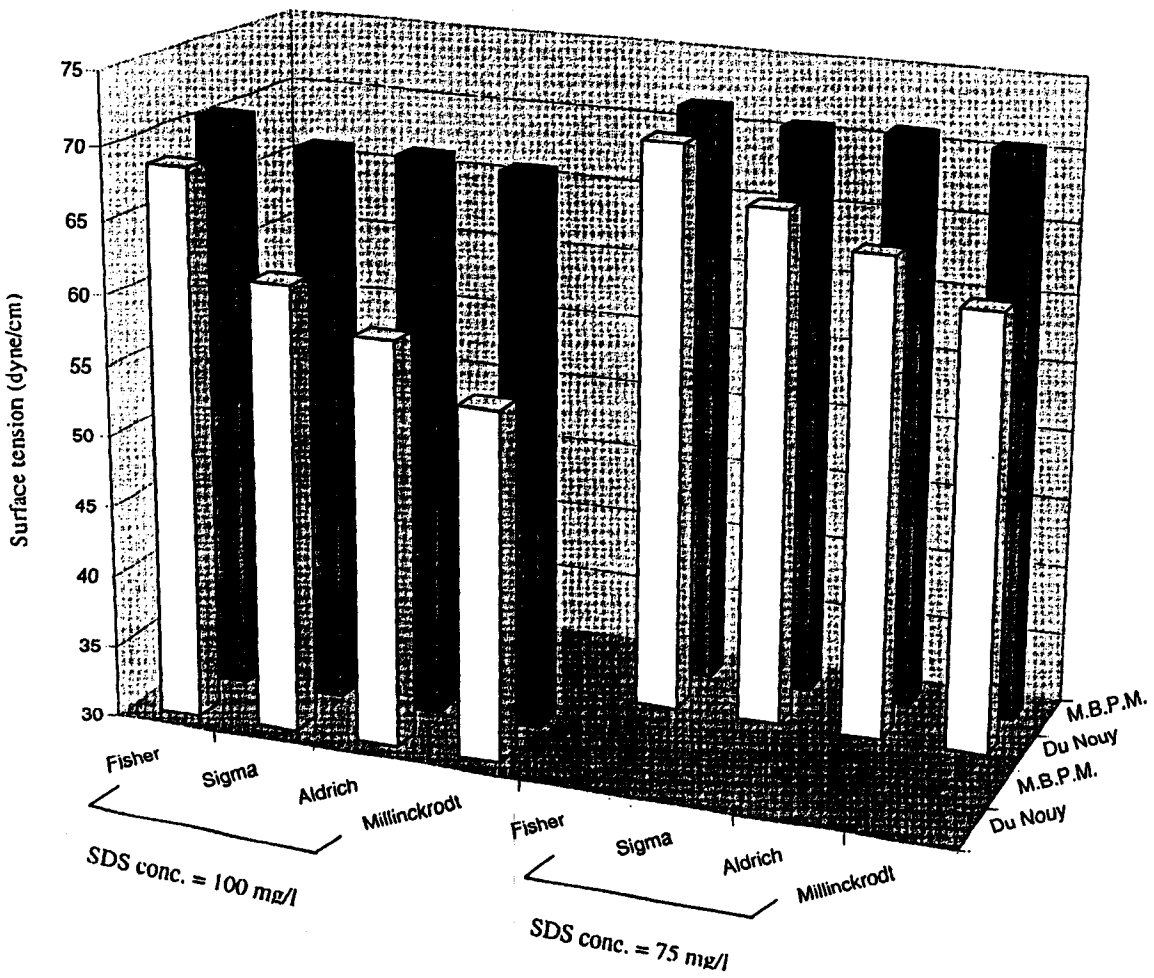

surface age:
MBPM - 6 min.
Du Nouy - 30 min.

purity of SDS:
Fisfer - 99.7%
Sigma - 95%
Aldrich - 70%
Millinckrodt - 95%

Figure 46. Impurity effect on surface tension.

can not be used for bubble life beyond 2 min. Adam and Shute (1938) reported that only by patiently maintaining constant pressure was he able to observe bubble life up to about 10 min. The reason is that the volume of an escaping bubble is extremely small (~1 mm^3), and minute temperature changes produce a slow pressure drift.

E. Applications

1. There are many applications of surface tension measurement (refer to Literature Review), and one is to detect polluted water. Sridhar (1984) used the Du Noüy Ring Method to determine water treatment plant performance, Gunde *et al.* (1992) used the Drop Volume Method. However, MBPM has never used in this application because of the short surface life it can provide. Nevertheless, it is interesting to know the DST behavior of water from a wastewater treatment plant. Therefore, three samples (primary, secondary and filtered secondary effluents) were collected from the Tapia plant (Las Virgines, California) and analyzed using the MBPM and the Du Noüy Ring Method. The results of this analysis (Figure 47) proved the difficulty of using MBPM for this application.

Many attempts have been made to prove that there is (or is not) a relationship between surface tension and the α-value during aeration. Du Noüy surface tension measurements of simulated wastewater have been used. The results either inconclusive (Stenstrom and Gilbert, 1981) or suggested no relationship (Wagner, 1996). The probable reason is that surface tension does not obtain equilibrium at short bubble life,

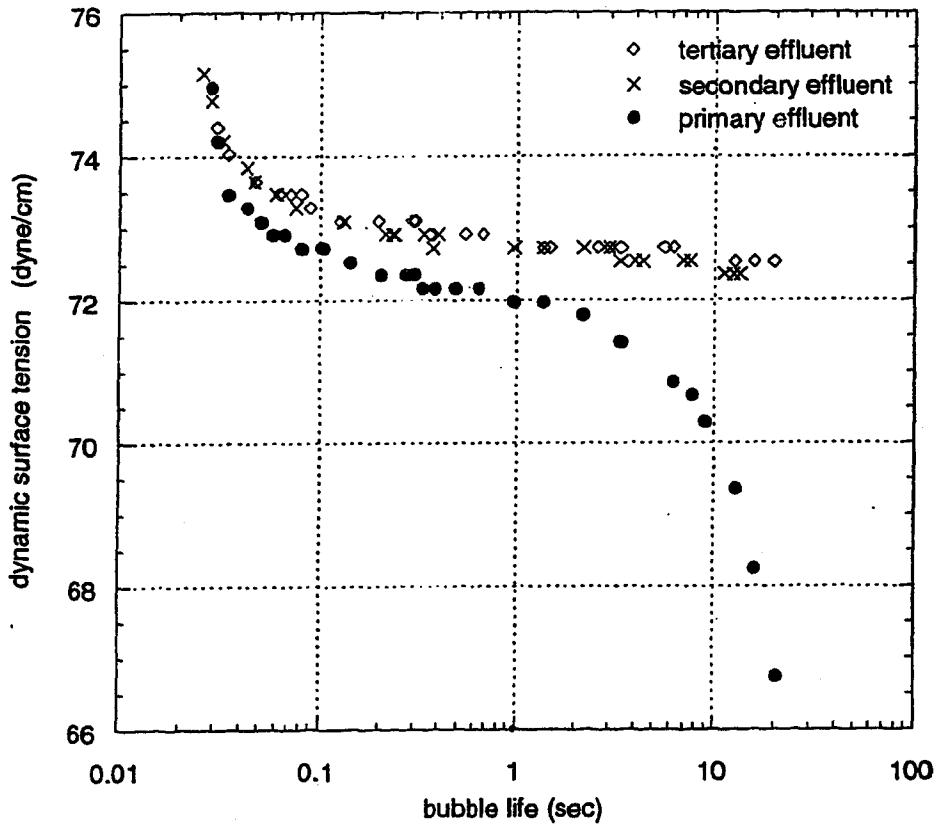

Figure 47. DST of wastewater effluents.

Note: The equilibrium surface tension from Du Noüy method are

Primary effluent	37.77 dyne/cm
Secondary effluent	63.68 dyne/cm
Tertiary effluent	64.40 dyne/cm

Tertiary effluent is filtered secondary effluent.

which is most important for oxygen transfer. Relating equilibrium surface tension with mass transfer rate is not an appropriate choice. Figure 47 showed the DST of primary effluent that typically enters an aeration tank for biological treatment. Apparently, during bubble aeration, the surface tension of primary effluent varies with time and is not even close to equilibrium surface tension (36.63 dyne/cm in this study). This result suggests that DST is a much better choice for characterizing oxygen transfer.

III Preliminary Aeration Studies

The device showed in Figure 35 has a feature of measuring OTR and DST simultaneously. Each bubble created and released at the tip of capillary gave three types of information: bubble life, dynamic surface tension of the solution, and oxygen transfer coefficient of the aeration vessel (glass tube). Consequently, this device is very useful in correlating the relationship between DST and OTR. However, prior to using this device for this purpose, the error results from any sources have to be studied.

A. Dissolved Oxygen (DO) Probe Lag Study

The ASCE Clean Water Test procedure was used to measure transfer coefficients. Probe lag-induced error is known to alter the results of this test. In 1989, Philichi and Stenstrom studied a series of lab-scale reaeration experiments used DO probes with various lag times. They concluded that to limit the error in $K_L a$ estimation to less than 1%, the product of $K_L a$ and probe lag constant should be less than 0.02. The micro-oxygen electrode (MI-730, Microelectrodes, Inc.) that need for this research was not included in

Philichi's study. It is necessary to know the magnitude of the error by using this DO probe. A probe lag test was performed (Figure 48). The $K_L a$ obtained from this test was 3.7 hr^{-1} and probe lag constant was 1.63 sec (4.53 x 10^{-4} hr). The effect of probe lag, based on Philichi's study, was very small because the product of $K_L a$ and probe lag constant was less than 0.002.

B. Error Analysis

Errors often are introduced from experimental measurements and analytical instruments. These errors can not be overlooked because they can influence the accuracy or interpretation of the experimental data. This section is to analyze the uncertainties in the experimental results due to the measurements.

The inaccuracy in calculating $K_L a$ results from three possible error sources: temperature, water volume, and air flow-rate measurements. The error of the thermometer , graduate cylinder, and flowmeter that used in this research was ±0.3°C, ±0.2ml, and ±0.05ml/min, respectively. At a bubble life equals 0.106 sec, all measurements showed there was no effect in $K_L a$ result within the error range of water volume and flow-rate measurements. However, the temperature measurements using a traditional thermometer (analog reading) did show the uncertainty in $K_L a$ results, alternately, in α factor results (Figure 49). Notice that either at long or short bubble life, the error in α factor is significant. This

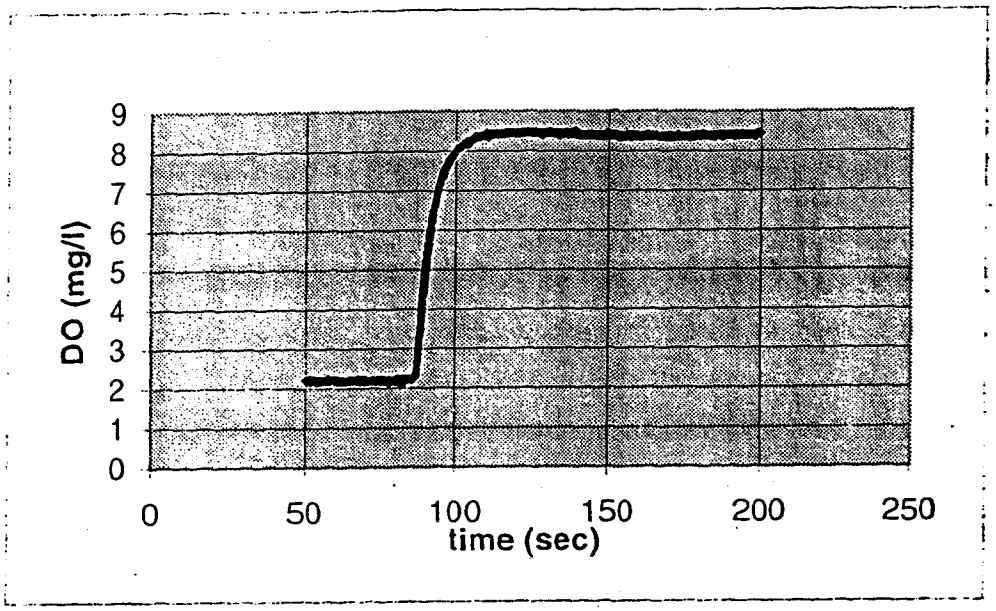

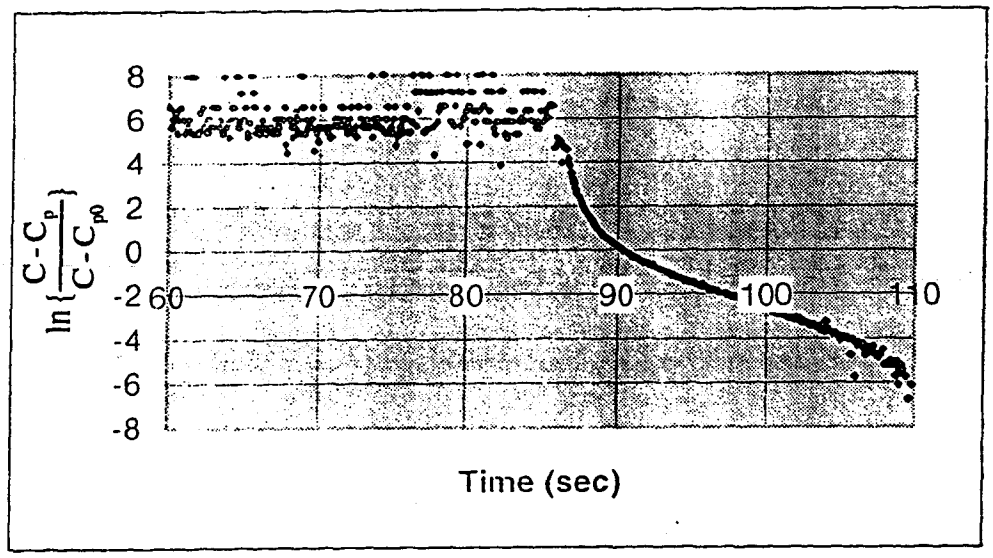

Figure 48. Probe Lag Analysis.

Note: C: tank DO concentration, mg/l
C_p: DO indicated by the probe, mg/l
C_{p0}: initial probe indication, mg/l

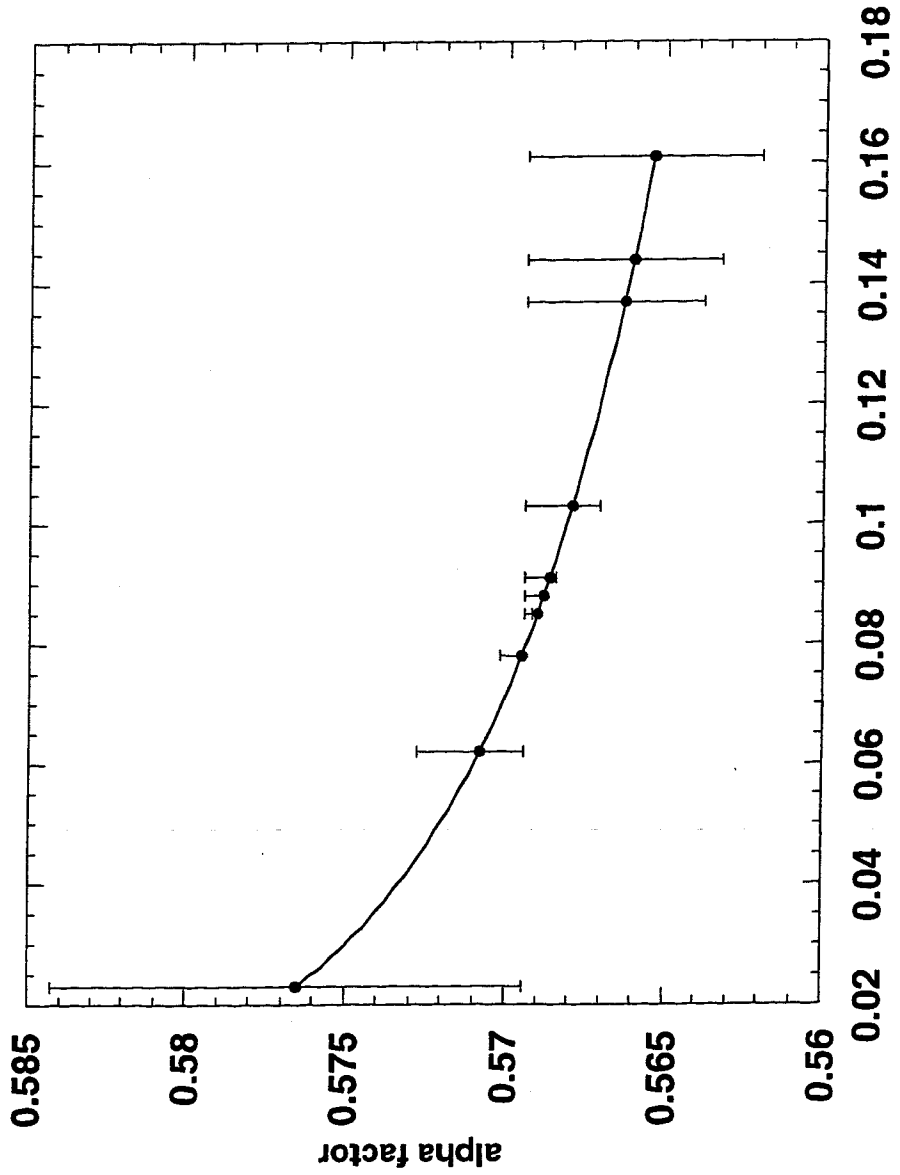

Figure 49. Estimated error for alpha factor subject to 0.3 °C error in measuring temperature.

research is mainly interested in $K_L a$, or α factor, behavior at short bubble life, therefore, the traditional thermometer was replaced by a digital thermometer (COOPER INSTRUMENT CORP., Electro-therm, TM99A) in order to eliminate the error results from temperature measurement.

C. Model Surfactant Selection and Deoxygenate Reagent Dosage Determination

The most important criteria for selecting the model surfactants was these two compounds must have very different diffusivity. This means one surfactant molecule diffuses very quickly to the bubble surface while the other diffuses slowly. This character will show on DST curve, ideally, as the high diffusivity compound has a very steep surface tension decline curve and the low diffusivity compound has a slow decline. This is required for the two model surfactants to have very different surface tension at the same bubble life. In addition, these two representative surfactant compounds selection were also based on the following factors:

(1). The vapor pressure of the model surfactants must be low, so that they will not evaporate during aeration;

(2). The model surfactants should be non-toxic and non-oxidized during aeration;

(3). The model surfactants must be as pure as possible in order to eliminate the unpredictable impurity effects during DST measurement, and

(4). The DST of the model surfactants were previously studied by researchers.

As a result of intensive literature search, in addition to Dodecyl Sodium Sulfite, iso-amyl alcohol (Addison, 1944) was chose as the second model surfactant in this study. The DST of both surfactants is showed in Figure 52; the characteristic of both surfactants as following:

Suface Active Agent	Molecular Weight	Purity	Vapor Pressure [KPa]	Diffusivity [cm^2/sec] @ 25°C
Sodium Dodecyl Sulfate ($CH_3(CH_2)_{11}OSO_3Na$)	288.38	99.7%	N/A	~ 10^{-6}
Iso-amyl Alcohol ($(CH_3)_2CHCH_2CH_2OH$)	88.15	99.9%	0.315 @ 25°C	~ 10^{-5}

To better represent the primary effluent in wastewater aeration unit, 5 - 15 mg/l SDS was ideal concentration for synthetic surfactant water, however, the device (Figure 35) can not detect dynamic surface tension depreciation at this concentration range during aeration. In fact, the dynamic surface tension detection limit of this device is that 45 mg/l for SDS and 0.020%(v/v) for iso-amyl alcohol. Therefore, we chose 50 mg/l and 0.025% (v/v) as concentration of SDS and iso-amyl alcohol, respectively.

The clean water used in the Standard Clean Water Test was tap water. However, the DST test at high purity SDS (99.7%, Fisher Scientific) dissolved in tap water showed an "impurity" effect (Figure 50 and 51), while in NANO water it showed no effect (Figure 51). Notice that, in section II-B of this chapter, the DST difference between tap water and DI water was negligible. The conclusion is true if the DST measuring device has higher surfactant detection limit, so that, the existence of trace amount of surface-active agent in the tap water is not detectable. However, the competition of adsorption between two surface-active agents will appear as soon as the DST of tap water is lowered by the

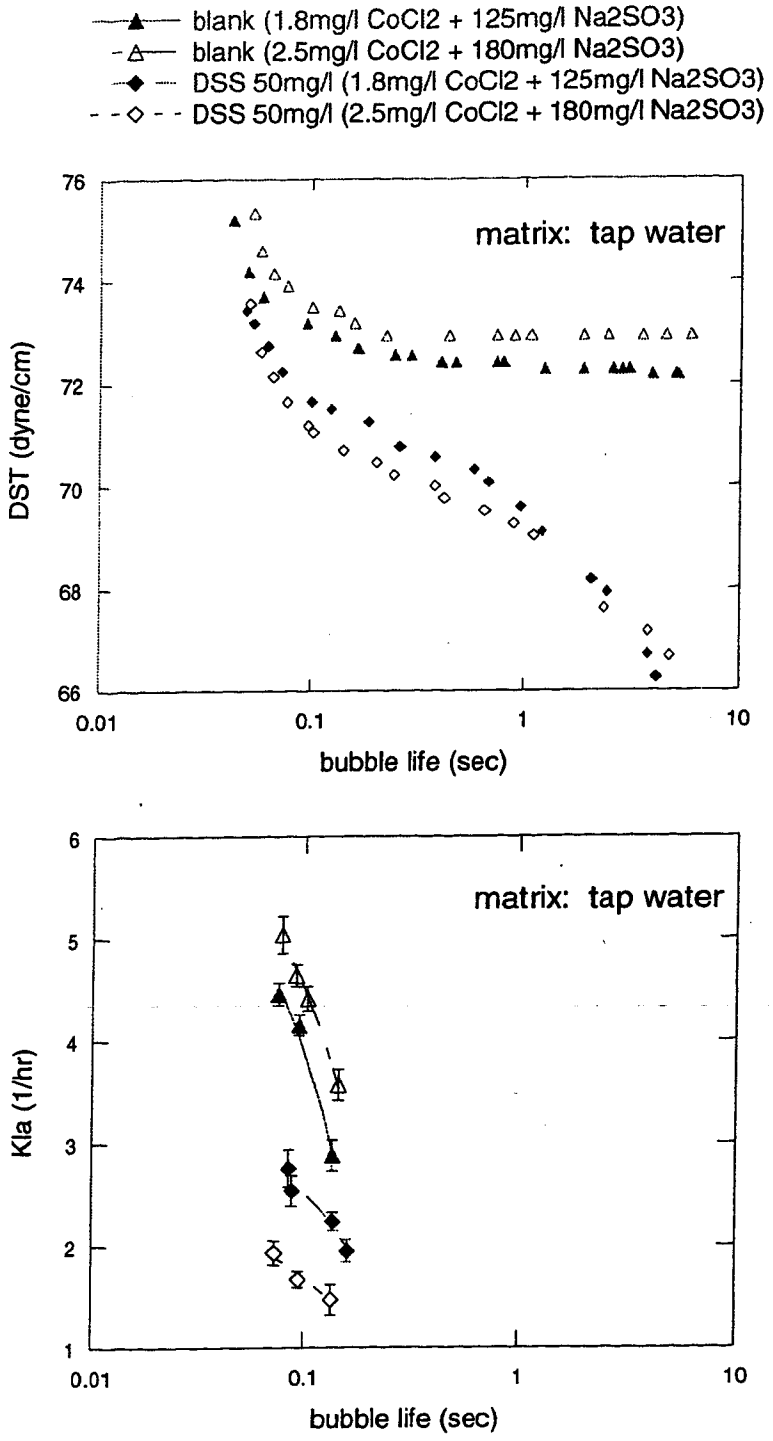

Figure 50. The dosage of deoxygenation chemical affects on dynamic surface tension and oxygen transfer rate.

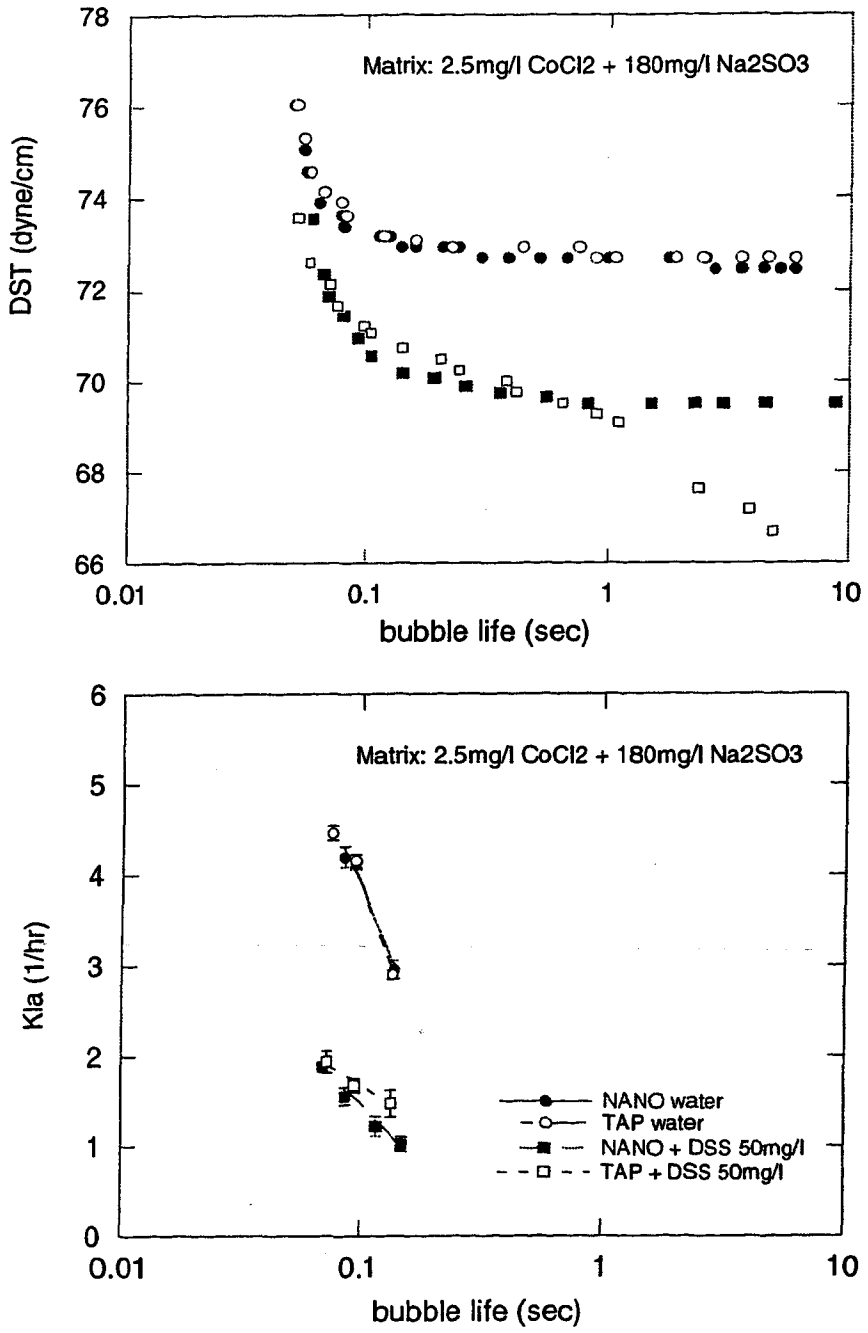

Figure 51. Water Quality Influences on Both Dynamic Surface Tension and Oxygen Transfer Coefficient.

dominant surface-active agent. To avoid the complication of impurity issue, both NANO water and pure surfactants were used in this research.

Sodium Sulfite and Cobalt Chloride Hydride, the deoxygenation chemical for clean water test, are salts. As mentioned in literature review, they have impact on DST of both water and SDS (Figure 50). Moreover, the higher dose of salts, the larger effect on DST. However, the effect of dosage of both chemicals on deoxygenation procedure has not been studied before. It was found that the dosages of both salts needed for deoxygenation of the surfactant water before clean water test must be experimentally determined.

The test water was freshly prepared by adding surfactant and deoxygenation chemicals (Na_2SO_3 and $CoCl_2 \cdot 6H_2O$) to 1000 ml tap (or NANO) water for each aeration test. The ASCE guidelines were used to estimate the mass of deoxygenation chemicals required for lowering dissolved oxygen concentration to less than 0.5mg/l. However, this research found the final DO concentration, before reaeration, depends on the sequence of chemicals' additon (Table 6) and the type and concentration of surfactant in test water (Table 7). Notice in Table 6(a), adding surfactant to the deoxygenated tap water arose final DO concentration. The reason for this phenomenon is unknown, but is probably related to binding the cobalt catalyst. But, Table 6(b) revealed that adding surfactant before adding deoxygenated chemicals is right sequence for preparing test water. Therefore, the dosage of Na_2SO_3 and $CoCl_2 \cdot 6H_2O$ depended on the type and amount of surfactant were used and it must be experimentally determined each time. In order to assure the soluble cobalt concentration in test water was sufficient (0.1 - 0.5mg/l), a series

Table 6. The Sequence of Chemical Addition Affected the Final DO Concentration of Test Water.

(a).

(1) Water type	DO of water [mg/l]	(2) $CoCl_2 \cdot 6H_2O$ [mg/l]	DO after Adding (2) [mg/l]	(3) Na_2SO_3 [mg/l]	DO after Adding (2)&(3) [mg/l]	(4) Surface Active Agent	Final DO [mg/l]
Tap water	6.242	1.08	7.597	107.92	0.45	0.01% (v/v) iso-amyl alcohol	5.380
Tap water	6.324	1.03	7.351	108.26	0.44	0.05% (v/v) acetic acid	2.053
Tap water	6.160	1.07	7.474	103.15	0.41	5 (mg/l) SDS	2.957

(b).

(1) Water type	DO of water [mg/l]	(2) Surface Active Agent	DO after Adding (2) [mg/l]	(3) $CoCl_2 \cdot 6H_2O$ [mg/l]	DO after Adding (2)&(3) [mg/l]	(4) Na_2SO_3 [mg/l]	Final DO [mg/l]
Tap water	6.357	11.05% (v/v) SDS	7.721	1.03	8.090	108.50	0.329
Tap water	6.411	5.43 mg/l Tergitol	7.844	1.01	8.419	110.13	0.370
Tap water	6.375	5.58 mg/l Aerosol OT	7.287	1.22	8.201	115.90	0.411

Temperature = 22.4 °C
Salinity = 0 mg/l
Dissoved Oxygen (DO) concentration = 8.624 mg/l @ 22.4 °C

Table 7. The Final Dissolved Oxygen Concentration for Different Surfactants after Adding Same Amount of Deoxygenation Chemicals

(1) Water Type	*DO of Water [mg/l]	(2) Surface Active Agent	DO after Adding (2) [mg/l]	(3) $CoCl_2 \cdot 6H_2O$ [mg/l]	DO after Adding (2) & (3) [mg/l]	(4) Na_2SO_3 [mg/l]	Final DO [mg/l]
Tap Water	6.357	5.89 mg/l DSS	7.515	1.01	8.213	107.72	0.205
Tap Water	6.368	50.23 mg/l DSS	7.146	1.06	8.008	107.00	0.616
Tap Water	6.467	0.01% (v/v) Acetic Acid	8.583	1.08	8.624	107.55	6.899
Tap Water	6.475	0.1% (v/v) Acetic Acid	8.295	1.03	8.501	108.50	8.213
Tap Water	6.411	5.43 mg/l Tergitol	7.843	1.01	8.419	110.13	0.370
Tap Water	6.371	10.03 mg/l Tergitol	8.583	1.03	8.624	111.47	1.930

*DO: dissolved oxygen concentration

of experiments were performed using atomic absorption hydride generation technique (3300, Perkin Elmer) to determine soluble cobalt concentration before adding sodium sulfite (Table 8). The results showed that certain amounts of soluble cobalt had reacted with surfactant and remaining concentration was sufficient for the catalyzing deoxygenation reaction. This chemical reaction between the soluble cobalt and surfactant must release some form of oxygen in water, therefore, the DO concentration rose to nearly saturation level (Table 7). Another important phenomenon revealed in Table 8 was that surfactant solutions made of NANO water required more deoxygenation chemicals than solutions made from tap water.

IV. Simultaneous DST and $K_L a$ Measurements

As mentioned earlier, the device (Figure 35) measures DST and $K_L a$ simultaneously. During an experiment, both the changes of system pressure and dissolved oxygen concentration were collected by Daqview and processed using Microsoft Excel. Although Daqview allows sample collection in multiple channels, all channels must use the same sampling rate. However, the required sampling rate for DST (250/sec) and $K_L a$ (2/min) are quite different. Consequently, the aeration test was started at 2/min sampling rate until near completion. The sampling rate was then increased to 250/sec to record the system pressure changes due to bubble creation and release.

Simultaneous DST and $K_L a$ measurements ware performed on both SDS and iso-amyl alcohol solutions, with experimentally determined deoxygenating chemical dosage. In

Table 8. The Concentration of Soluble Cobalt and Sodium Sulfite Effect on Final DO Concentration.

Water Type	Surfactant		$CoCl_2 \cdot 6H_2O$ [mg/l]	Soluble Cobalt Conc. Added [mg/l]	Soluble Cobalt Conc. From AA* [mg/l]	Na_2SO_3 [mg/l]	Dissolved Oxygen Conc. @20°C [mg/l]
Tap Water	SDS	50.08 [mg/l]	1.841	0.456	0.245	125.70 (185%)†	0.0
NANO Water	SDS	50.35 [mg/l]	1.865	0.462	0.260	125.45 (185%)	4.3
NANO Water	SDS	50.57 [mg/l]	2.503	0.620	0.403	163.17 (240%)	1.2
NANO Water	SDS	50.50 [mg/l]	2.503	0.620	0.403	180.04 (265%)	0.0
NANO Water	Iso-amyl Alcohol	0.020% (v/v)	3.028	0.750	0.400	300.09 (442%)	1.8
NANO Water	Iso-amyl Alcohol	0.020% (v/v)	3.028	0.750	0.400	350.30 (515%)	0.3
NANO Water	Iso-amyl Alcohol	0.025% (v/v)	3.028	0.750	0.418	400.32 (589%)	0.2

* Atomic Absorption.
† The amount of excess of stochiometric amount.

Figure 52, the DST of iso-amyl alcohol declined sharply within first 0.1 second and reached equilibrium surface tension at 0.4 second of bubble life. However, after gradually decline, the DST of SDS finally reached equilibrium at bubble life of 2 seconds. This outcome was expected. Notice that, although the diffusivity of iso-amyl alcohol is higher than of SDS, the molecular size of iso-amyl alcohol (5 carbons) is much smaller than of SDS (12 carbons). This implies longer time is needed for iso-amyl alcohol transport to subsurface layer. Therefore, at the same surface life, the bubble surface of iso-amyl alcohol solution is cleaner for higher oxygen transfer. A close examination of $K_L a$ at different bubble life (Figure 52) revealed two information: (1) The oxygen transfer rate is highest as bubble surface freshly formed. As bubble's life increases, the surfactant molecule starts to adsorb to the bubble surface, which results in decreasing in transfer rate. (2) At the same bubble life, the DST of iso-amyl alcohol is higher than of SDS. This implies the bubbles, which are covered only by iso-amyl alcohol, have more vacant site for oxygen transfer. Consequently, the $K_L a$ of the solution only contains iso-amyl alcohol is higher than the solution only contains SDS at the same surface life. In addition, since higher gas flow-rate generates shorter bubble life, the $K_L a$ is larger at higher flow-rate (Figure 53). This is consistent with the results we have been known from other researchers' work.

In order to clearly show the relationship among $K_L a$, DST, and bubble life, a re-plot of Figure 52 was showed in Figure 54. In 1988, Masutami and Stentrom related $K_L a$ to the

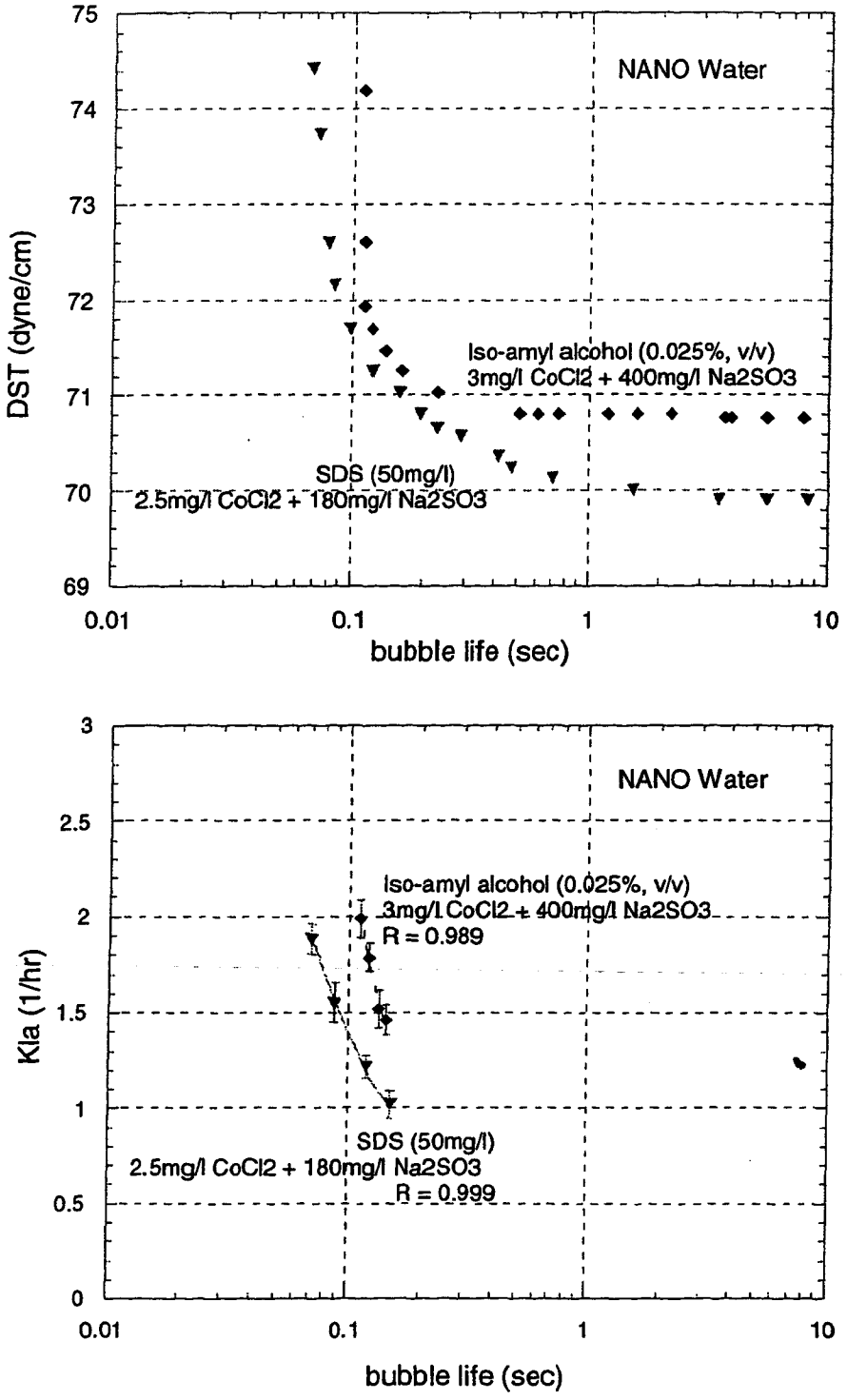

Figure 52. The DST and Kla Results for Both SDS and Iso-amyl Alcohol Solutions Using Simultaneous Measurement.

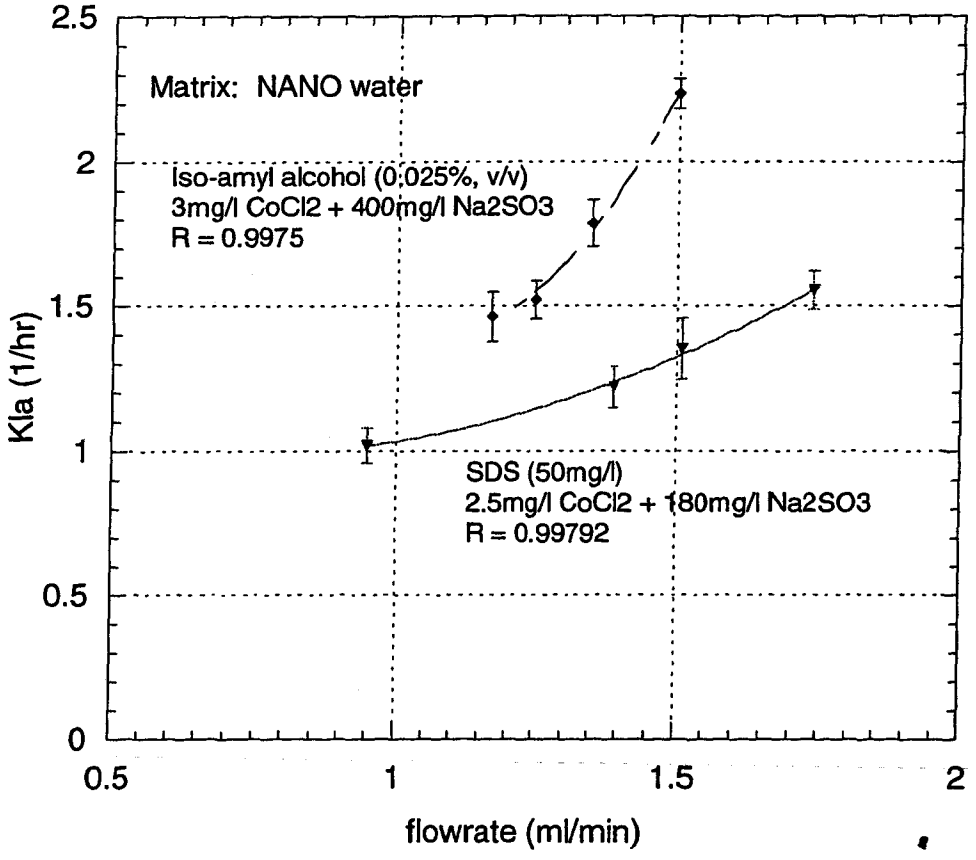

Figure 53. Kla Relationship with Gas Flowrate.

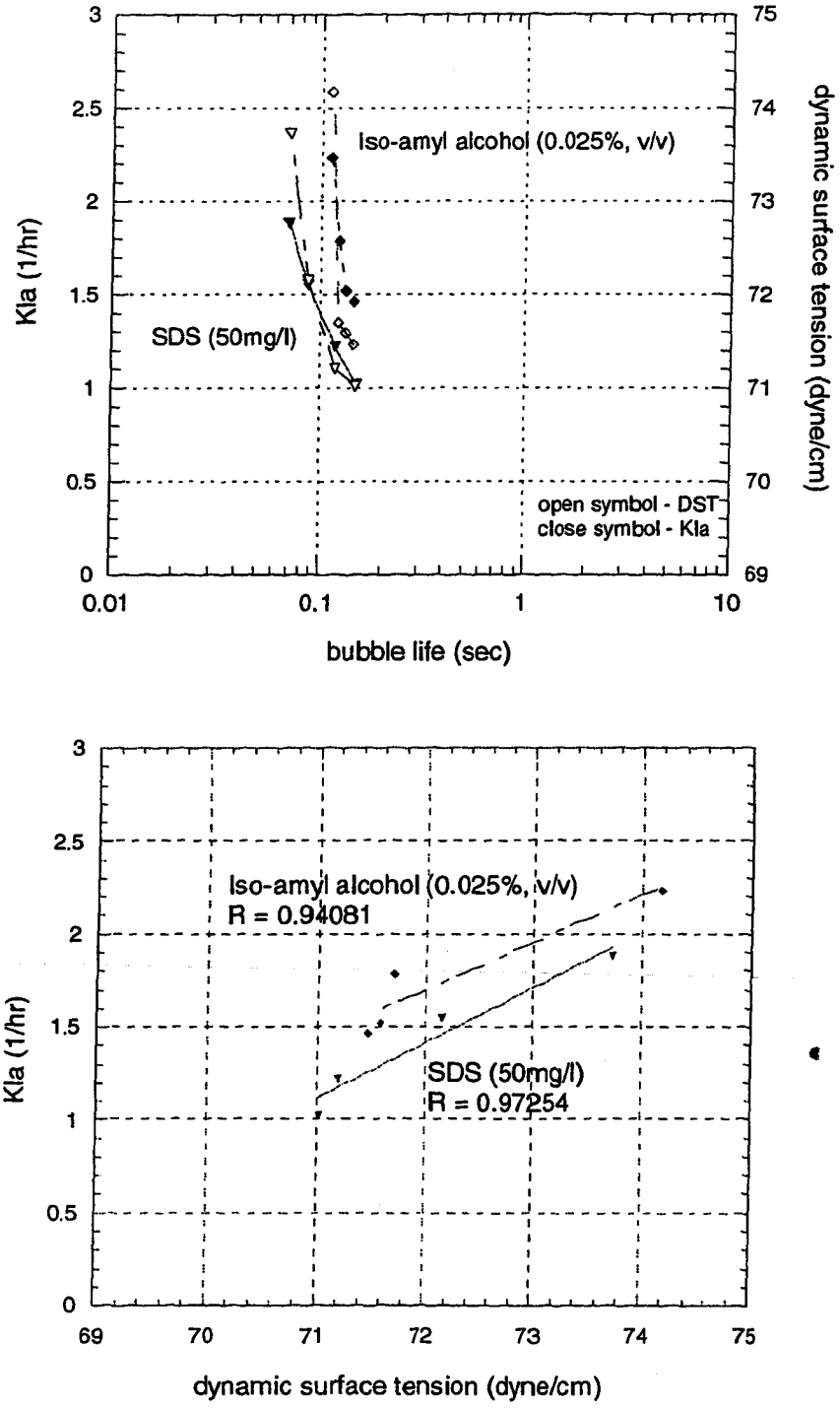

Figure 54. Replot of Figure 52.

slope of DST. In this work, with more advanced design in experimental device, the results shown in Figure 54 confirmed that $K_L a$ value at very short bubble life was very close to the slope of DST. However, to safely conclude $K_L a$ and DST have linear relationship as shown in Figure 54, more aeration tests at different bubble life will be necessary.

The total volumetric oxygen transfer coefficient is a function of liquid film transfer coefficient (K_L) and total transfer surface area (a). Lower K_L may be compensated by larger total transfer surface area, gives higher $K_L a$. Theoretically, K_L increases with bubble retention time during clean water aeration. However, when there are surfactants in the water, the K_L reduces because the surfactant adsorbs onto the bubble surface, that, not only decreases the mobility of the bubble interface but also the internal gas circulation (hydrodynamic effect). But, as soon as the bubble surface is completely covered by surfactant, internal circulation resumes, the K_L will increase again. Figure 55 has shown the K_L changes with retention time for iso-amyl alcohol and SDS. As mentioned earlier, the molecule of iso-amyl alcohol is very small, therefore, longer time is required for iso-amyl alcohol molecule transporting to subsurface and diffusing onto the surface. In other words, retention time from 1.2 to 1.26 second is not long enough for iso-amyl alcohol molecules completely covering the bubble surface. Consequently, K_L decreased in this retention time because the surface tension gradient result from iso-amyl alcohol molecule adsorption. On the other hand, the surfactant SDS completely covered the bubble surface

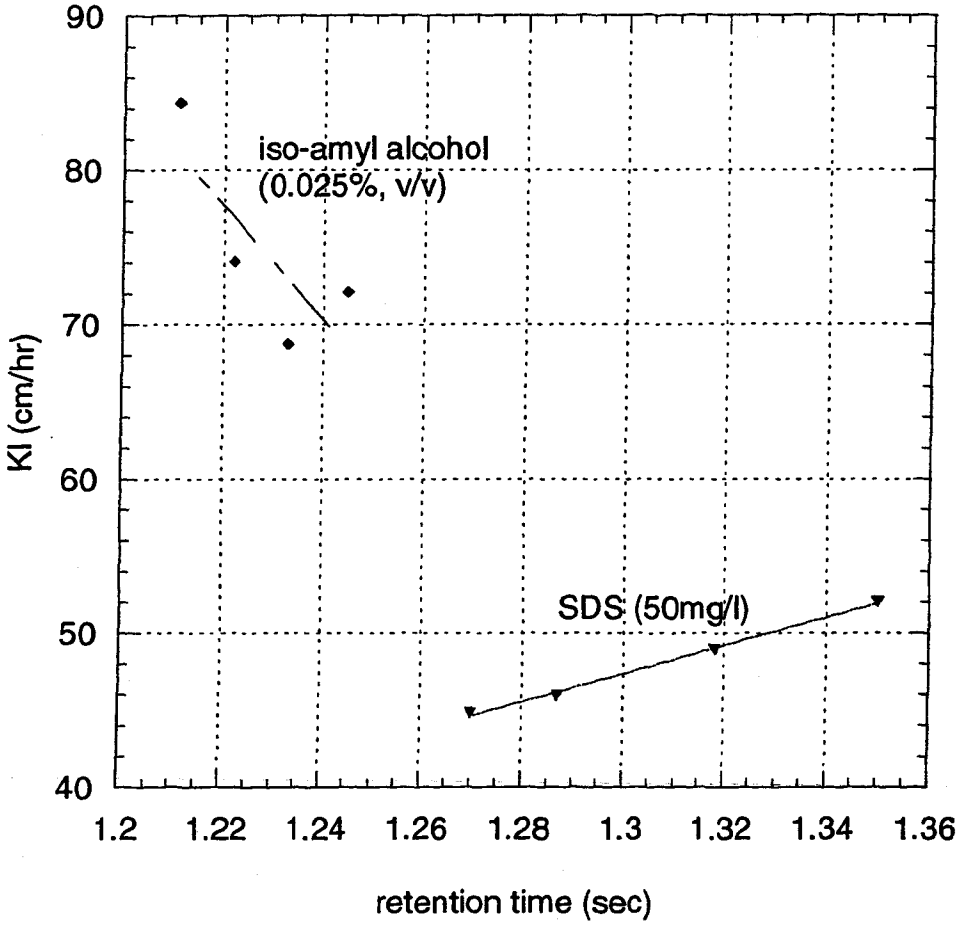

Figure 55. Liquid Film Transfer Coefficient Versus Bubble Retention Time

in the time of 1.26 to 1.36 second. As result of this, the surface tension gradient disappeared and K_L increased in this time range.

The bubble size and terminal rise velocity were used to calculate retention time. Bubbles were photographed during aeration, however, the bubble diameter measuring tool, a ruler with 0.1 cm graduation, was not sufficient enough to distinguish the bubble diameter differences between both surfactant solutions. In addition, the depth of aeration column was too shallow (28 cm) to ascertain differences between the bubble with terminal velocity 25.1 cm/sec and 24.8 cm/sec.

The aeration systems are an important requirement for normal activated sludge plant operation. Over the past several decades, many improvements have been made in process water testing procedures for evaluating bubble diffuser aeration systems. Neverthless, the problem in translating clean water results to process conditions still remains unsolved. British surfactant-enhanced aeration test requires 5 g/m^3 of an arbitrary anionic surfactant into clean water in order to simulate the oxygen transfer rate of aeration systems in wastewater.

It is known that surfactants influence α value during bubble aeration. Many researchers tried to relate the surface tension to α value. However, this research found that α value is a time function. The α value is largest as bubble freshly created. As bubble surface aged the α value decreses, and the rate of α value drops is surfactant dependent (Figure 56).

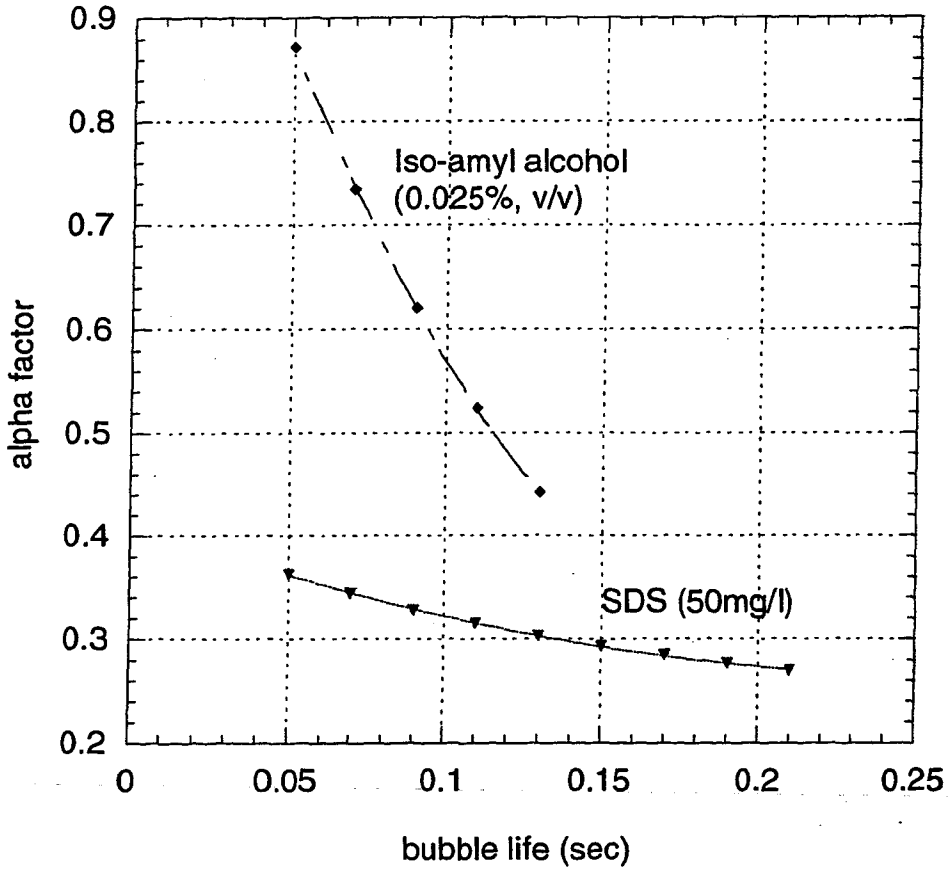

Figure 56. Different Surfactants Effect on Alpha Fators

In Figure 56, there are only two surfactants were used in this study, however, it is clear that at the same bubble age (flow-rate), the α value is not a single value. For wastewater contains mixtures of surfactant, a range of α values should be used for designing the aeration tanks.

CONCLUSIONS

Previous attempts to correlate static surface tension (SST) to oxygen transfer rate of a new surface have had very limited success. In 1988, dynamic surface tension (DST) effect on oxygen transfer in activated sludge system was studied in our laboratory. The results showed that DST, along with other easily measured aeration parameters (i.e. SST and gas flow-rate), were useful to estimate the volumetric oxygen transfer ($K_L a$) and liquid film oxygen transfer coefficients (K_L).

To continue this research, a second DST device was constructed, which was an improvement over the previous device. The new device measured DST and $K_L a$, simultaneously, for sodium dodecyl sulfate and iso-amyl alcohol solutions. The results were used to correlate the $K_L a$, DST and bubble life.

The following specific findings are made relative to this research:

1. The DST difference between tap and NANO (or DI) water is negligible if the measuring device has high detection limits, so that the small amounts of impurity (also a surface-active agent) in tap water are not detectable. However, the surfactant solution made of tap water showed the slow reduction in DST over long bubble life, but the solution made of NANO water showed no effect. The reason for this is the

competition of adsorption between surface-active agent and impurity can be detectable as soon as the DST of tap water was lowered by the surfactant.

2. The dosage of deoxygenating chemicals, $CoCl_2.6H_2O$ and Na_2SO_3, for different surfactant solutions or for the same surfactant solution but different concentrations must be experimentally determined. The experimental results showed the dose for surfactant solution made of tap water was higher than made of tap water alone. In order to calculate α factor (the ratio of the transfer rate in process water to clean water) correctly, the amount of $CoCl_2.6H_2O$ and Na_2SO_3 added to surfactant solution and matrix water must be the same.

3. Simultaneously measured DST and $K_L a$ has shown the $K_L a$ reduction rate, at short bubble life, is parallel to the DST reduction rate. Furthermore, the DST and $K_L a$ showed a linear relationship. An attempt was made to correlate K_L, DST, and bubble life. A random relationship was obtained.

FUTURE RESEARCH

The device, which was built in this research has demonstrated the feasibility of usage in studying the impact of surfactant in oxygen transfer. Moreover, it also demonstrated the feature of relating the oxygen transfer rate to dynamic surface tension by measuring both parameters simultaneously. Further research, however, is necessary to improve the device's capability, so that a more general and accurate relationship between OTR and DST can be obtained. The following are suggestions for future research area.

(1) Flow-rate measurement. The traditional analog flow meter is very difficult to control or measure the low gas flow-rate. There are many alternatives such as, a digital flow-rate controller, syringe pump, HPLC pump, or using water flow to displace air to create the gas flow, can be researched in order to increase the accuracy of gas flow-rate measurement.

(2) The dosage of soluble cobalt and sodium sulfite effect on surfactant solution deoxygenation mechanism needs to further investigation. It is suggested both total cobalt and soluble cobalt for different surfactant solutions were measured so that a stoichometric relationship between surfactant and soluble cobalt can be established.

REFERENCES

Adam N.K. and H.L. Shute (1938), "Anomalies in the Surface Tension of Paraffin Chain Salts", *Trans. Faraday Soc.*, 34, 758-765.

Adamson A.W. (1976), *Physical Chemistry of Surfaces*, 3rd Ed., John Wiley & Sons, New York, NY, 1-43.

Addison C.C. (1943), "The properties of Freshly Formed Surfaces. Part I. The Application of the Vibrating-jet Technique to Surface-tension Measurements on Mobile Liquids", *J. Chem. Soc.*, 535-541.

Addison C.C. (1944), "The properties of Freshly Formed Surfaces. Part II. The Rate of Adsorption of iso Amyl Alcohol at the Air-Water Surface", *J. Chem. Soc.*, 252-256.

Addison C.C. and S.K. Hutchinson (1948), "The Properties of Freshly-formed Surfaces. Part IX. Expansion of Soluble Films of Sodium Dodecyl Sulphate at Air-Water and Toluene-Water Interfaces", *J. Chem. Soc.*, 943-948.

Addison, C.C. (1945), " VII. The Measurement of Surface and Interfacial Tensions at Fresh Surfaces by the Vibrating Jet Method", *Philosophical Mag.* 36, 253, 73-100.

Akers, R.J. (1976), *Foams*, Academic Press, London.

Akita K. and F. Yoshida, (1974), "Bubble Size, Interfacial Area, and Liquid-Phase Mass Transfer Coeffeicient in Bubble Columns", *Ind. Engr. Chem., Process Des. Develop.*, v.13, n.1, 84-91.

Andrews G.F., R. Fike, S. Wong (1988), "Bubble hydrodynamics and mass transfer at high Reynold number and surfactant concentration", *Chem. Engr. Sci.*, 43, 7, 1467-1477.

Austin M., B.B. Bright, E.A. Simpson (1967), "The Measurement of the Dynamic Surface Tension of Manoxol OT Solutions for Freshly Formed Surfaces", *J. Colloid and Interface Sci.*, 23, 108-112.

Boyle W.C., P.M. Berthonex, and T.C. Rooney (1974), "Pitfalls in Parameter Estimation for Oxygen Transfer Data", ASCE, *J. of The Environmental Engineering Division*, 100, EE2, 391-408.

Bass S.J., and G.L. Shell (1977), "Evaluation of Oxygen Transfer Coefficients of Complex Wastewaters, *Proceedings, 32nd Purdue Industrial Waste Conference*, Ann Arbor Science, Ann Arbor, Mich., 953-967.

Bardavid S.M., G.C. Pedora and M. Katz (1994), "Surface Tensions of Some Nonelectrolyte Binary Liquid Mixtures", J. *Colloid and Interface Sci.*, 165, 264-268.

Barnhart, E.L. (1969), "Transfer of Oxygen in Aqueous Solutions", *J. Sanit. Engr. Div.*, ASCE, 95, 645-661.

Batchelor G.K., F.R.S. (1967), *An Introduction to Fluid Dynamics*, Cambridge University press, 474-481.

Bendure R.L. (1971), "Dynamic Surface Tension Determination with the Maximum Bubble Pressure Method", *J. Colloid and Interface Sci.*, 35, 2, 238-248.

Bernardin C.P. (1993), *C/MATH Toolchest for Engineering and Scientific Applications*, PTR Prentice Hall, Englewood Cliffs, New Jersey.

Bird R.B., W.E. Stewart and E.N. Lightfoot (1960), *Transport Phenomena*, John Wiley & Sons, New York.

Boucher E.A., T.M. Grinchuk, A.C. Zettlemoyer, (1967), *J. Colloid Interface Sci.*, 23, 600.

Bogaert, R. van den and P. Joos (1979), "Dynamic Surface Tensions of Sodium Myristate Solutions", *J. Phys. Chem.*, 83, 17, 224-2248.

Brennen C.E. (1995), *Cavitation and Bubble Dynamics*, Oxford University Press, New York.

Brown L.C. (1978), Oxygen Transfer Parameter Estimation: In *Proceedings : Workshop Toward an Oxygen Transfer Standard*, 27-40, EPA publication no. 600/9-78-021.

Burcik E.J. (1950), "The Rate of Surface Tension Lowering and its Role in Foaming", *J. Colloid Sci.*, 5, 421-436.

Campbell H.J., R.D. Ball, and J.H. O'Brien (1976), "Aeration Testing and Design - A Critical Review", Presented at the January 13, 8th Mid-Atlantic Industrial Waste Conference, held at Neward, Del.

Carver C.E., Jr. (1955),Adsorption of Oxygen in Bubble Aeration, in *Biological Treatment of Sewerage and Industrial Wastes*, v. 1, Reinhold Publishing Corporation, New York.

Clift R., J.R. Grace, and M.E. Weber (1978), *Bubbles, Drops and Particles*, Academic Press, New York.

Caskey J.A. and W.B. Barlage (1971), "An improved Experimental Technique for determining Dynamic Surface Tension of Water and Surfactant Solutions", *J. Colloid Interface Sci.*, 35, 1, 46-52.

Cusslor E.L. (1984), *Diffusion, Mass Transfer in Fluid Systems.* Cambridge University Press, Cambridge.

Dankworts, P.V. (1951), "Significance of the Liquid-Film Coefficient in Gas Absorption", *Ind. Engr. Chem.*, 43, 1460-1467.

Davidson J.F. and D. Harrison. (1963), *Fluidised Particles*, Cambridge University Press.

Davidson L. and E.H. Amick Jr. (1956), "Formation of Gas Bubbles at Horizontal Orifices", AIChE, 2, 3, 337-342.

Davies O.L. (1967), *Design and Analysis of Industrial Experiments*, 2nd Ed., Hafner.

Defay R. and G Pe'tre', (1991) "Dynamic Surface Tension" in : *Surface and Colloid Science*, Vol. 3, (Editor) E. Matijevic, Wiley-Interscience, New York.

Defay R. and R.J. Hommelen ((1958), "I. Measurement of Dynamic Surface Tensions of Aqueous Solutions by the Oscillating Jet Method", *J. Colloid Science*, 13, 553-564.

Downing A.L. (1960), "Aeration in the activated Sludge process", *J. of the Institute of Public Health Engr.*, 49, 80-118.

Doyle M.L. and W.C. Boyle (1985), Translation of Clean to Dirty Water Oxygen Transfer Rates, in *Proc. Seminar Workshop on Aeration System Design, Testing, Operation and Control*, EPA publication no. 600/19-85-45.

Drogaris, G. and P. Weiland (1983), "Coalescence behavior of gas bubbles in aqueous solutions of n-alcohols and fatty acids", *Chemical Engineering Science*, v38, n9, 1501-1506.

Du Nouy P. Lecomte (1919), "A new apparatus for measuring surface tension", *J. Gen. Physio.*, 1, 521-524.

Durham K. (1961), *Surface Activity and Detergency*, Macmillan & Company Limited, London.

Dushkin C.D. and Tx. H. Ilier (1994), "Dynamic Surface Tension of Micellar Solutions Studied by the Maximum Bubble Pressure Method. 2. Theory of the Solutions Below C.M.C.", *Colloid Polym. Sci.*, 272, 1157-1165.

Eckenfelder W.W. Jr., (1959), "Absorption of Oxygen from Air Bubbles in Water", *J. Sanitary Engineering Division*, SA4, 89-99.

Eckenfelder W.W., Jr. and D.L. Ford (1968), "New Concepts in Oxygen Transfer and Aeration", in *Advance in Water Quality Improvement*, (edited by Gloyna, E.F. and Eckenfelder W.W., Jr.), University of Texas Press, 215-236.

Elworthy P.H. and K.J. Mysels (1966), "The Surface Tension of Sodium Dodecylsulfate Solutions and the Phase Separation Model of Micelle Formation", *J. Colloid and Interface Sci.*, 21, 331-347.

Eversole W.G., G.H. Wagner and E. Stackhouse (1941), "Rapid Formation of Gas Bubbles in Liquids", *Ind. Engr. Chem.*, 33, 11, 1459-1462.

Fainerman V.B. (1992), "Adsorption Kineticcs from Concentrated Micallar Solutions of Ionic Surfactants at the Water-Air Interface", *Colloids and Surfaces*, 62, 333-347.

Fainerman V.B., A.V. Makievski and R. Miller (1993), "The Measurement of Dynamic Surface Tensions of Highly Viscous Liquids by the Maximum Bubble Pressure Method", *Colloids and Surfaces A : Physicochemical and Engineering Aspects*, 75, 229-235.

Fainerman V.B., R. Miller, P. Joos (1994), "The Measurement of Dynamic Surface Tension by the Maximum Bubble Pressure Method", *Colloid and Polymer Sci.*, 272, 731-739.

Fetter C.W. (1993), *Contaminant Hydrogeology*, Macmillan Publishing Company, New York.

Field J.A., J.A. Leenheer, K.A. Thorn, L.B. II Barber, C. Rostad, D.L. Macalady, S.R. Daniel (1992), "Identification of Persistent Anionic Surfactant-Derived Chemicals in Sewage Effluent and Groundwater", *J. Contaminant Hydrology*, 9, 55-78.

Filippov L.K. (1994), "Dynaimc Surface Tension of Aqueous Surfactant Solutions. 2. Diffusion - Kinetic - Vonvetive Controlled Adsorption", *J. Colloid and Interface Sci.*, 164, 471-482.

Frend B.B. and H.Z. Frend (1930), "A Theory of the Ring Method for the Determination of Surface Tension", *Amer. Chem. Soc. J.*, 52, 1772-1782.

Fujimoto T. (1985), *New Introduction To Surface Active Agents*, Sanyo Chemical Industries, Ltd., Kyoto, Japan.

Gal-Or B., G.E. Klinzing and L.L. Tarlarides (1969), "Bubble and Drop Phenomena", *Ind. Engr. Chem.*, 61, 2, 21-34.

Garner, F.H. and D. Hammerton (1954), "Circulation Inside Gas Bubbles", *Chem. Engr'. Sci.*, 3, 1-11.

Garrett P.R. and D.R. Ward (1989), "A Re-Examination of the Measurement of Dynamic Surface Tensions Using the Maximum Bubble Pressure Method", *J. Colloid and Interface Sci.*, v.132, n.2, 475-490.

Geankoplis C.J. (1983), *Transport Processes and Unit Operation*, 2 Ed. Allyn and Bacon, Inc., Boston.

Gilanyi T., Chr Stergiopoulos, and E. Wolfram (1976), "Equilibrium Surface Tension of Aqueous Surfactant Solutions", *Colloid & Polymer Sci.*, 254, 1018-1023.

Gilbert R.G. (1979), Measurement of alpha and beta factors. In *Workshop Toward an Oxygen Transfer Standard* (Edited by Boyle W.C.), 147-162. EPA publication no. 600/9-78-021.

Goldfinger G. (1970), *Clean Surface : Thin Preparation and Characterization for Interfacial Studies*, Chapter 13, Marcel Dekker, Inc. New York.

Gomezplata A. and T.M. Regan (1970), "Mass Transfer", *Industrial and Engineering Chemistry*, 62, 12, 140-147.

Gunde R., M. Davies and S. Hartland (1992), "Surface Tension of Wastewater Samples Measured by the Drop Volume Method", *Environ. Sci. Technol.*, 26, 1036-1040.

Gurol, M.D. and S. Nekoninaini (1985), "Effect of Organic Substances on Mass Transfer in Bubble Aeration", *J. Water Pollut. Control Fed.*, v.57,n.3, 235-240.

Haberman W.L. and R.K. Morton (1954), " An Experimental Study of Bubbles Moving in Liquids", *Amer. Soc. Civ. Engr. Trans.*, 227-250.

Hallowell C.P. and D.E. Hirt (1994), "Unusual Characteristics of the Maximum Bubble Pressure Method Using a Teflon Capillary", *J. Colloid and Interface Sci.*, 168, 281-288.

Hansen R.S., M.E. Purchase, T.C. Wallace and R.W. Woody (1958), "Extension of the Vibrating Jet Method for Surface Tension Measurement to Jets of Non-Uniform Velocity Profiles", *J. Phys. Chem.*, 62, 210-214.

Hanson R.S. and T.C. Wallace (1959), " The Kinetics of Adsorption of Organic Acids at the Water-Air Interface", *J. Phys. Chem.*, 63, 1085-1091.

Hardy C.D. and E.R. Baylor (1975), "Surface Tension Reductions and Urban Wastes in the New York bight", *J. Geophysical Research*, 80, 18,2696-2699.

Harkins W.D. and F.E. Brown (1919), "The Determination of Surface Tension (Free Surface Energy), and the Weight of Falling Drops : The Surface Tension of Water and Benzone By the Capillary Height Method", *J. Amer. Chem. Soc.*, 41, 499-524.

Harkins W.D. and H.J. Jordon (1930), "A Method for the Determination of Surface and Interfacial Tension from the Maximum Pull on a Ring", *Amer. Chem. Soc. J.*, 52, 1751-1772.

Harlsins W.D. (1949), "Determination of Surface and Interfacial Tension" in *Technique of Organic Chemistry*, Vol. 1, part 1, (Editor) Weissberger A., Interscience publishers, Inc., New York.

Hayes W.B., B.W. Hardy and C.D. Holland (1959), "Formation of Gas Bubbles at Submerged Orifices"' AIChE *J.*, 319-324.

Hermann L. (1965), "Dynamic Surface Tension of Detergent Solutions at Constant and Variable Surface Area", *Journal of Colloid Science*, 20, 50-61.

Higbie, R. (1935), "The rate of absorption of a pure gas into a still liquid during short periods of exposure", AIChE *Trans.*, 31, 365-388.

Hommelen J.R. (1959), "The Elimination of Errors Due to Evaporation of the solute in the Determination of Surface Tension", *J. Colloid Sci.*, 14, 385-400.

Huang H.J. and M.K. Stenstrom, "Evaluation of Fine Bubble Alpha Factors in Near Full-Scale Equipment", *J. Water Pollut. Control Fed.*, 57, 1143.

Hughes R.R., A.E. Handlos, H.D. Evans and R.L. Maycock (1955), "The Formation of Bubbles at Single Orifices", *Chem. Engr. Progress*, 51, 12, 557-563.

Huh C. and S.G. Mason (1975), "A Rigorous Theory of Ring Tensiometry", *Colloid Poly. Sci.*, 253, 566-580.

Ippen T. and C.E. Carver, Jr. (1954), "Basic factors of oxygen transfer in aeration systems", *Sewage Works J.*, 26, 813-820.

Jiang B., R.L. Varty, and L.W. Sigurdson (1993), "The Acceleration of a Single Bubble Rising from a Nozzle in Water", ASME, Fed-Vol. 165, Gas-Liquid flows - 1993, 161-169.

Jiang B., R.L. Varty, and L.W. Sigurdson (1993), "The Acceleration of a Single Bubble Rising from a Nozzle in Water", *Fed-Vol.165, Gas-Liquid Flows - 1993, ASME*, 161-169.

Joos P. and E. Rillaerts (1981), "Theory on the Determination of the Dynamic Surface Tension with the Drop Volume and Maximum Bubble Pressure Methods", *J. Colloid and Interface Sci.*, 79, 1, 96-100.

Joos P., J.P. Fang and G. Serrien (1992), "Comments on some Dynamic Durface Tension Measurements by the Dynamic Bubble Pressure Method", *J. Colloid and Interface Sci.*, 151, 1, 144-149.

Kalinske A.A., (1978), Problems Encountered in Steady-State Field Testing of Aerators and Aeration Systems: In *Proceedings: Workshop Toward an Oxygen Transfer Standard*, 27-40, EPA Publication no. 600/9-78-021.

Keitel, G. and V. Onken (1981), "Errors in the determination of mass transfer in gas-liquid dispersions", *Chemical Engineering Science*, v.3.6, n.12, 1927-1932.

Kippenhaum C. and D. Tegeler (1970), "A Bubble Growth Experiment for the Determination of Dynamic Surface Tension", AIChE *J.*, 314-316.

Kloubek J. (1972), "Measurement of the Dynamic Surface Tension by the Maximum Bubble Pressure Method. II. Calculation of the Effective Age of the Solution - Air Interface", *J. Colloid and Interface Sci.*, v41, n1, 1-6.

Kloubek J. (1972), "Measurement of the Dynamic Surface Tension by the Maximum Bubble Pressure Method III. Factors Influencing the Measurements at High Frequency of the Bubble Formation and an Extension of the Evaluation to Zero Age of the Surface", *J. Colloid and Interface Sci.*, v.41, n.1, 7-16.

Kloubek J. (1972), "Measurement of the Dynamic Surface Tension by the Maximum Bubble Pressure Method. IV. Surface Tension of Aqueous Solutions of Sodium Dodecyl Sulfate", *J. Colloid and Interface Science*, 41, 1, 17-22.

Kragh A.M. (1964), "Effect of Gelatin and Salts on the Dynamic Surface Tension of Manoxol OT", *Trans. Faraday Soc.*, 60, 225-232.

Kubiak A. and P Dejmek. (1993), "Application of Image Analysis to Measurement of Dynamic Surface Tension Using Oscillating Jet Method", *J. Dispersion Science and Technology*, 14(6), 661-673.

Kuffner R.J. (1961), "The Measurement of Dynamic Surface Tensions of Solutions of Slowly Diffusing Molecules by the Maximum Bubble Pressure Method", *J. Colloid Sci.*, 16, 497-500.

Lee Y.H., G.T. Tsao and P.C. Wankat (1980), "Hydrodynamic Effect of Surfactants on Gas-Liquid Oxygen Transfer", AIChE *J.*, v.26, n.6, 1008-1012.

Leibson I., E.G. Holcomb, A.G. Cacoso, and J.J. Jacmic (1956), "Rate of Flow and Mechanics of Bubble Formation from Single Submerged Orifices", AIChE, 296-306.

Leonard J.H. and G. Houghton (1963), "Mass Transfer and Velocity of rise phenomena for single bubbles", *Chemical Engr. Sci.*, 18, 133-142.

Levich V.G. (1962), Motion of Drops and Bubbles in Fluid Media, in *Physicochemical Hydrodynamics*, Prentice-Hall, Inc., Engleqood Cliffs, N.J.

Lewis W.K. and W.G. Whitman (1924), "Principles of Gas Absorption", *Industrial and Engineering Chemistry*, 16, 12, 1215-1220.

Libra J.A. (1993), *Stripping of Organic Compounds in an aerated stirred Tank Reactor*, VDI - Verlag GmbH, Dusseldorf, Germany.

Lin J.N., S.K. Banerji, and H. Yasuda (1994), "Role of Interfacial Tensions in the Formation and the Detachment of Air Bubbles. 1. A Single Hole on a Horizontal Plane Immersed in Water", *Langmuir*, 10, 936-942.

Lin J.N., S.K. Banerji, and H. Yasuda (1994), "Role of Interfacial Tensions in the Formation and the Detachment of Air Bubbles. 2. A Single Orifice on an Inclined Plane Immersed in Water", *Langmuir*, 10, 943-948.

Lin J.N., S.K. Banerji, H. Yasuda (1993), "Role of Interfacial Tension in the Formation and the Detachment of Air Bubble. 1. A Single Hole on a Horizontal Plane Immersed in Water", *Langmuir*, 10, 936-942.

Lin J.N., S.K. Banerji, H. Yasuda (1994), "Role of Interfacial Tensions in the Formation and the Detachment of Air Bubbles. 2. A Single Orifice on an Inclined Plane Immersed in Water", *Langmuir*, 10, 943-948.

Llorens J., C. Mans, and J. Costa (1988), "Discrimination of the effects of surfactants in gas absorption", *Chem. Engr. Sci.*, v.43, n.3, 443-450.

Lunkenheimer K., K.D. Wantke (1981), "Determination of the Surface Tension of Surfactant Solutions applying the method of Lecomte Du Nouy (Ring Tensiometer)", *Colloid & Polymer Sci.*, 259, 354-366.

Macleod C.A. and C.J. Radke (1994), "Surfactant Exchange Kinetics at the Air/Water Interface from the Dynamic Tension of Growing Liquid Drops", *J. Colloid and Interface Sci.*, 166, 73-88.

Makievski A.V., V.B. Fainerman and P. Joos (1994), "Dynamic Surface Tension of Micellar Trifon X-100 Solutions by the Maximum-Bubble-Pressure Method", *J. Colloid and Interface Sci.*, 166, 6-13.

Mancy K.H. and D.A. Okun (1960), "Effects of Surface Active Agents on Bubble Aeration", *J.Wat. Pollut. Control Fed.*, 32, 351-364.

Mancy K.H. and D.A. Okun (1960), "Effects of Surface Active Agents on Bubble Aeration", *J.Wat. Pollut. Control Fed.*, 37, 212-227.

Masutani G.K. (1988), "Dynamic Surface Tension Effects on Oxygen Transfer in Activated Sludge", Dissertation, Civil Engineering, University of California, Los Angeles.

McKinney R.E. and J.R. Stokenberg (1978), On Site Evaluation : steady state vs. Non steady state Testing. In *Proceedings : Workshop Toward an Oxygen Transfer Standard,* 195-204. EPA publication no. 600/9-78-021.

Miller R. (1980), "Zur Adsorptionskinetik an der Oberfläche wachsender Torpfen", *Colloid Polymer Sci.*, 258, 179-185.

Miller R. and G. Kretzschmar (1991), "Adsorption Kinetics of Surfactants at Fluid Interfaces", *Adv. in Colloid and Interface Sci.*, 37, 97-121.

Miller R., P. Joos and V.B. Fainerman (1994), "Dynamic Surface and Interfacial Tensions of Surfactant and Polymer Solutions", *Adv. Colloid and Interfacial Sci.*, 49, 249-302.

Motarjemi M. and G.J. Jameson (1978), "Mass Transfer from Very Small Bubbles - the Optimum Bubble Size for Aeration", *Chemical Engr. Sci.*, 33, 1415-1423.

Motarjemi M. and G.J. Jameson (1979), "The Effect of Bubble Size on the Efficiency of Oxygen Utilization in Aeration Processes". Paper presented at the Society of Chemical Industry Meeting, *New Processes of Waste Treatment and Recovery*, September, London.

Munson B.R., D.F. Young, T.H. Okiishi (1990), Flow Over Immersed Bodies, in : *Fundamentals of Fluid Mechanics*, John Wiley & Sons, Inc., New York.

Mysels K.J. (1989), "Some Limitations in the Interpretations of Time Dependence of Surface Tension Measure by the Maximum Bubble Pressure Method", *Langmuir*, 5, 442,447.

Mysels K.J. (1986), "Improvements in the Maximum Bubble Pressure Method of Measuring Surface Tension", *Langmuir*, 2, 428-432.

Mysels K.J. (1986), "Surface Tension of Solutions of Pure Sodium Dodecyl Sulfate", *Langmuir*, v.2, n.4, 423-428.

Mysels K.J. (1990), "The Maximum Bubble Pressure Method of Measuring Surface Tension, Revisitied", *Colloid and Surface*, 43, 241-262.

Mysels K.J. and A.T. Florence (1970), "Techniques and Criteria in the Purification of Aqueous Surfaces" in *Clean Surfaces: Their Preparation and Chracteristics for Interfacial Studies*, (Editor) Goldfinger G., Marcel Dekker, Inc., New York, 227-265.

Mysels K.J. and A.T. Florence (1973), "The Effect of Impurities on Dynamic Surface Tension - Basis for a Valid Surface Purity Criterion", *J. Colloid and Interface Sci.*, v.43, n.3, 577-582.

Mysels K.J. and R.E. Stafford (1990), "Time and Concentration Resolved Surface Tension", *Colloids and Surfaces*, 51, 105-114.

Netzel D.A., G. Hoch and T.I. Marx (1964), " Adsorption Studies of Surfactants at the Liquid-Vapor Interface : Apparatus and Method for rapidly determining the Dynamic Surface Tension", *J. Colloid Sci.*, 19, 774-785.

O'Connor D.J. (1963), "Effects of Surface Active Agents on Re-aeration", *J. Air Wat. Pollut.*, 5, 123-130.

Oko M.V. and R.L. Venable (1971), "The Effects of Divalent Metal Ions on the Micellar Properties of Sodium Dodecyl Sulfate", *J. Colloid and Interface Sci.*, 35, 1, 53-59.

Owens D.K. (1969), "The Dynamic Surface Tension of Sodium Dodecyl Sulfate Solutions", *J. Colloid Interface Sci.*, 29, 3, 496-501.

Padday J.F., D.R. Russel (1960), "The Measurement of the Surface Tension of Pure Liquid and Solutions", *J. Colloid Sci.*, 15, 503-511.

Padday J.F. (1969) "Theory of Surface Tension" in *Surface and Colloid Science*, vol. 1, part I, (Eitor) Matijevic E., Wiley - Interscience, New York.

Pasveer A. (1956), "Research on Activated Sludge. VII. Efficiency of the diffused air system", *Sewerage and Industrial Wastes Journal*, 28-29.

Peary H.S., D.R. Rowe and G. Tchobanoglous (1985), *Environmental Engineering*, Mcgraw-Hill Publishing Company, New York.

Perry R.H. (editor) (1984), *Perry's Chemical Engineers' Handbook*, McGraw-Hill Book Company, 6th edition, 5-65 - 5-68.

Philichi T.L., Stenstrom M.K. (1989), "Effects of Dissolved Oxygen Probe Lag on Oxygen Transfer Parameter Estimation", *J. Water Pollution Control Federation*, 61, 1, 83-86.

Pierson F.W. and S. Whitaker (1975), "Studies of the Drop-Weight Method for Surfactant Solutions, I. Mathematical Analysis of the Adsorption of Surfactants at the Surface of a Growing Drop", *Journal of Colloid and Interface Science*, 54, 2, 203-218.

Pierson F.W. and S. Whitaker (1975), "Studies of the Drop-Weight Method for Surfactant Solutions, II. Experimental Results for Water and Surfactant Solutions", *Journal of Colloid and Interface Science*, 54, 2, 219-230.

Quigley C.J., A.I. Johnson and B.L. Harris (1955), "*Size and Mass Transfer Studies of Gas Bubbles*" in : *Mass Transfer --- Transport Properties*, Chemical Engineering Progress Symposium Series, 16, 51, AIChE, New York.

Rideal E.K. and K.L. Sutherland (1952), "The Variation of the Surface Tension of Solutions with Time, Solutions of Alcohol", *Trans., Faroday Soc.*, 48, 1109-1123.

Roberson J.A. and C.T. Crowe (1993), Drag and Lift, in : *Engineering Fluid Mechanics*, 5th edition, Houghton Mifflin Company, Boston.

Roberson J.A.; C.T. Crowe (1993), *Engineering Fluid Mechanics*, 5th edition, Houghton Mifflin Company, Boston.

Rodrigue D., Kee D. De, Fong C.M.C.F. (1996), "An Experimental Study of the Effect of Surfactants on the Free Rise Velocity of Gas Bubbles", *J. Non-Newtonian Fluid Mech.* 66, 213-232.

Roll J.B. and J.E. Myers (1964), "Measurement of Dynamics Surface Tension in Bubbling Systems", *J. Chem. Engr. Data*, 9, 2, 256-258.

Rosen M.J. (1978), *Surfactants and Interfacial Phenomena*, John Wiley & Sons, New York.

Ross S. and R.M. Haak (1958), "Inhibition of Foaming. IX. Changes in the Rate of Attaining Surface Tension Equilibrium in Solutions of Surface-Active Agents on addition of Foam-Inhibitors and Foam Stabilizers", *J. Phys. Chem.*, 62, 1260-1264.

Schmidt F. and H. Steyer (1926), "neue Untersuchungen Über die zeitliche Änderung der Spannung reiner Waerober flächen ", *Annalen Der Physik*, 384, 442-464.

Schmit F.L., J.D. Wren, and D.T. Redman (1978), "The Effect of Tank Dimensions and Diffusion Placement of Oxygen Transfer", *J. of Water Pollution Control Federation*, v.50, n.7, 1750-1767.

Schramm L.L. and W.H.F. Green (1992), "An absolute Differential Maximum Bubble Pressure Surface Tensiometer Employing Displaced Capillaries", *Colloid & Polymer Sci.*, 270, 694-706.

Shorter J.A., W.J. De Bruyn, J. Hu, E. Swartz and P. Davidovits (1995), "Bubble Column Apparatus for Gas-Liquid Heterogeneous Chemistry Studies", *Enviro. Sci. Tech.*, 29, 5, 1171-1178.

Springer T.G. and R.L. Pigford (1970), "Influence of Surface turbulence and surfactants on gas transport through liquid interfaces", *Ind. Engr. Chem. Fundam.*, v.9, n.3, 458-465.

Sridhar M.K.C. (1984), "Surface Tension of Polluted Waters and Treated Wastewater", *Environ. Pollution, Series B*, 7, 49-69.

Standard - Measurement of Oxygen Transfer in Clean Water (1993), Published by the American Society of Civil Engineers, New York, NY.

Standard Methods for the Examination of Waters and Wastewaters (1975), 14th ed., American Public Health Association, Washington, D.C.

Standard Guidelines for In-Process Oxygen Transfer Testing (1993), Published by the American Society of Civil Engineers, New York, NY.

Stenstrom M.K. and R.G. Gilbert (1981), "Effects of Alpha, Beta and Theta Factor upon the Design, Specification and Operation of Aeration Systems", *Water Research*, v.15, 643-654.

Stenstrom M.K., L.C. Brown and H.J. Huang (1981), "Oxygen Transfer Parameter Estimation", ASCE, *J. of The Environmental Engineering Division*, 107,EE2, 379-397.

Sugden S. (1922), "XCVII. - The Determination of Surface Tension from the Maximum Pressure in Bubbles", *J. Chem. Soc.*, 121, 858-866.

Sugden S. (1924), "V. - The Determination of Surface Tension from the Maximum Pressure in Bubbles. Pert II.", *J. Chem. Soc.*, 125, 27-41.

Sutherland K.L. (1954), "The Oscillating Jet Method for the Measurement of Surface Tension", *Australian J. Chem.*, 7, 319-328.

Tarlarides L.L., C.A. Conlaloglon, M.A. Zeitlin, G.E. Klinzing, and Gal-Or B. (1970), "Bubble and Drop Phenomena", 62, 11, 6-27.

Tchobanoglous G.; E.D. Schroeder (1987), *Water Quality : Characteristics, Modeling, Modification*, Addison - Wesley Publishing Company, California.

Thomas W.D.E. and L. Potter (1975), "Solution/Air Interfaces, I. An Oscillating Jet Relative Method for Determining Dynamic Surface Tensions", *Journal of Colloid and Interface Science*, v.50, n.3, 397-412.

Valentin F.H.H. (1967), *Absorption in Gas-Liquid Dispersions*, E. & F.N. Spon Ltd., London.

Van Krerelen D.W. and P.J. Hoftijzer (1950), "Studies of Gas-Bubble Formation", *Chem. Engr. Progress*, 46, 1, 29-35.

Vandegrift A.E. (1967), "Experimental Evidence that water has no Dynamic Surface Tension", *J. Colloid Interface Sci.*, 23, 43-45.

Varty R.L. (1991a), "Development of a Mathematical Model for a Bubble Rising above an Orifice", *Proc. of the Thirteenth Canadian Congress of Applied Mechanics*, Winnipeg, Manitoba, June 2-6, 464-465.

Ward A.F.G. and L. Tordai (1949)," Time-Dependence of Boundary Tensions of Solutions. I. The Role of Diffusion in Time-Effects", *J. Chem. Phys.*, 14, 453-461.

Weber M.E. (1975), "The Effect of Surface Active Agents on Mass Transfer from Spherical Cap Bubbles", *Chem. Engr. Sci.*, v.30, 1507-1510.

Yu B. and Y. Shi (1988), "Foam Fractionation Technique. III. Study on Dynamic Adsorption Behavior of Surfactants at the Gas-Liquid Surface using MBPM", *J. East China Institute of Chemical Technology*, 14, 5, 579-587.

Zickefoose C.S. and P.T. Karney (1987), *Manuals of Practice for Water Pollution Control*, Water Pollution Control Federation, manual of practice FD-13, ASCE, Manuals and Reports on Engineering Practice No. 63.

Zlokarnik, M. (1978), "Sorption characteristics for gas-liquid contacting in mixing vessels", *Advances in Biochemical Engineering*, v.8, 133-151.